APPLICATION OF THE SUB-REGION MIXED ENERGY PRINCIPLE TO NUMERICAL MODELLING OF PRESTRESSED CLAD CABLE NETS

A thesis
submitted to the University of Warwick
in supplication for the Degree of
Doctor of Philosophy

by

JIAN SHAN

Department of Engineering
University of Warwick

September 1990

To the memory of my mother

*

To my wife and my daughter

Acknowledgements

The author wishes to thank the Civil Engineering Group, headed by Dr. D. Anderson, of the Department of Engineering, for financial support for this work. Financial support was also obtained from the Committee of Sino-British Friendship Scholarship during the first year of the work.

Thanks are due to Dr. W. J. Lewis for supervision and many helpful discussions during the work.

The author is also indebted to Dr. J. T. Mottram, for advice in the use of PAFEC package.

The author wishes to acknowledge the facilities provided by the Department of Engineering, University of Warwick.

Synopsis

The sub-region mixed energy principle is applied to the analysis of prestressed clad cable net structures, with the emphasis on the interaction between the cable net and the cladding panels. The sub-region mixed energy principle is reformulated with special consideration of the conditions under which the principle is applicable to geometrically non-linear problems. The established governing equations are solved using the dynamic relaxation technique. Comparison of the results from the proposed numerical approach and from an experimental model shows good agreement.

Two numerical models, a five-force model and a four-force model, are developed to represent the behaviour of flat or warped quadrilateral panels. The flexibility matrices of these models are calculated using the finite element method. The influence of curvature of the panels on flexibility, and the influence of different finite element meshes on the results of flexibility analysis are investigated. The five-force model is proved to be capable of expressing any self-balanced nodal forces applied to a panel.

Several computer programs for the analysis of clad network structures are introduced. These programs are the result of optimisation of dynamic relaxation, involving viscous and kinetic dampings respectively, and different selections of

parameters that control the speed of convergence of the method, mainly the fictitious masses. Numerical examples are calculated and the effects of using these programs on the rate of convergence of the solution are discussed.

Contents

Notation

$X, Y, Z\ (X_1, X_2, X_3)$	Cartesian coordinates
$u, v, w\ (u_1, u_2, u_3)$	Displacements in X, Y, Z directions
ξ, η	Local natural coordinates
$\bar{F}_i^{(e)}$	Body force of sub–region e in X_i direction (prescribed)
T_i	Surface force
e_{ij}	Strain
σ_{ij}	Stress
$A\ (e_{ij})$	Density of strain energy
Π	Functional of the sub–region mixed energy principle
Π_{P1}	Total potential energy of sub–region 1
Π_{C2}	Total complementary energy of sub–region 2
H_{21}	Additional energy item on the interface S_{12} between sub–region 1 and sub–region 2
M	Total number of cable members
M_c	Total number of cladding panels
N	Total number of nodes in the structure
N_j	Total number of links connected to node j
$\{\Delta\}$	Nodal displacement vector of the structure
$\{P\}$	Load vector
U_m	Strain energy stored in the m–th cable member
E	Young's modulus
A	Cross–section area of a cable member
F_{jk}	Internal force in cable link j–k

F_{jk}^{0}	Initial (prestress) force in cable link $j-k$
L_{jk}^{0}	Initial (prestressed) length of cable link $j-k$
L_{jk}	Current length of cable link $j-k$
δL_{jk}	Increase in current length L_{jk}
t_{jk}	Tension coefficient of cable link $j-k$
$\{\bar{F}\}^{(e)}$	Nodal force vector of the e−th panel in local coordinates
$\{\bar{\Delta}\}^{(e)}$	Nodal displacement vector of the e−th panel in local coordinates
$[\bar{f}]^{(e)}$	Flexibility matrix of the e−th panel
$[\bar{K}]^{(e)}$	Stiffness matrix of the e−th panel
λ	Factor for the fifth force in the five−force model
R_{ji}	Residual force at node j , in X_i direction
m_{ji}	Mass, concentrated at node j , in X_i direction
c_{ji}	Viscous damping coefficient
$\dot{\Delta}_{ji}$, $\ddot{\Delta}_{ji}$	Velocity and acceleration, respectively
δt	Time increment
K^t	Kinetic energy of the structure at the moment t
B1, C1	Alternative parameters for dynamic relaxation procedure
s_{ji}	Stiffness component at node j inX_i direction

CHAPTER 1

Introduction

1.1 Brief review of tensile structure development

As is widely believed, the idea of tensile structures originally arose from our natural surroundings [1]: spider webs, vinelike plants hanging between trees, etc. have inspired our ancestors in the ancient times to span space in a similar way.

It is reported [2,3] that as early as 285 BC, a bamboo rope bridge was built in southwest China. The first record of an iron-chain bridge built in China can be traced back to roughly the same age (206 BC). These can be regarded as the embryonic form of modern suspension bridges.

The use of tensile structure in architecture began much later (1950's in Europe) than in bridges (early 17th century in Europe), if the very early use of tents is not taken into account. The advantages displayed in suspension bridges attracted

architects and engineers and encouraged them to employ the same type of structure in building design. The main advantages of tensile structures are:

- low cost,
- flexibility of form, giving rise to unusual shapes,
- possibility to meet the ever increasing need for longer, unobstructed (column-free) spans.

The first doubly curved suspension roof structure used in architecture was the one for the Raleigh Arena in North Carolina, designed by Mathew Nowicki in 1952 [4] (Fig. 1.1). Since then various tensile building structures have appeared worldwide. These structures are built for various purpose: stadia and skating rinks, concert halls and theatres, supermarkets and factories, exhibition pavillions, cooling towers, hangars, etc., among which many are truly magnificent and elegant (Figs. 1.2 and 1.3). For small spans, tensile structures can also provide competitive alternatives to conventional designs [5].

Fig. 1.1 Saddle shaped roof of Raleigh Arena, N. Carolina

Fig. 1.2 German Federal Pavilion at Expo '68 Montreal

(Photographs on this page are copied from Ref. [6])

Fig. 1.3 Heart Tent of the Diplomatic Club, Riyadh

(Copied from photograph provided by Buro Happlod Consulting Engineers)

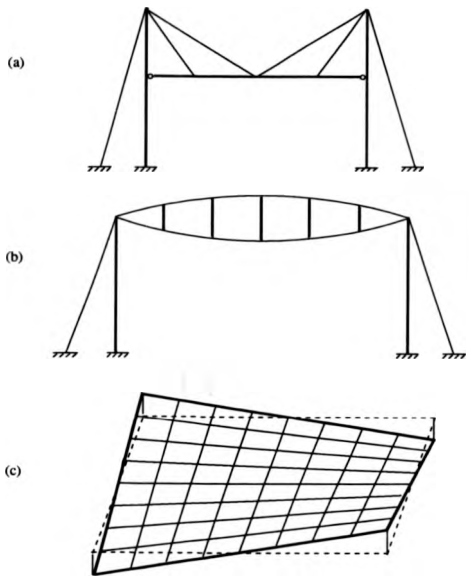

Fig. 1.4 Classification of cable structures

(a) Cable stayed roof (beam)

(b) Cable girder (c) Cable net

1.2 General properties of cable net structures and the materials

Broadly speaking, any structure containing steel cables as resisting members can be referred to as a cable structure. In this sense, cable stayed roofs, cable girders and cable nets are all examples of cable structure (Fig. 1.4). These structures fall into two categories according to the way the cables are stressed: the suspended type consisting of freely hanging cables, which are stressed by means of dead weight, as shown in Fig. 1.4(a), and prestressed ones, where the cable members are tensioned prior to the application of dead load, as shown in Figs. 1.4(b) and (c). The work in this thesis deals mainly with prestressed cable net structures, characterised by a geometrically non-linear response to external static loadings. The method of analysis and computer programs developed during this study are also applicable to other types of cable structures, such as cable girders.

1.2.1 Cables

There are many variations in cables for use in building structures, as shown in Fig. 1.5[5]. Cables shown in Figs. 1.5(a) and (b) are wire ropes, composed of six wire strands spun around an independent wire rope core. These cables are relatively flexible and are mainly used in small lightweight nets. For heavier applications, the suitable constructions are spiral-strand or locked coil, as shown in Figs. 1.5(c) and (d). A spiral-strand is composed of only round wires, whereas in the construction of a locked coil there are two types of wires, i.e. round and shaped.

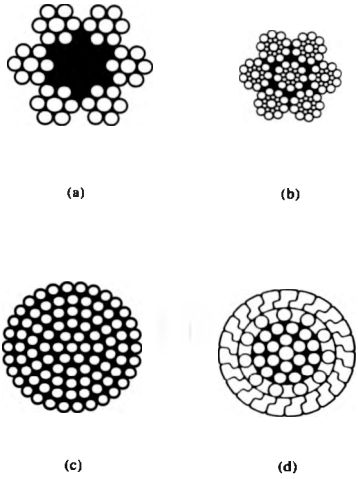

Fig. 1.5 Structural cables

(a) 6 × 7 independent wire rope cable

(b) 6 × 19 independent wire rope cable

(c) Spiral-strand (d) Locked coil

Because of the construction of cables as described above, the relationship between elongation and load during tensile test of a cable is much more complex than that of a single wire. During the period of initial stretch, the wires and strands are relatively loose, allowing relative movements to take place and the cable to stretch under a relatively small load: in this period the ratio of tensile stress to elongation is very low. To ensure against too large a deformation in a cable, the initial or constructional stretch must be eliminated before working loads are applied, namely, prestress is necessary.

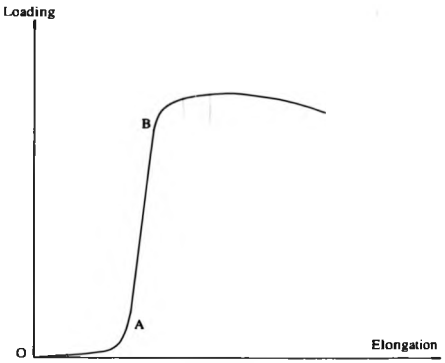

Fig. 1.6

When sufficiently stressed, the cables behave according to the Hooke's law, i.e. elongation is proportional to the applied load. This continues until the elastic limit is exceeded. The process of loading from the initial stage to final fracture is roughly illustrated in Fig. 1.6, in which the period of initial stretch is represented by the section between points O and A. In this thesis, one of the basic assumptions concerning the cables is that they remain linearly elastic under applied load, i.e. they are assumed to work within the zone between points A and B in Fig. 1.6 where the elongation-load behaviour is linear.

1.2.2 Cladding materials

There is also a variety of cladding materials used in cable structures. Sheets or panels made of steel, copper, concrete, plywood or laminated timber, even glass, and various fabric materials such as pvc-polyester and terylene are employed. Except for fabric materials, corrugated metal sheets and timber, these materials can be assumed to be isotropic: this is an assumption about the properties of cladding adopted in this thesis. Cladding materials are also assumed to be working within the elastic zone and hence, the roofing panels are calculated as elastic plates or shells.

1.2.3 Geometrical non-linearity of cable structures

Cable structures represent not only a new style in architecture, but also a different type, from the conventional structures, in structural mechanics. In traditional structural analysis, no attention is paid to geometrical changes when equilibrium alone is considered, because these changes are so small that all the internal forces in question can be regarded as to always act in their initial directions. In conventional structures, deformations and stresses are assumed to be proportional to the value of external loads, provided the loads are applied within elastic limits. Cable structures, however, behave differently.

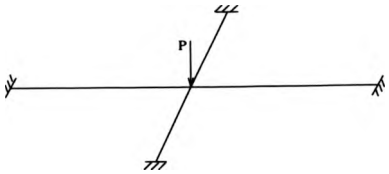

Fig. 1.7 A flat net

Cable structures in nature are mechanisms which adjust their shapes to applied loads so a minimum increase in force is achieved. The change in shape is so noticeable that it must be taken into account when equilibrium is considered, otherwise the derived equilibrium equations will be erroneous. For the flat net shown in Fig. 1.7, under a vertical load, equilibrium is impossible if the deformation of the net is ignored.

As loads increase, the shape of the structure changes continuously and significantly, resulting in an ever changing global stiffness matrix, even if the structure remains elastic. It follows that the magnitudes of the displacements and internal forces of the structure are not proportional to the magnitude of the loading. The non-linearity displayed here is classified as geometrical non-linearity because it is related purely to geometrical changes. This is the essential characteristic mechanical property of cable structures.

Because of geometrical non-linearity, the analysis of cable structures is more difficult than that of conventional ones. It tends to be further complicated when the interaction between the bare cable structure and the cladding material is taken into account. This problem is the main subject of the thesis.

1.3 Objectives and scope of thesis

The main aim of the work presented in this thesis is to develop a numerical approach for the analysis of clad cable net structures. For this purpose, the sub-region mixed energy principle (SMEP) is reformulated taking into account the geometrically non-linear behaviour of the structures. Two numerical models are developed to represent the behaviour of cladding panels, so that their contribution to global stiffness of the composite structure can be assessed. The established governing equations are solved in an iterative procedure using the dynamic relaxation technique. The research work concerning the cladding-network interaction has, so far, resulted in two publications, i.e. Refs. [7] and [8]. Comparison of the results from the proposed numerical approach and from an experimental model shows good agreement. A dynamic relaxation technique is optimised to give the fastest convergence and the results of this work are demonstrated on numerous examples of cable net structures.

The chapter following the introduction, is devoted to a literature survey, mainly on the topic of cable net building structures, with the emphasis on theoretical analysis and numerical methods dealing with geometrically non-linear problems.

The SME principle, which forms the theoretical foundation of the work, is stated and derived in Chapter 3. The derivation, restricted to linear problems, is given in Section 3.4, and then, in Section 3.6, special consideration is paid to the conditions under which the principle is applicable to geometrically non-linear

problems. To give a full assessment of the capacity of the principle, its early applications to some linear problems are also introduced in Section 3.5.

In Chapter 4, general assumptions concerning the behaviour of clad cable net structures are presented and the SME principle is applied to establish the governing equations. The solution of these equations is discussed in Chapter 7, after suitable numerical models are built for representation of the cladding panels.

Chapters 5 and 6 deal with the numerical modelling of cladding panels in two stages: firstly, with modelling of relatively simple rectangular panels (Chapter 5), and then the arbitrary quadrilateral ones (Chapter 6). Two numerical models, i.e. the five-force model and the four-force model, for the flexibility analysis of rectangular panels, are presented in Chapter 5. Later, these are generalised to include arbitrary quadrilateral panels and presented in Chapter 6. The flexibility matrices of these models are calculated using the finite element method. The influence of curvature of the panels on their flexibility and the influence of different finite element meshes on the results of flexibility analysis are discussed in Sections 5.4 and 5.5, respectively. The validity of the five-force model in expressing any self-balanced nodal forces applied to a quadrilateral panel is proved in Section 6.2.

The solution of the governing equations using the dynamic relaxation method is presented in Chapter 7. The method makes use of D'Alembert principle describing a body in motion. Static equilibrium is reached as a result of decaying motions with viscous or kinetic damping. These are discussed in Section 7.3.

Chapter 8 introduces four computer programs, which are the result of optimisation of dynamic relaxation, involving viscous and kinetic dampings respectively and careful selection of parameters that control the speed of convergence of the method, mainly the fictitious masses.

Chapter 9 provides a number of numerical examples of clad cable net structures, calculated using the programs introduced in Chapter 8. The results produced with the four-force model and the five-force model are analysed. They are further compared with the results for the corresponding bare net obtained by ignoring the stiffening effect of the panels. Comparison between numerical results and experimental measurements for a partly clad hyperbolic paraboloid cable net model is performed. Experimental data for the model are obtained from Ref. [9]. The effects of using different programs on the rate of convergence of the solution are discussed in Section 9.3.

Finally, in Chapter 10, the main work is concluded, and comments on the approach presented in the thesis and the SME principle, together with suggestions for further work are given.

CHAPTER 2

Literature Survey

The information contained in this chapter includes the following three aspects:

(i) the sub-region generalised variational principle in elasticity,

(ii) the theoretical and experimental work on the problem of interaction between cable net and its cladding,

(iii) numerical approaches to the solution of governing equations for geometrically non-linear problems.

Further information concerning the architectural aspects of cable structures can be found in the work of Frei Otto [10], and study of an individual cable behaviour is given in the work of H. Irvine [11]. There is also an introductory book by H. Buchhlodt [5] which provides sufficient information about structural systems, materials, loadings, static and dynamic analysis, and design considerations, to enable interested engineers to carry out their own designs.

2.1 Sub-region generalised variational principle in elasticity

In elasticity, the principle of minimum potential energy and the principle of minimum complementary energy are well known. They can be stated as follows [12]:

> Principle of minimum potential energy (PMPE) *Of all displacement fields which satisfy the prescribed constraint conditions, the correct state is that which makes the total potential energy of the structure a minimum.*

and

> Principle of minimum complementary energy (PMCE) *Of all states of stress which satisfy the equation of equilibrium, the correct state is that which makes the total complementary energy of the structure a minimum.*

In the two basic energy principles the independent variables are single type functions, i.e. the displacement type for PMPE and the stress type for PMCE. In addition, these functions are conditional: in PMPE, the displacement fields must satisfy the prescribed constraint conditions, including the strain-displacement relationship inside the body and the prescribed constraint conditions on the boundary; in PMCE, the stress state must satisfy the condition of equilibrium both inside the body and on the boundary.

In the fifties, various generalised variational principles were proposed. In 1950 and 1958, a new principle was suggested by E. Reissner [13,14], taking both displacement and stress as independent variable functions. This became known as Hellinger-Reissner variational principle. In 1954, H. Hu [15] proposed "generalised principle of potential energy" and "generalised principle of complementary energy" and pointed out that the Reissner's variational principle could be regarded as a special case of the generalised principle of potential energy. K. Washizu [16] presented similar work in 1955 and their principles are now known as Hu-Washizu principles.

In the above principles, more than one of the three types of functions (stress, strain and displacement) are taken as independent variables and, compared with PMPE and PMCE, the constraint conditions on these functions e.g. the strain-displacement relationship, are relaxed to a greater or lesser extent. If all the three types of functions are taken as independent variables and the conditions of equilibrium, the strain-displacement relationship, the stress-strain relationship and all the boundary conditions are relaxed, a completely generalised variational principle can be derived. This is achieved using the Lagrange multiplier method [17] which provides a universal approach for developing generalised variational principles (W. Chien [18]).

Another development of generalised variational principles in elasticity is achieved by dividing the object under consideration into a number of sub-regions, where the stress, strain and displacement are partly or wholly taken as

independent variables and the constraint conditions, including the condition of continuity of these variables at the interface between sub-regions, are partly or completely relaxed. The Lagrangian multiplier method is used once again, yielding the corresponding partly or completely generalised sub-region variational principles [18–20].

Generalised variational principles find wide use in elasticity [21–23]. For problems with complex boundary conditions, it is very difficult to find a family of functions which satisfies the boundary conditions, and hence the application of PMPE, for example, is limited. A suitable generalised variational principle, however, can be easily used in this case, because the boundary conditions can be ignored when the approximate functions are chosen. For problems in which different characteristics are shown in different parts of the object, sub-region variational principles are recommended.

The sub-region mixed energy principle developed in this study is a partly generalised variational principle. The object is divided into two sub-regions and in each sub-region the independent variable is specified as a single type function, but different from that in the other sub-region. The detailed information about the principle, including its derivation and its application in linear and geometrically nonlinear problems, is given in Chapter 3.

2.2 Theoretical and experimental work associated with the problem of cladding-network interaction

In most of the published work concerning the analysis of cable net structures, the stiffening effects of cladding material on the cable net are usually disregarded. The cable net is considered as the main load-carrying part of the structure, with the cladding transmitting the load onto it. As H. Buchholdt pointed out [5],

> *The cladding will not, unless it is the form of a concrete shell, significantly increase the stiffness of a roof. It is, however, the major source of structural damping.*

To assess the contribution of cladding to the global stiffness of the structure exactly, theoretical or experimental investigation into the interaction between the cable net and the cladding is necessary. The relevant work in this area has been carried out by E. Bryan *et al* [24–26] on steel building design problems, which takes the stiffening effect of cladding into account. His argument is significant [25]:

> *Whether a building is designed for this effect or not, interaction will always occur to affect profoundly the structural behaviour. If the effect is disregarded, it must not be imagined that the resulting design is always conservative since, because the cladding is so stiff, it usually attracts a great deal of load to itself and so may well be overstressed, even at working loads.*

The findings of this work have been utilised in several national and international codes of practice [27]. Although it is basically a linear problem, because the displacements involved are usually small, the positive conclusion is inspiring as the same problem in cable structures needs to be considered.

Experimental data on the problem of cable-cladding interaction in cable structures is available in Ref.[9], where a partly clad hyperbolic paraboloid (HYPAR) cable net is studied. The information provided there is used to verify the numerical approach proposed in this thesis.

In Ref.[9] a theoretical treatment of the cable-cladding interaction problem is given. Effort is made to express explicitly the relationship between the nodal forces and the nodal displacements of an individual cladding panel. The solution, including the non-linear effects due to the large out-of-plane displacement, is based on Pucher's equilibrium equations of thin shells [28]. This approach, however, is not satisfactory: it fails to give numerical results due to divergence of the solution [9,29].

2.3 Numerical methods for the solution of geometrically non-linear problems

There are two basic problems concerning cable net structures:

(i) form finding problems, in which the initial configuration of a net consistent with given prestress and boundary conditions is to be found,

(ii) analysis problems, including static and dynamic analysis of a structure of known initial configuration.

The corresponding theories are called by Buchholdt *et al* [30,31] the *configuration theory* and the *deformation theory*, respectively. This thesis is dealing with the response of cable nets to static loading and hence is concerned with the deformation theory.

One of the earlier approaches of the deformation theory was to replace the cable net by a membrane and use a shell theory to get a approximate solution [32,33]. As some authors pointed out [30], such a solution would be further away from the original problem than that obtained by a process of discretisation of the structure. But, according to Krishna and Agrawal [34], it gave fairly accurate results for shallow networks.

Another approach is to apply a linear analysis to the non-linear problem, corrected during the iterative process of elimination of the residual forces [35–39].

The accuracy of this approach depends on the validity of the stiffness matrix adopted, and, for highly non-linear problems divergence in the solution may occur. This approach is similar to the modified Newton-Raphson method, as discussed in Section 2.3.3.

In Ref.[40] Hussey mentions the possibility of calculating the deformation of cable nets by minimisation of the total potential energy of the structure. This method is adopted by Buchholdt in Ref.[41] and thereafter forms a unifying approach to the analysis of both linear and non-linear structures. According to this approach, the position of equilibrium is reached in an iterative process of minimising the total potential energy [42,43]. This approach can be explained as a process in which a point in the displacement space moves, step by step, from higher energy surfaces to lower energy surfaces, until the minimum energy point is reached. Here the term "energy surface" means the collection of all the points in the displacement space, each representing a position of the structure, for which the total potential energy is constant. For a two-degree-of-freedom structure, the displacement space is a plane and the energy surfaces are a series of close lines, as shown in Fig. 2.1.

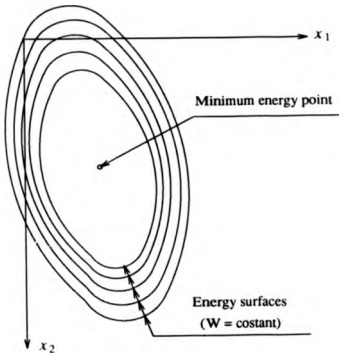

Fig. 2.1 Energy surfaces in the displacement space of a two-degree-of-freedom structure

The minimisation can be carried out by means of various iterative methods, *e g.* the method of steepest descent [51], the method of conjugate gradients [15,44,45], the Newton-Raphson method [15,46] and the dynamic relaxation method [46–50].

2.3.1 The method of steepest descent

In the method of steepest descent, each iteration is carried out by moving from a higher energy surface, in the direction of the steepest descent vector, to a lower energy surface. The length of the move is hS_k, S_k being the full length to reach a point where the total potential energy is a minimum in the direction of the steepest descent vector (in k–th iteration) and h a value between 0 and 1. Only at the beginning of each iteration is the move truly in the direction of steepest descent; the smaller the value of h, the more closely the calculation follows the real steepest descent path. On the other hand, too small a value of h will slow down the process. Unfortunately, there is no method to find an optimum value of h, and for cable structures the optimum value of h varies from case to case.

2.3.2 The method of conjugate gradients

This method is regarded as a more powerful technique of minimisation than the method of steepest descent [44,45]. In this approach, the steepest descent vector is modified at the beginning of each iteration to include the vector from the previous iteration and hence forming a conjugate vector. But the optimisation of h remains a problem.

2.3.3 The Newton-Raphson method

The Newton-Raphson method can also be regarded and developed as an approach to minimise the total potential energy [5,51,52], but it can more easily be understood by the alternative names such as the instantaneous or tangential stiffness method. At the beginning of each iteration, the global tangent stiffness matrix is calculated according to the current geometry. The displacement increment for the iteration is then calculated from the current unbalanced force and the tangent stiffness matrix.

The disadvantage of the Newton-Raphson method is that when used for the solution of cable structures, numerical instability may occur if the calculated stiffness matrix is positive semi-definite or indefinite. Another drawback of the method is that the tangent stiffness matrix has to be reset for each iteration. For this reason, a modified Newton-Raphson method, in which the stiffness matrix is kept constant throughout or reset at intervals may be more efficient [46].

2.3.4 The dynamic relaxation method

The dynamic relaxation method represents another approach in the minimisation of the total potential energy of the structure. Devised by J. Otter in 1964 [53], and first applied to cable net structures by A. Day and J. Bunce in 1970 [47], it is the method adopted in this study to analyse the static response of clad cable net

structures.

According to the dynamic relaxation approach, the total potential energy of the structure is minimised in a process of decreasing vibration about the position of equilibrium. In static problems, fictitious masses and a damping system are introduced into the structure, and, according to the theory of vibration [54], a group of equations of dynamic equilibrium can be written. For discrete structures these equations are:

$$R_{ji} = m_{ji}\ddot{\Delta}_{ji} + c_{ji}\dot{\Delta}_{ji} \qquad (2.1)$$

where R_{ji} is the residual force component at node j and in the direction i; m_{ji} and c_{ji} are the fictitious mass component and damping coefficient, respectively; $\ddot{\Delta}_{ji}$ and $\dot{\Delta}_{ji}$ are the components of acceleration and velocity, respectively. The finite difference representation of eq. (2.1) constitutes the recurrent formulae in the iterative procedure, in which the residual forces are gradually reduced to negligibly small values and the static equilibrium is approached.

The damping system employed in eq. (2.1) is viscous damping, which applies resistance to the movement of the structure and the components of which are proportional to the corresponding components of velocity. An alternative and effective damping system in the dynamic relaxation can be provided by the so called kinetic damping as suggested by Cundall [48]. In this procedure the vibration of the structure is undamped, i.e. $c_{ji} = 0$ in eq. (2.1), and the total kinetic energy, E_k of the structure is traced. Once a peak value of E_k is found, the vibration is forced to stop, i.e. all the velocity components are set to zero, and the vibration is then

restarted from the current position. This procedure is found to be generally stable and rapidly convergent when dealing with large local disturbances and hence is ideally suited for form finding problems (configuration theory) of cable net structures [49,50].

Study of the efficiency of various numerical methods for the analysis of cable net structures have been carried out by Lewis [55] and Barnes [46]. As the result of these studies, the dynamic relaxation method was recommended to be the most efficient method in terms of numerical stability and the speed of convergence.

CHAPTER 3

Sub–region Mixed Energy Principle

3.1 Introduction

The sub-region mixed energy principle [19,20], abbreviated to SMEP in this thesis, is used to establish the governing equations for the problem of interaction between a cable network and its cladding. The SMEP can be regarded as a corollary of the sub-region generalised variational principle in elasticity [18]. For simplicity, however, in this chapter the SMEP will be derived directly, rather than be treated as a special case of the generalised, but more complicated principle.

In this chapter, the following three sections are concerned with the statement and the derivation of SMEP for linear problems. In Section 3.5 the application of SMEP to some linear problems is introduced. Special consideration is given in Section 3.6 to the conditions under which the principle is applicable to non-linear problems.

In the present chapter tensor notation is used to shorten the writing of equations involving quantities with subscripts. The conventions adopted are briefly listed in Appendix A.

3.2 Functional of SMEP

An elastic body is assumed to be divided into two sub-regions (Fig. 3.1). The body force in direction i (i = 1, 2, 3) of a certain sub-region e (e = 1 or 2) is $F_i^{(e)}$. Here and throughout this chapter a *tilde* $\tilde{\ }$ over a character is used to indicate that the corresponding force or displacement is prescribed. The volume of the sub-region is V_e and the surface is S_e.

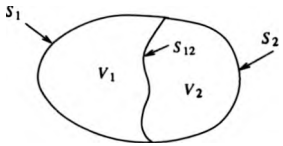

Fig. 3.1 Two sub-regions in an elastic body

The surface S_e consists of three parts in general:

$$S_e = S_{ue} + S_{\sigma e} + S_{12}$$

in which S_{ue} is the part of the boundary surface where displacements u_i are prescribed, $S_{\sigma e}$ is the part of the boundary surface where surface forces $\bar{T}_i$ are prescribed and S_{12} is the interface between the two sub-regions.

Sub-region 1 is a region of potential energy in which displacements u_i (i = 1, 2, 3) are taken as the independent variational functions. For the sake of simplification, the following conditions of compatibility are assumed to be satisfied *a priori*:[1]

$$u_i = \bar{u}_i \qquad at \ S_{u1} \tag{3.1}$$

and

$$e_{ij} = \frac{1}{2}\,(u_{i,j} + u_{j,i}) \qquad in \ V_1 \tag{3.2}$$

where e_{ij} (i, j = 1, 2, 3) are strains.

Sub-region 2 is a region of complementary energy in which stresses σ_{ij} (i, j =1, 2, 3) are taken as the independent variational functions. For the sake of simplification, the following conditions of equilibrium are assumed to be satisfied *a priori*:

[1] These conditions, i.e. eqs. (3.1) and (3.2), as well as the following eqs. (3.3) and (3.4), may be relaxed, resulting in a rather more complicated form of the functional and a rather more generalised energy principle [18].

$$T_i = \tilde{T}_i \qquad at \quad S_{\sigma 2} \tag{3.3}$$

and

$$\sigma_{ij,j} + \tilde{F}_i = 0 \qquad in \quad V_2 \tag{3.4}$$

The functional of SMEP can be written as follows:

$$\Pi = \Pi_{P1} - \Pi_{C2} + H_{21} \tag{3.5}$$

where Π_{P1} = the total potential energy of sub–region 1;

Π_{C2} = the total complementary energy of sub–region 2;

H_{21} = an additional energy item on the interface S_{12},which represents the work done by the interface forces of sub–region 2 on the interface displacements of sub–region 1.

According to the foregoing definitions of Π_{P1} , Π_{C2} and H_{21}, and the conditions (3.1)-(3.4), the three energy items on the right-hand side of eq. (3.5) can be expressed as follows:

$$\Pi_{P1} = \iiint_{V_1} [\, A(e_{ij}) - \tilde{F}_i u_i \,]\, dV - \iint_{S_{\sigma 1}} \tilde{T}_i u_i \, dS \tag{3.6}$$

$$\Pi_{C2} = \iiint_{V_2} [\, \sigma_{ij} e_{ij} - A(e_{ij}) \,]\, dV - \iint_{S_{u2}} T_i u_i \, dS \tag{3.7}$$

$$H_{21} = \iint_{S_{12}} u_i^{(1)} T_i^{(2)} \, dS \tag{3.8}$$

Therefore, eq. (3.5) can be rewritten as follows:

$$\Pi = \iiint_{V_1} [\, A(e_{ij}) - \hat{F}_i u_i \,]\, dV - \iint_{S_2} \hat{T}_i u_i \, dS$$

$$-(\iiint_{V_2} [\, \sigma_{ij} e_{ij} - A(e_{ij}) \,]\, dV - \iint_{S_3} T_i \bar{u}_i \, dS \,)$$

$$+ \iint_{S_{12}} u_i^{(1)} T_i^{(2)} \, dS \qquad (3.9)$$

In eqs. (3.6), (3.7) and (3.9), $A(e_{ij})$ is the density of strain energy.

3.3 Sub-region mixed energy principle

The sub-region mixed energy principle can be stated as follows:

Amongst all the possible answers to the unknown functions, that is, u_i in sub-region 1 and σ_{ij} in sub-region 2, fulfilling the conditions of eqs. (3.1), (3.3) and (3.4), the real answer leads to a stationary value of Π, defined by eq. (3.5) or (3.9).

Hence

$$\delta\Pi = 0 \qquad (3.10)$$

which will give the governing equations of the unknown functions.

3.4 Derivation of SMEP for linear problems

For linear problems a complete derivation of the generalised form of SMEP can be found in Refs.[18] and [19]. As a particular case, the SMEP used in this thesis can be derived simply by using the virtual displacement principle in sub-region 1 and the virtual force principle in sub-region 2 [56].

Consider sub-region 1. The forces and the stresses and their corresponding displacements and strains in this region are listed in Table 3.1. The variations of displacements and the consequent variations of strains (determined by eq. (3.2)) are also listed in this table. At S_{u1}, the variations of displacements are equal to zero because the displacements are prescribed.

Take δu_i and δe_{ij} as a set of virtual displacements. According to the virtual displacement principle, we have

$$\iiint_V [\, \sigma_{ij}\, \delta e_{ij} - \bar{F}_i\, \delta u_i \,]\, dV - \iint_{S_{t1}} \bar{T}_i\, \delta u_i\, dS - \iint_{S_{12}} T_i\, \delta u_i\, dS = 0 \qquad (3.11)$$

Table 3.1 Forces/stresses and displacements/strains and their variations in sub-region 1

Position	Forces /stresses	Displacements /strains	Variations of displacements/strains
in V_1	$\bar{F}_i$, σ_{ij}	u_i , e_{ij}	δu_i , δe_{ij}
at $S_{\sigma 1}$	$\bar{T}_i$	u_i	δu_i
at S_{u1}	T_i*	$\bar{u}_i$	0
at S_{12}	T_i**	u_i	δu_i

* Support reaction ** Interface force

Consider sub-region 2. The forces and the stresses and the corresponding displacements and strains in this region are listed in Table 3.2. The variations of stresses which satisfy $\delta\sigma_{ij,j} = 0$ (according to eq. (3.4)) and the consequent variations of surface forces ($\delta T_i = \delta\sigma_{ij} n_j$, n_j being the direction cosine of the outward normal of the surface) are also listed in the table. At $S_{\sigma 2}$, the variations of forces are zero because the forces are prescribed.

Take $\delta\sigma_{ij}$ and δT_i as a set of virtual forces. According to the virtual force principle, we have

$$\iiint_{V_1} e_{ij}\,\delta\sigma_{ij}\,dV - \iint_{S_{u1}} u_i\,\delta T_i\,dS - \iint_{S_{12}} u_i\,\delta T_i\,dS = 0 \qquad (3.12)$$

Table 3.2 Forces/stresses and their variations and displacements/strains in sub-region 2

Position	Forces /stresses	Displacements /strains	Variations of forces/stresses
in V_2	$\bar{F}_i$, σ_{ij}	u_i, e_{ij}	0, $\delta\sigma_{ij}$
at $S_{\sigma 2}$	$\bar{T}_i$	u_i	0
at S_{u2}	T_i^*	$\bar{u}_i$	δT_i
at S_{12}	T_i**	u_i	δT_i

* Support reaction ** Interface force

Subtracting eq. (3.12) from eq. (3.11) and rearranging terms gives

$$\{ \iiint_{V_2} [\, \sigma_{ij}\, \delta e_{ij} - \bar{F}_i\, \delta u_i \,]\, dV - \iint_{S_{\sigma 2}} \bar{T}_i\, \delta u_i\, dS \,\}$$

$$- \{ \iiint_{V_2} e_{ij}\, \delta\sigma_{ij}\, dV - \iint_{S_{u2}} \bar{u}_i\, \delta T_i\, dS \,\}$$

$$- \iint_{S_{12}} [\, T_i^{(1)}\, \delta u_i^{(1)} - u_i^{(2)} \delta T_i^{(2)} \,]\, dS = 0 \qquad (3.13)$$

The superscripts of the quantities relevant to S_{12} denote the sub-region to which these quantities belong. Because the displacements are continuous at S_{12} and $T_i^{(1)}$ and $T_i^{(2)}$ represent the action and reaction of sub-region 1 and sub-region 2, respectively, we have

$$u_i^{(1)} = u_i^{(2)} \tag{3.14}$$

and

$$T_i^{(1)} = -T_i^{(2)} \tag{3.15}$$

Substituting eqs. (3.14) and (3.15) into (3.13) gives

$$\{ \iiint_{V_1} [\sigma_{ij} \delta e_{ij} - \bar{F}_i \delta u_i] \, dV - \iint_{S_{\sigma 1}} \bar{T}_i \delta u_i \, dS \}$$

$$- \{ \iiint_{V_1} e_{ij} \delta \sigma_{ij} \, dV - \iint_{S_{u2}} \bar{u}_i \delta T_i \, dS \}$$

$$+ \{ \iint_{S_{12}} [T_i^{(2)} \delta u_i^{(1)} + u_i^{(1)} \delta T_i^{(2)}] \, dS \} = 0 \tag{3.16}$$

where the three expressions in brackets are equal to $\delta\Pi_{P1}$, $\delta\Pi_{C2}$ and δH_{21}, respectively.

Comparing eq. (3.16) with (3.5), we have

$$\delta\Pi = 0$$

which validates the sub-region mixed energy principle for linear problems.

3.5 Application of SMEP to some linear problems

The application of SMEP allows different unknowns to be considered in different parts of a structure, so that, for some problems, a more efficient approach can be found than that based on the traditional minimum potential principle or the minimum complementary energy principle. This section includes the application of SMEP to linear structural mechanics and linear fracture mechanics.

3.5.1 Sub-region mixed method in structural analysis

As is well known [56,57], there are two general methods used for the analysis of statically indeterminate structures. The first is the force or flexibility method, in which sufficient releases are introduced into the structure to make it statically determinate. The second is the displacement or stiffness method, in which sufficient additional restraints are introduced into the structure to prevent movements, including translations and rotations, of the joints. The governing equations of both methods can be established using suitable energy principles – the minimum potential energy principle for the displacement method, or the minimum complementary energy principle for the force method. Therefore the two methods can be regarded as the applications of these energy principles [56].

The force method and the displacement method are applicable to any structure, but one or the other method may be preferable for a given case. Considering only the number of primary unknowns involved, the force method is preferable when the degree of static indeterminacy of the structure (the number of releases required) is lower than its degree of kinematic indeterminacy (the number of additional restraints required), while the displacement method is preferable if the opposite is true.

There are composite structures, consisting of, say, two parts, one of which has higher degree of static indeterminacy, the other has higher degree of kinematic indeterminacy. In this case, obviously, the best way is to use different methods of analysis for different parts of the structure. This produces the third approach in structural analysis – the mixed method, or, more accurately, the sub-region mixed method.[2]

Example 3.1

Consider the plane frame shown in Fig. 3.2(a). It can be naturally divided into two parts, that is, ABC and BDEFG, the former providing a part of the supports of the latter.

[2] There is another kind of mixed method which takes displacements and forces as the primary unknowns in the same part of a structure and is called " the sub-term mixed method " [56].

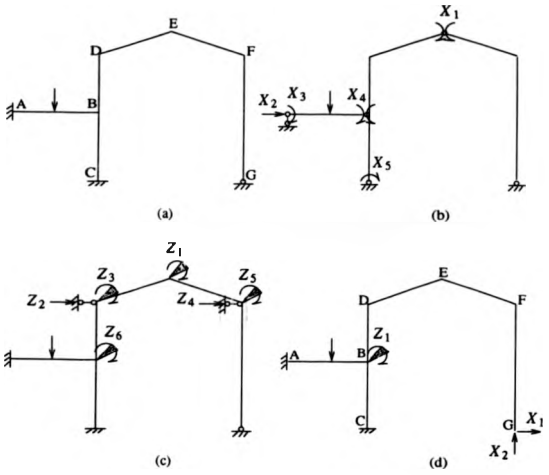

Fig. 3.2 Plane frame in Example 3.1

(a) original structure (b) structure resulting from force method

(c) structure resulting from displacement method

(d) structure resulting from sub-region mixed method

It is easy to see that the degrees of static and kinematic indeterminacy of ABC are 3 and 1 respectively, and those of BDEFG are 2 and 6. In BDEFG, the six unknown displacements at the joints include the rotation at G where a corresponding additional restraint is not necessarily to be introduced when the displacement method is applied. Therefore, if the force method or the displacement method is applied alone to the whole frame, the number of simultaneous equations to be solved is 5 or 6, respectively. The structures resulting from the force method and the displacement method are shown in Figs. 3.2(b) and (c), respectively; in which the unknown forces (including forces and force moments) are denoted by X and the unknown displacements (including translations and rotations) by Z. The shaded triangles represent the additional restraints to rotations of the joints.

Fig. 3.2(d) shows the resulting structure when the sub-region mixed method is used where one additional restraint is introduced at B (displacement method) and two releases are introduced at G (force method). The total number of unknowns is 3 (one displacement and two forces).

The governing equations of sub-region mixed method can be established using SMEP [56]. Therefore this method can be regarded as an application of the principle.

3.5.2 Sub-region mixed finite element method and its application to the calculation of stress intensity factors

The sub-region mixed finite element method applied to two and three dimensional continuum problems is a logical extension of the sub-region mixed method described in Example 3.1. One of the two sub-regions, or both, are replaced by their equivalent systems composed of discrete finite elements. The sub-region mixed energy is then expressed in terms of nodal displacements of sub-region 1 and nodal forces of sub-region 2, or by some other suitable variables chosen to describe the relevant fields. The stationary condition of the functional, given by eq. (3.10), leads to a set of simultaneous algebraic equations involving two types of unknowns: the displacement type and the stress type, and two kinds of equations defining equilibrium and compatibility, respectively.

This method was first applied to the calculation of the stress intensity factor in two-dimensional crack problems of mode I (the opening mode) by Long, Zhi, Kuang and Shan in 1980 [58]. As an example, a strip with a single edge crack which is normal to the edge, as shown in Fig. 3.3, was studied.

The vicinity of the crack-tip was taken as the complementary energy region (the C-region) where a singular element of the stress type was placed; the remaining area of the strip was taken as the potential energy region (the P-region) where a number of conventional elements of the displacement type were arranged. The

mesh is also shown in Fig. 3.3.

In the C-region, the stress field was assumed to be the first term in the known series of stress function which is the main part near the crack-tip and the only unknown in this region was therefore the stress intensity factor. This and the nodal displacements in the P-region constituted the primary unknowns.

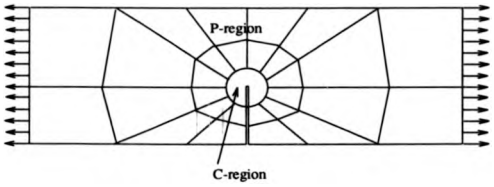

Fig. 3.3 Strip with a single crack normal to the edge, studied by sub-region mixed finite element method

This approach for calculating stress intensity factors was examined by numerical examples and proved to be an efficient method by which the same accuracy was achieved with less computational effort compared with other methods. In 1984, the method was applied further to the plane crack problems of mixed mode.[59]

3.6 SMEP for geometrically non-linear problems

In Section 3.4 it has been shown, by applying the virtual displacement principle in the sub-region of potential energy and the virtual force principle in the sub-region of complementary energy, that SMEP is valid for linear problems. The validity of the principle for geometrically non-linear problems is now considered.

Cable structures, which have been discussed in Chapter 1, belong to a category of geometrically non-linear structures which behave in a manner similar to mechanisms. In these structures, despite the materials remaining elastic, and that the local deformations of the members can be regarded as small, the global deformation of the structure is so large that it cannot be ignored when equilibrium is considered. The stress-strain relationship is linear, but the strain-displacement relationship and the relationship between loading and deformation are non-linear in general.

Re-examining the derivation of the sub-region mixed energy principle in Section 3.4 shows that the use of the virtual displacement principle in sub-region 1 is always valid, regardless whether the problem is linear or not, because here the virtual displacements are variations of displacements and hence are small. The question is whether or not the use of the virtual force principle in sub-region 2 is valid for a geometrically non-linear problem.

The answer to this question depends on what frame of reference is being used. If the behavior of the structure is observed from a global coordinate system, as is usual when linear problems are dealt with, the answer is "No", because of the large displacements. If, instead, the sub-region 2 is observed from a local coordinate system which is fixed to the sub-region and hence moving with it, the answer is "Yes" as the rigid body movements are effectively eliminated and the resulting strain-displacement relationship is linear. In this case, eq. (3.12) is correct even if the displacements and the strains are finite, because the virtual work can be calculated through an integral process with the displacements and the strains proportionally increasing, and for every small increment the differential of virtual work is zero.

Consequently, eq. (3.13) is correct if all the quantities related to sub-region 2 are observed from the local coordinate system. In eq. (3.13), $T_i^{(1)}\delta u_i^{(1)}$ is the dot product of two vectors $\mathbf{T}^{(1)}$ and $\delta\mathbf{U}^{(1)}$ which is an invariant whatever reference system is used. Therefore, the remaining equations in Section 3.4 are correct and the following conclusion can be drawn:

The sub-region mixed energy principle as stated in Section 3.3 applies to geometrically non-linear problems provided all the quantities related to sub-region 2 and to the interface S_{12} in eq. (3.9) are observed from a local coordinate system which always coincides with this sub-region.

This conclusion suggests an amendment to the definition of the functional of the sub-region mixed energy principle. For a geometrically non-linear problem, the difference in the definition of SMEP can be illustrated by the following example.

Example 3.2

Fig. 3.4 shows two hinged bars, loaded by a single lateral force P. The length of each bar is l, the cross section area is A and the Young's modulus is E. The displacement of joint C is vertical because of symmetry. We are to establish an equation relating the displacement Δ to the force P.

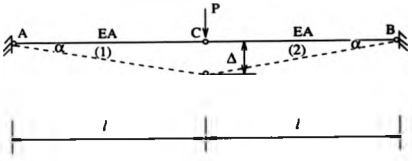

Fig. 3.4 Two bar structure in example 3.2

The structure is divided into two sub-regions:

Sub-region 1 – bar AC, with the displacement Δ of joint C as the primary unknown.

Sub-region 2 – bar BC, with its axial force F as the primary unknown.

With the sub-regions divided this way, the 'interface' between them is the joint point C.

The potential energy of sub-region 1 is

$$\Pi_{P1} = \frac{1}{2}\frac{EA}{l}(\sqrt{l^2+\Delta^2} - l)^2 - P\Delta \qquad (a)$$

The complementary energy of sub-region 2 is

$$\Pi_{C2} = \frac{1}{2}\frac{l}{EA}F^2 \qquad (b)$$

The mixed term of energy at the joint point is

$$H_{21} = F(\sqrt{l^2+\Delta^2} - l) \qquad (c)$$

(Note: here the displacement corresponding to the internal force F should be seen from the local system of reference which always coincides with bar BC, i.e. it is the extension of the bar.)

The sub-region mixed energy then is

$$\Pi = \frac{1}{2}\frac{EA}{l}(\sqrt{l^2+\Delta^2} - l)^2 - P\Delta - \frac{1}{2}\frac{l}{EA}F^2 + F(\sqrt{l^2+\Delta^2} - l) \qquad (d)$$

Letting $\frac{\partial \Pi}{\partial \Delta} = 0$ and $\frac{\partial \Pi}{\partial F} = 0$ gives

$$\frac{EA}{l}(\sqrt{l^2+\Delta^2}-l)\frac{\Delta}{\sqrt{l^2+\Delta^2}}-P+F\frac{\Delta}{\sqrt{l^2+\Delta^2}}=0 \qquad (e)$$

and

$$-\frac{l}{EA}F+(\sqrt{l^2+\Delta^2}-l)=0$$

or

$$F=\frac{EA}{l}(\sqrt{l^2+\Delta^2}-l) \qquad (f)$$

Substituting eq. (f) into (e) gives

$$2\frac{EA}{l}(\sqrt{l^2+\Delta^2}-l)\frac{\Delta}{\sqrt{l^2+\Delta^2}}-P=0$$

which is the equation required, and is clearly correct.

If the mixed energy term is simply calculated as the dot product of vectors Δ and **F**, as it is calculated in a linear case, then

$$H_{21}=F\,\Delta\sin\alpha \qquad (c')$$

the right hand side of which is approximately equal to $\frac{F\Delta^2}{l}$ when α is small. However, for small values of α, the right hand side of eq. (c), describing the mixed energy for the non-linear case, is approximately equal to $\frac{1}{2}\frac{F\Delta^2}{l}$. The difference between eqs. (c) and (c') is not neqligible. For a highly non-linear structure like this example, the misapplication of the linear form of SMEP always results in large error.

CHAPTER 4

Derivation of Governing Equations

4.1 Introduction

In this short chapter, cable roof structures under static loadings are analysed with the interaction between cable system and cladding system being taken into account. Based on the general assumptions in Section 4.2, the sub-region mixed energy principle is applied to establish the governing equations, described in Section 4.3. The solution of the governing equations is presented in Chapter 7, which follows two chapters dealing with numerical models of cladding panels.

4.2 General assumptions

The analysis of clad cable roof structures discussed in this thesis is based on the following assumptions:

(i) The structures are composed of prestressed cable links and panels, and the panels are connected to the cables at cable intersections;

(ii) The cables possess extensional stiffness only and remain linearly elastic under applied external loadings;

(iii) The panels are made of isotropic materials, possess in-plane stiffness only and remain linearly elastic under applied external loadings;

(iv) The external loadings are applied at the cable intersections only.

Cable intersections are called nodes or joints. A subsection between two neighbouring nodes is called a cable member or a cable link. According to assumptions (i) and (iv), cable links (or members) remain straight under external loadings.

4.3 Governing equations

Let the structure under analysis be divided into two sub-regions:

Sub-region 1 – the unclad cable structure, with the cable node displacements being taken as primary unknowns;

Sub-region 2 – the cladding panels, with their nodal forces (detailed in the next two chapters) being taken as primary unknowns.

The total potential energy of sub-region 1 is

$$\Pi_{P1} = \sum_{m=1}^{M} U_m - \{\Delta\}^T\{P\} \tag{4.1}$$

where U_m = the strain energy stored in the m−th cable member;

M = the total number of cable members;

$\{\Delta\}$ = the nodal displacement vector;

$\{P\}$ = the load vector.

In eq. (4.1), $-\{\Delta\}^T\{P\}$ represents the potential energy of external loadings. The total strain energy stored in cable members, $\sum_{m=1}^{M} U_m$, is a function of the nodal displacement vector $\{\Delta\}$. For a linear problem it can be expressed as a quadratic form of $\{\Delta\}$: $\sum_{m=1}^{M} U_m = \frac{1}{2}\{\Delta\}^T[K]\{\Delta\}$, $[K]$ being the global stiffness matrix of the sub-region; for a non-linear problem as the present one, the total strain energy cannot be expressed in this way.

The total complementary energy of sub-region 2 is

$$\Pi_{C2} = \sum_{e=1}^{M_2} \frac{1}{2}\{\bar{F}\}^{(e)T}[\bar{f}]^{(e)}\{\bar{F}\}^{(e)} \tag{4.2}$$

where $\{\bar{F}\}^{(e)}$ = the nodal force vector of the e–th panel in its local coordinates;[3]

$[\bar{f}]^{(e)}$ = the flexibility matrix of the e–th panel;

M_c = the total number of cladding panels.

For rectangular panels and arbitrary quadrilateral panels, the nodal force vector $\{\bar{F}\}$ and the flexibility matrix $[\bar{f}]$ are discussed in Chapters 5 and 6, respectively.

According to general assumption (i), the "interface" between the two sub-regions is composed of all the joints where the panels are connected to cable members. Hence the additional energy item H_{21}, defined in Section 3.2 , is the total work done by the nodal forces of panels on the displacements of cable joints:

$$H_{21} = \sum_{e=1}^{M_c} \{\bar{F}\}^{(e)T} \{\bar{\Delta}\}^{(e)} \tag{4.3}$$

where $\{\bar{\Delta}\}^{(e)}$ is the nodal displacement vector of the e-th panel, corresponding to $\{\bar{F}\}^{(e)}$ and compatible with $\{\Delta\}$ and is therefore a function of $\{\Delta\}$, which will be discussed in Chapters 5 and 6.

Substitution of eqs. (4.1), (4.2) and (4.3) into eq. (3.5) gives

[3] Here and throughout this chapter and the succeeding Chapters 5 and 6, a bar '-' over a character is used to indicate that the corresponding force or displacement is observed from the local coordinate system.

$$\Pi = \sum_{m=1}^{M} U_m - \{\Delta\}^T\{P\}$$

$$- \sum_{e=1}^{M_c} \frac{1}{2}\{\bar{F}\}^{(e)T}[\bar{f}]^{(e)}\{\bar{F}\}^{(e)}$$

$$+ \sum_{e=1}^{M_c} \{\bar{\Delta}\}^{(e)T}\{\bar{F}\}^{(e)} \qquad (4.4)$$

by which the sub-region mixed energy Π is expressed in terms of cable nodal displacements $\{\Delta\}$ and panel nodal forces $\{\bar{F}\}^{(e)}$ ($e = 1, 2, ..., M_c$).

In eq. (4.4) the quantities related to sub-region 2 and to the interface S_{12}, i.e. $\{\bar{F}\}^{(e)}$ and $\{\bar{\Delta}\}^{(e)}$, are observed from a local coordinate system which coincides with sub-region 2 (the panels). As concluded in Section 3.6, under this condition the SMEP is applicable to the present geometrically non-linear problem.

Comparing eq. (4.4) with eq. (3.10) leads to the conclusion that every partial derivative of the right-hand-side in eq. (4.4) with respect to any component of $\{\Delta\}$ or $\{\bar{F}\}^{(e)}$ ($e = 1, 2, ..., M_c$) must be zero. This gives the governing equations of the primary unknowns.

Letting

$$\frac{\partial \Pi}{\partial \Delta_\mu} = 0$$

gives

$$\sum_{m=1}^{M} \frac{\partial U_m}{\partial \Delta_{ji}} - P_{ji} + \sum_{e=1}^{M_e} \frac{\partial (\bar{\Delta})^{(e)T}}{\partial \Delta_{ji}} (\bar{F})^{(e)} = 0$$

$$(j = 1, 2, ..., N;\ i = 1, 2, 3) \qquad (4.5)$$

where j = cable node number;

N = the total number of cable nodes;

i = coordinate number (i = 1, 2, 3 corresponds to coordinate X, Y and Z, respectively).

Letting

$$\frac{\partial \Pi}{\partial \bar{F}_k^{(e)}} = 0$$

gives

$$-\sum_{r=1}^{R_e} \bar{f}_{kr}^{(e)} \bar{F}_r^{(e)} + \bar{\Delta}_k^{(e)} = 0$$

$$(e = 1, 2, ..., M_e;\ k = 1, 2, ..., R_e) \qquad (4.6)$$

where e = panel number;

k = local force number in panel 'e';

R_e = the total number of forces in panel 'e'; for a quadrilateral panel, R_e = 4 or 5, corresponding to the four or five force model, respectively, as explained in the next two chapters.

Eqs. (4.5) and (4.6) are the governing equilibrium and compatibility equations,

respectively, of the clad cable structure. Eq. (4.6) can be rewritten in a compact form as the following:

$$[\overline{f}]^{(e)}\{\overline{F}\}^{(e)} = \{\overline{\Delta}\}^{(e)} \tag{4.7}$$

or

$$\{\overline{F}\}^{(e)} = [\overline{K}]^{(e)}\{\overline{\Delta}\}^{(e)} \tag{4.8}$$

where

$$[\overline{K}]^{(e)} = ([\overline{f}]^{(e)})^{-1} \tag{4.9}$$

which is the stiffness matrix of the e-th panel (e = 1, 2, ..., M_c).

Eqs. (4.7) and (4.8) are the flexibility equation and the stiffness equation of the e-th panel, respectively, in which the physical meanings are apparent. In Chapter 7, explicit explanation is given about the physical meaning of eq. (4.5) and a dynamic relaxation approach to solve these equations is discussed.

CHAPTER 5

Numerical Models of Rectangular Panels

5.1 Introduction

In practice, two way cable nets are widely used. The panels connected with this type of net at cable intersections have four sides, which are assumed to be straight lines. Although these panels can be warped, i.e. the four sides of a panel may not be necessarily in one plane, they are referred to as quadrilateral panels for convenience.

To start with, a simple case of rectangular panels is discussed in this chapter. Here, the term 'rectangular panels' refers to flat or warped panels with shallow curvatures and rectangular projections of their boundaries on plan. A general discussion of arbitrary quadrilateral panels is given in Chapter 6.

In this chapter, two numerical models, i.e. the five-force model and the four-force model, are presented for the flexibility analysis of rectangular panels. The five-

force model is discussed in depth in Section 5.2 while only a brief discussion of the four-force model is included. The comparison of the two models, using numerical examples, is given in Chapter 9. Sections 5.4 and 5.5 discuss the influence of curvature of a panel on its flexibility and the influence of the change in the size of finite element mesh on the resulting flexibility matrix.

5.2 Five-force model

It is assumed in Section 4.2 that the cladding panels are made of isotropic materials and possess in-plane stiffness only. As far as membrane action is concerned, the nodal force vector of a rectangular panel has eight components. With three equilibrium equations to be fulfilled, only five of the eight forces can be taken as independent variables. A five-force model is thus considered, as shown in Fig. 5.1. The model has five self-balanced, generalised forces, denoted by $\bar{F}_1$, $\bar{F}_2$, $\bar{F}_3$, $\bar{F}_4$ and $\bar{F}_5$ in local coordinates.[1]

Forces $\bar{F}_1$, $\bar{F}_2$, $\bar{F}_3$ and $\bar{F}_4$ are coupled forces, each acting along a side of the panel. The forces are considered positive when tensile. They cause symmetrical deformation of the panel, as shown in Fig. 5.2(b) which illustrates the effect of force $\bar{F}_1$ for example. The displacements corresponding to these forces are the extensions

[1] See the footnote in Section 4.3, pp. 51.

of the sides of the panel. Force $\bar{F}_5$ represents two pairs of forces, acting along the diagonals, equal and opposite, i.e. one tensile and the other compressive. This generalised force causes antisymmetrical deformation, i.e. angular distortion of the panel, illustrated in Fig. 5.3(b). The displacement corresponding to $\bar{F}_5$ is the change in the difference between lengths of the diagonals.

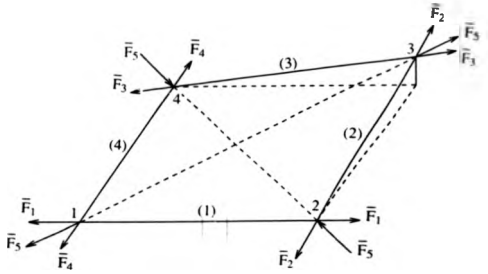

Fig. 5.1 Five-force model of a rectangular panel

The relationship between the five forces and their corresponding displacements can be given in the following flexibility equations:

$$\{ \bar{\Delta} \} = [\bar{f}] \{ \bar{F} \} \tag{5.1}$$

where

$$\{ \bar{\Delta} \} = [\bar{\Delta}_1 \; \bar{\Delta}_2 \; \bar{\Delta}_3 \; \bar{\Delta}_4 \; \bar{\Delta}_5]^T$$

is the generalised displacement vector, and

$$[\bar{f}] = \begin{bmatrix} \bar{f}_{11} & \bar{f}_{12} & \bar{f}_{13} & \bar{f}_{14} & \bar{f}_{15} \\ \bar{f}_{21} & \bar{f}_{22} & \bar{f}_{23} & \bar{f}_{24} & \bar{f}_{25} \\ \bar{f}_{31} & \bar{f}_{32} & \bar{f}_{33} & \bar{f}_{34} & \bar{f}_{35} \\ \bar{f}_{41} & \bar{f}_{42} & \bar{f}_{43} & \bar{f}_{44} & \bar{f}_{45} \\ \bar{f}_{51} & \bar{f}_{52} & \bar{f}_{53} & \bar{f}_{54} & \bar{f}_{55} \end{bmatrix} \tag{5.2}$$

is the flexibility matrix.

In the flexibility matrix, $\bar{f}_{kr}$ ($k, r = 1, 2, 3, 4, 5$) represents the generalised displacement in the direction of Δ_k caused by a unit force in the direction of F_r. For example, $\bar{f}_{11}$ is the extension of side 1 when $\bar{F}_1 = 1$ and all the other forces are zero; $\bar{f}_{23}$ is the extension of side 2 when $\bar{F}_3 = 1$ is applied only; $\bar{f}_{55}$ is the difference between lengths of the diagonals caused by $\bar{F}_5 = 1$.

According to the reciprocal theorems of Betti [60], the flexibility matrix is symmetrical, i.e. $\bar{f}_{kr} = \bar{f}_{rk}$ ($k, r = 1, 2, 3, 4, 5$). In addition, because of the symmetry[2] of the rectangular panel itself, the following equations are true:

$$\bar{f}_{12} = \bar{f}_{14} = \bar{f}_{32} = \bar{f}_{34} = \bar{f}_{21} = \bar{f}_{41} = \bar{f}_{23} = \bar{f}_{43}, \tag{5.3a}$$

$$\bar{f}_{13} = \bar{f}_{31}, \tag{5.3b}$$

$$\bar{f}_{24} = \bar{f}_{42}, \tag{5.3c}$$

$$\bar{f}_{11} = \bar{f}_{33}, \tag{5.3d}$$

$$\bar{f}_{22} = \bar{f}_{44}. \tag{5.3e}$$

[2] Warped rectangular panels can be roughly considered symmetrical when they are shallow, and calculation shows that eqs. (5.3) and (5.4) can be used for these panels with satisfactory accuracy.

$$\bar{f}_{15} = \bar{f}_{25} = \bar{f}_{35} = \bar{f}_{45} = \bar{f}_{51} = \bar{f}_{52} = \bar{f}_{53} = \bar{f}_{54} = 0. \qquad (5.4)$$

The coefficients in eq. (5.4) are zero, because the deformation caused by forces $\bar{F}_1$, $\bar{F}_2$, $\bar{F}_3$ and $\bar{F}_4$ are symmetrical and independent of force $\bar{F}_5$, which produces antisymmetrical deformations only.

From eqs. (5.3) and (5.4) it can be seen that there are only 6 values to be found to determine the 25 coefficients in the flexibility matrix. In the case of a square panel, the number is further reduced to 4, because the coefficients in eqs. (5.3b) and (5.3c) are equal, as well as those in eqs. (5.3d) and (5.3e). These values can be calculated by the finite element method, or measured through experiments.

A mesh of elements is suggested in Fig. 5.2(a), when the finite element method is employed to calculate the coefficients in the first column of the flexibility matrix of a rectangular panel[3]. Because of symmetry, only a half of the panel is considered. The mesh is refined in the area of stress concentration, i.e. where the unit force is applied. The deformation of the panel under the force $\bar{F}_1 = 1$ is shown in Fig. 5.2(b). Given the three values of extensions δ_1, δ_2 and δ_3, the flexibility coefficients can be expressed as follows:

$$\bar{f}_{11} = 2\,\delta_1, \quad \bar{f}_{21} = \bar{f}_{41} = -\,\delta_2, \quad \bar{f}_{31} = -\,2\,\delta_3.$$

These give the three values of the five unknown coefficients in eqs. (5.3). To find the other two, the unit force $\bar{F}_2 = 1$ or $\bar{F}_4 = 1$ is applied and the resulting displacements are calculated or can be measured experimentally.

[3] In the figures throughout the thesis, a short bar with two pinned ends represents a restriction on the displacement in the corresponding direction.

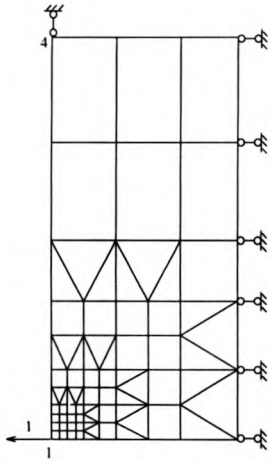

(*a*)

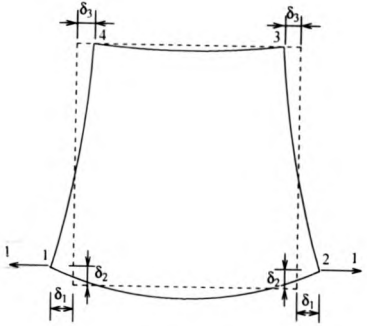

(*b*)

Fig. 5.2 (a) Finite element mesh for calculation of $\bar{f}_{k1}$ (k = 1, 2, 3, 4)

(b) Deformation of the panel under $\bar{F}_1 = 1$

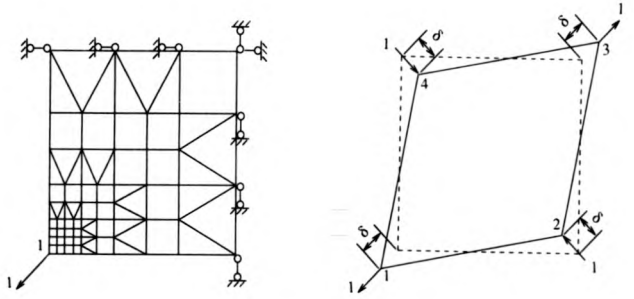

(*a*) (*b*)

Fig. 5.3 (a) Finite element mesh for calculation of $\bar{f}_{55}$

(b) Deformation of the panel under $\bar{F}_5 = 1$

Fig. 5.3(a) shows a mesh of elements for the calculation of the flexibility coefficient $\bar{f}_{55}$. Because the panel has two symmetrical axes and the force is antisymmetrical about both of them, as shown in Fig. 5.3(b), only a quarter of the panel needs to be considered. Again, the mesh is refined near the corner of the panel. Once the extension δ has been found, the flexibility coefficient, $\bar{f}_{55}$, is simply given as

$$\bar{f}_{55} = 4\,\delta$$

which, according to the definition of $\bar{f}_{55}$, gives the difference between the lengths of the diagonals, induced by $\bar{F}_5 = 1$.

In Figs. 5.2(a) and 5.3(a) the meshes are composed of mainly rectangular elements, varied in size, with bilinear shape functions. Triangular elements of constant strains are inserted into the rectangular ones. An alternative to this is to use the quadrilateral isoparametric elements which are more adaptable to changes in both sizes and shapes of the elements, as shown in Fig. 5.4.

The calculation of the flexibility matrix may be carried out using either purpose written programs or available commercial packages. In this thesis, most of the calculations (especially those for panels with arbitrary shapes and curvature) are carried out using the PAFEC package [61] with isoparametric plate or shell elements. For the flat square panel in the following Example 5.1, a finite element program was written, restricted to meshes with rectangular and triangular elements, as shown in Figs. 5.2(a) and 5.3(a). The program gives exactly the same results (to 5 significant figures) as those obtained from the PAFEC using the same data.

Example 5.1

To illustrate the calculation of the flexibility matrix based on the five-force model, a flat square panel is chosen, as shown in Fig. 5.4(a). Material properties of the panel are: Young's modulus $E = 0.62 \times 10^8\ kN/m^2$, Poisson ratio $\nu = 0.33$, and the thickness $t = 0.9 \times 10^{-3} m$.

Although for an individual load case it may be beneficial to consider only a half or a quarter of the panel, taking symmetry into account, it is generally not the case when different combinations of loads are involved. A mesh over the whole panel, as shown in Fig. 5.4(a), needs to be then considered. This not only avoids repetitive data input concerning different meshes, but also saves computational work, because for all the load cases the computer needs to assemble the global stiffness matrix once only.

The mesh in Fig. 5.4(a) is composed of the second-order quadrilateral isoparametric plate elements [60,62] each having eight nodes. The panel is supported to prevent rigid body movement. In the case of $\bar{F}_1 = 1$ being applied (Fig. 5.4(b)), there is no reaction in the supports. In Fig. 5.4(c), the applied forces and the resulting support reactions compose the diagonal load $\bar{F}_5 = 1$.

The output of nodal displacements is listed in Table 5.1 where u_j and v_j (j = 1, 2, 3, 4) are the nodal displacements in x direction and y direction, respectively.

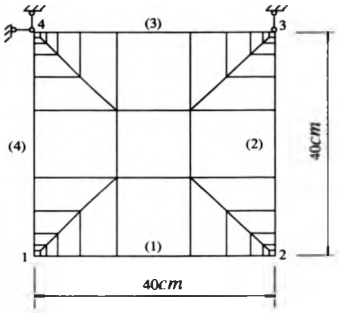

(a)

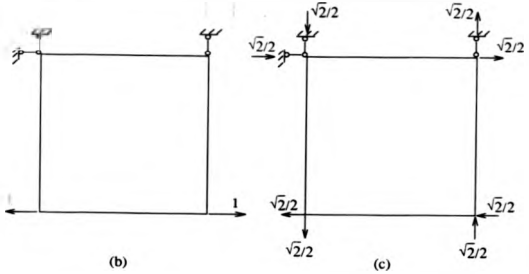

(b) (c)

Fig. 5.4 Panel in Example 5.1

(a) Finite element mesh

(b) $\bar{F}_1 = 1$ (c) $\bar{F}_5 = 1$

Table 5.1 Nodal displacements of the panel
in Example 5.1 (Fig. 5.4) (Unit : *mm*)

Forces	u_1	v_1	u_2	v_2	u_3	v_3	u_4	v_4
$\bar{F}_1 = 1$	-0.197	0.115	0.192	0.115	-0.005	0	0	0
$\bar{F}_5 = 1$	-0.247	0.000	-0.247	0.000	0.000	0	0	0

Based on the data in Table 5.1, the corresponding flexibility coefficients are calculated as shown below:

i) First column (displacements caused by $\bar{F}_1 = 1$):

$$\bar{f}_{11} = u_2 - u_1 = 0.192 + 0.197 = 0.389$$

$$\bar{f}_{21} = v_3 - v_2 = 0 - 0.115 = -0.115$$

$$\bar{f}_{31} = u_3 - u_4 = -0.005 - 0 = -0.005$$

$$\bar{f}_{41} = v_4 - v_1 = 0 - 0.115 = -0.115$$

$$\bar{f}_{51} = 0$$

ii) Fifth column (displacements caused by $\bar{F}_5 = 1$):

$$\bar{f}_{15} = \bar{f}_{25} = \bar{f}_{35} = \bar{f}_{45} = 0$$

$$\bar{f}_{55} = \frac{\sqrt{2}}{2}\{[(u_3 - u_1) + (v_3 - v_1)] - [(u_2 - u_4) + (v_4 - v_2)]\}$$

$$= \frac{\sqrt{2}}{2}\{[(0 + 0.247) + (0 - 0)] - [(-0.247 - 0) + (0 - 0)]\}$$

$$= 0.349$$

The remaining columns of the flexibility matrix of the panel are obtained from symmetry, and hence:

$$[\bar{f}] = \begin{bmatrix} 0.389 & -0.115 & -0.005 & -0.115 & 0 \\ -0.115 & 0.389 & -0.115 & -0.005 & 0 \\ -0.005 & -0.115 & 0.389 & -0.115 & 0 \\ -0.115 & -0.005 & -0.115 & 0.389 & 0 \\ 0 & 0 & 0 & 0 & 0.349 \end{bmatrix}$$

5.3 Four-force model

The four-force model is produced by simply ignoring the fifth force in the five-force model. Hence the corresponding flexibility matrix consists of 4 × 4 elements, as given by equation (5.5):

$$[\bar{f}] = \begin{bmatrix} \bar{f}_{11} & \bar{f}_{12} & \bar{f}_{13} & \bar{f}_{14} \\ \bar{f}_{21} & \bar{f}_{22} & \bar{f}_{23} & \bar{f}_{24} \\ \bar{f}_{31} & \bar{f}_{32} & \bar{f}_{33} & \bar{f}_{34} \\ \bar{f}_{41} & \bar{f}_{42} & \bar{f}_{43} & \bar{f}_{44} \end{bmatrix} \qquad (5.5)$$

In the four-force model, the antisymmetrical force is assumed to be zero even if the angular distortion is caused. Hence, employing the four-force model results in a decrease in stiffness of the panel and, consequently, the whole structure. However, in the case where it can be ensured that the angular distortion is not significant, the four-force model can still be adopted and give quite accurate results. In the case of warped panels, discussed in the following section, it is shown that the stiffness coefficient relating the antisymmetrical force to the displacement of a thin panel is much smaller than the other principal coefficients of the stiffness matrix. This is further discussed in Chapter 8 where numerical examples are given and the analysis of the results is carried out.

5.4 Influence of curvature on flexibility of panels

A curved panel is more flexible than an otherwise identical flat one when they are stretched, because in the former there will be not only membrane strain but also bending strain induced by the applied forces. This difference in flexibility is similar to that of two bars, one curved and the other straight, subjected to the tensile forces acting at their ends, as shown in Fig. 5.5. Obviously, the relative displacement of the ends of the curved bar will be larger than that of the straight one, provided they are made of the same material, having the same length and cross section area and the same magnitude of the applied forces.

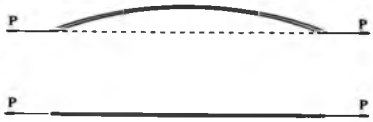

Fig. 5.5 A curved bar and a straight bar

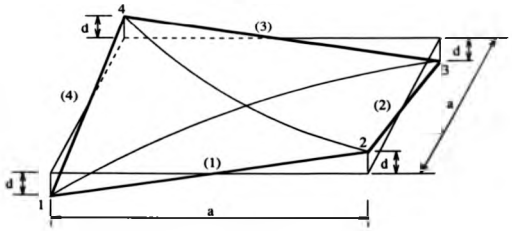

Fig. 5.6 A typical curved panel

To investigate the influence of curvature of a panel on its flexibility, the flexibility matrices of a series of panels are calculated by the finite element method using the PAFEC package. These panels are square in plan, with the same size and thickness and made of the same material, but different in curvature. A typical example of these is shown in Fig. 5.6, illustrating a hyperbolic paraboloid panel with four straight edges. The ratio a/d is taken as an indicator of curvature, where a is the length of the side, projected on plan, and d is the distance from the nodes of the panel to the reference plane. To make the results comparable, the meshes of elements used are the same in plan as that in Example 5.1 (Fig. 5.4(a)), composed of the second-order quadrilateral isoparametric shell elements, each having eight nodes.

Table 5.2 and Figs. 5.7 and 5.8 show the influence of curvature, measured by the a/d ratio, on flexibility coefficients $\bar{f}_{11}$, $\bar{f}_{21}$ (or $\bar{f}_{41}$), $\bar{f}_{31}$ and $\bar{f}_{55}$, respectively. In the bottom entry of Table 5.2 are the corresponding flexibility coefficients of the flat panel when a/d is infinitely large, i. e. $d = 0$. These are shown in Figs. 5.7 and 5.8 by dashed lines. The range of curvatures considered here corresponds to that of shallow panels.

From the results given in Table 5.2 and Figs. 5.7 and 5.8 the following conclusions can be drawn:

(i) Curvature of a warped panel does not influence significantly the coefficients related to a force acting along straight edges (*e.g.* the coefficients $\bar{f}_{11}$, $\bar{f}_{21}$, $\bar{f}_{31}$ and $\bar{f}_{41}$) because the stress field along these

directions is essentially a membrane action;

(ii) Curvature of a warped panel does influence significantly the coefficient $\bar{f}_{55}$, corresponding to forces acting along the two diagonals, i.e. the lines of principal curvatures, where the largest bending deformations develop because of the small bending stiffness.

Table 5.2 Flexibility coefficients of panels with different curvatures (indicated by a/d)

a/d	$\bar{f}_{11}$	$\bar{f}_{21}$ ($\bar{f}_{41}$)	$\bar{f}_{31}$	$\bar{f}_{55}$
40	0.5233	-0.0786	-0.0025	44.14
60	0.4891	-0.0816	-0.0024	21.10
80	0.4682	-0.0841	-0.0002	12.43
100	0.4540	-0.0866	0.0021	8.25
120	0.4435	-0.0889	0.0038	5.91
140	0.4355	-0.0910	0.0048	4.48
160	0.4293	-0.0931	0.0052	3.53
180	0.4242	-0.0949	0.0052	2.87
200	0.4200	-0.0968	-0.0050	2.40
∞	0.3895	-0.1153	-0.0054	0.3489

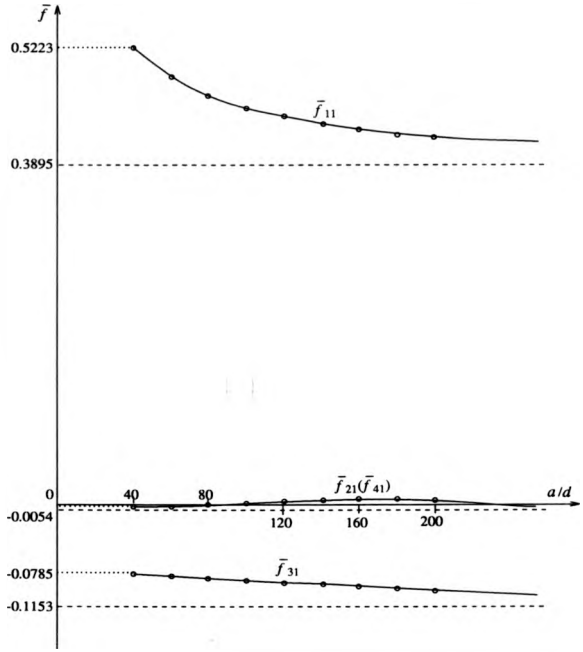

Fig. 5.7 Influence of curvature on flexibility coefficients $\bar{f}_{11}, \bar{f}_{21}(\bar{f}_{41})$ and $\bar{f}_{31}$

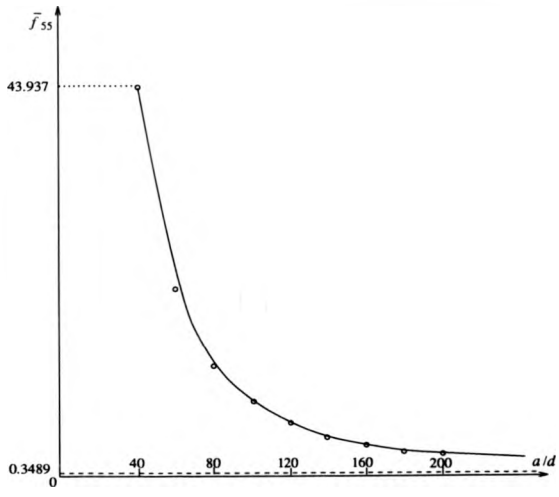

Fig. 5.8 Influence of curvature on flexibility coefficient $\bar{f}_{55}$

5.5 Influence of element mesh on calculated flexibility matrix

In this section, the effects of the size of finite elements upon the calculated flexibility matrix of warped panels are considered. Generally speaking, a coarse mesh results in smaller values of the flexibility coefficients than those resulted from a fine mesh because the latter has a higher degree of freedom and therefore is more flexible.

As an example, the flexibility matrix of a warped panel is calculated using different mesh sizes of elements. The panel is from the range of those studied in Section 5.4 (shown in Fig. 5.6) and has a shallow curvature, given by the ratio $a/d = 50$. The meshes used are shown by their projections on the reference plan in Fig. 5.9. The finest mesh, size (e), has been adopted for calculations in Section 5.4, and is the same in plan as that in Example 5.1 (Fig. 5.4(a)). The meshes vary from size (a) to (e), getting finer and finer in the corner areas, with the size of the smallest elements being reduced by a half each time. The calculated flexibility coefficients $\bar{f}_{11}$, f_{21}, $\bar{f}_{31}$ and $\bar{f}_{55}$ are listed in Table 5.3.

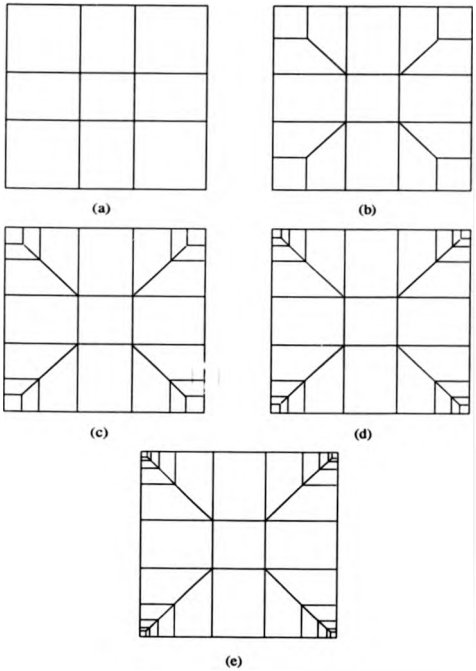

Fig. 5.9 Different meshes of a square panel (projections)

Table 5.3 Flexibility coefficients calculated using meshes in Fig. 5.9

Mesh	a	b	c	d	e
$\bar{f}_{11}$	0.2164	0.2658	0.3170	0.3685	0.4200
$\bar{f}_{21}$	-0.0317	-0.0480	-0.0643	-0.0806	-0.0968
$\bar{f}_{31}$	0.0050	0.0051	0.0050	0.0050	-0.0050
$\bar{f}_{55}$	2.23	2.28	2.32	2.36	2.40

The increase in magnitudes of $\bar{f}_{11}$ and $\bar{f}_{21}$ with the refinement of the mesh is considerable. Coefficient $\bar{f}_{55}$, however, is not so sensitive because it is related to the large deformation in the central area of the panel.

Here, a question is raised as to what mesh size should be chosen to yield a reliable flexibility matrix. In practice, the nodes at which the panels are joined to the structure have a finite size. They are not abstract dimensionless points as assumed in the numerical models. Therefore, over-refining an element mesh will not only cost unnecessary computational effort, but also give an unreliable result. One suitable treatment would be to adopt the real size of the panel node connector for the size of the smallest elements.

CHAPTER 6

Numerical Models of Arbitrary Quadrilateral Panels

6.1 Introduction

Two numerical models of rectangular panels have been introduced in Chapter 5. This chapter describes how these models can be extended to arbitrary quadrilateral panels, with the emphasis on, and generalization of, the five-force model. As has been explained in Chapter 5, the term "quadrilateral" panel may refer to a shallow-warped panel with four straight edges which are not in one plane.

For completeness, the five-force model is generalised further (in Section 6.2) to include any nodal forces applied to a flat quadrilateral panel, provided the panel is in equilibrium, and the bending stiffness can be ignored. This is extended to shallow-warped panels in Section 6.3. The model thus derived also applies to rectangular panels since they are a special case of quadrilateral panels. The four-force model is once again treated as a simpler case of the five-force model and is briefly discussed in Section 6.4.

6.2 Five-force model for arbitrary quadrilateral flat panels

6.2.1 Development of the model

An arbitrary quadrilateral flat panel, subjected to nodal forces resolved into components in the directions of the sides, is shown in Fig. 6.1(a). It remains true that there are five independent forces among the eight components, provided the panel is in equilibrium, since there are three equilibrium equations to be satisfied. The nodal forces can be divided into two groups, as shown in Figs. 6.1(b) and (c). For convenience they are referred to as "symmetrical" and "antisymmetrical" forces, respectively, although this is only true if the shape of the panel is symmetrical.

The state shown in Fig. 6.1(b) is a state of equilibrium, because each of the four pairs of forces is self-balanced. Hence, if the panel is in equilibrium in the case shown in Fig. 6.1(a), it should also be in equilibrium in the case given in Fig. 6.1(c). Again, because there are three equilibrium equations to be satisfied, there is only one independent force among the four forces shown in Fig. 6.1(c).

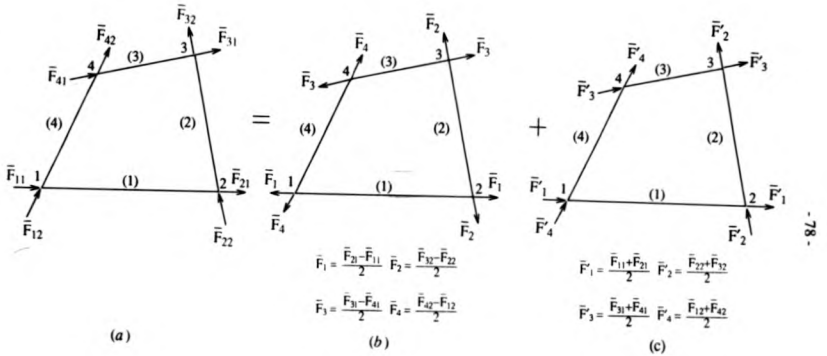

Fig. 6.1 Division of the nodel forces

(a) original (b) "symmetrical" (c) "antisymmetrical"

Consider the in-plane equilibrium equation

$$\sum M(1) = 0 \tag{6.1}$$

which means that the resultant moment about node 1 of all the forces, shown in Fig. 6.1(c), should be zero. Because the lines of action of $\bar{F}_1$ and $\bar{F}_4$ pass through node 1, it follows that the line of action of the resultant of $\bar{F}_2$ and $\bar{F}_3$ should also pass through node 1, that is to coincide with the diagonal 1-3. Repeating the same argument for all the other nodes leads to the conclusion that the resultant of any two forces acting at the same node act along the corresponding diagonal. The four resultants, $\bar{R}_1$, $\bar{R}_2$, $\bar{R}_3$ and $\bar{R}_4$ are shown in Fig. 6.2(a). They are equivalent to the forces shown in Fig. 6.1(c).

Furthermore, by using eq. (6.1) again, it is found that $\bar{R}_2 = \bar{R}_4$ in Fig. 6.2(a). Similarly, $\bar{R}_1 = \bar{R}_3$. The four resultants can therefore be denoted by $\bar{R}_1$ and $\bar{R}_2$, as shown in Fig. 6.2(b).

$\bar{R}_1$ and $\bar{R}_2$ are not independent of each other. It can be seen from Fig. 6.2(b) and Fig. 6.1(c) that their components in the direction of any particular side of the panel should be equal. Hence, from Fig. 6.2(b):

$$\bar{r}_{11} = \bar{r}_{21}, \quad \bar{r}_{12} = \bar{r}_{22}, \quad \bar{r}_{13} = \bar{r}_{23}, \quad \bar{r}_{14} = \bar{r}_{24}. \tag{6.2}$$

Referring to Fig. 6.2(b) and using the sine rule in triangles 1-j-k and 2-l-m, it is found that

$$\bar{r}_{11} = \frac{\bar{R}_1 \sin\alpha_1}{\sin(\alpha_1+\beta_1)}, \qquad \bar{r}_{21} = \frac{\bar{R}_2 \sin\alpha_2}{\sin(\alpha_2+\beta_2)}. \tag{6.3}$$

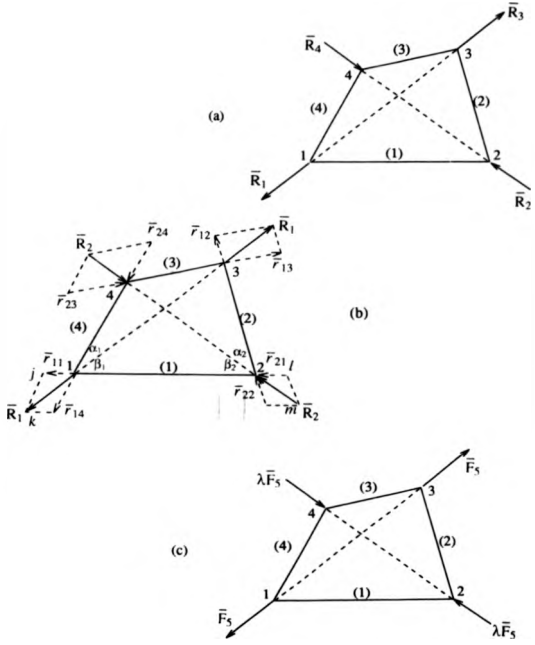

Fig. 6.2 The fifth force ($\bar{F}_5$)

Equating the right sides of the two equations in (6.3) leads to

$$\bar{R}_2 = \frac{sin\alpha_1 sin(\alpha_2+\beta_2)}{sin\alpha_2 sin(\alpha_1+\beta_1)} \bar{R}_1 \tag{6.4}$$

or

$$\bar{R}_2 = \lambda \bar{R}_1 \tag{6.5}$$

where

$$\lambda = \frac{sin\alpha_1 sin(\alpha_2+\beta_2)}{sin\alpha_2 sin(\alpha_1+\beta_1)} \tag{6.6}$$

which is a factor depending on the geometry of the panel only.

The factor λ can be expressed by the following, more general formula:

$$\lambda = \frac{d_2 sin(\alpha_2+\beta_2) sin(\alpha_4+\beta_4)}{d_1 sin(\alpha_1+\beta_1) sin(\alpha_3+\beta_3)} \tag{6.7}$$

the derivation of which is given in Appendix B. For a trapezium, λ simply equals the ratio between the lengths of the two diagonals; for isosceles trapezia, of which rectangles are a special case, $\lambda = 1$. For a quadrilateral without parallel sides, the calculation of λ can also be simplified. Values of λ for various quadrilaterals are given in Table 6.1 and are discussed in Appendix B. A short program is written for the calculation of λ and is listed in Appendix C.

Table 6.1 Values of λ of quadrilaterals

Shape	λ
Arbitrary quadrilaterals 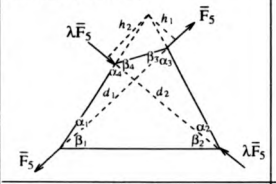	$\frac{d_2\sin(\alpha_2+\beta_2)\sin(\alpha_4+\beta_4)}{d_1\sin(\alpha_1+\beta_1)\sin(\alpha_3+\beta_3)}$ (general) $\frac{h_1}{h_2}$ (not parallelogram)
Trapezia 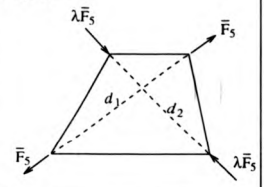	$\frac{d_2}{d_1}$
Isosceles trapezia (including rectangles)	1

The four forces in Fig. 6.2(a) (or Fig. 6.1(c)) can therefore be represented by only one force parameter, F_5, as shown in Fig. 6.2(c). And, to sum up, the eight forces shown in Fig. 6.1(a) can be represented by five generalised forces in Fig. 6.3, where a bar '-' over a force parameter emphasises that it is observed from local coordinates.

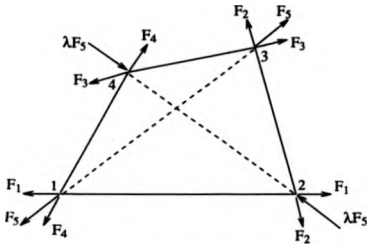

Fig. 6.3 Five-force model

6.2.2 Flexibility matrix

The displacement $\bar{\Delta}_k$ (k = 1, 2, 3, 4), corresponding to $\bar{F}_k$, is simply the extension of side k; while the displacement corresponding to $\bar{F}_5$ is

$$\bar{\Delta}_5 = \Delta_{13} - \lambda\, \Delta_{24}$$

where Δ_{13} and Δ_{24} are the extensions of the diagonals 1-3 and 2-4, respectively. The relationship between the forces and the displacements can still be given by eq. (5.4) with the flexibility matrix expressed by eq. (5.5). For an unsymmetrical panel, the reciprocities between flexibility coefficients in eqs. (5.6) and (5.7) (due to geometric symmetry), are no longer tenable, although the flexibility matrix is

always symmetrical.

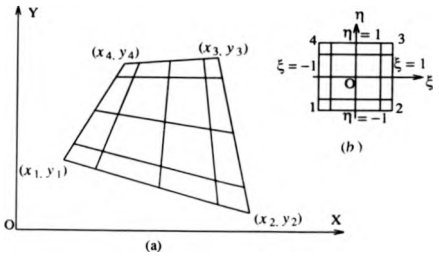

Fig. 6.4 Mesh of elements of a flat panel in
(a) global Cartesian coordinates;
(b) local natural coordinates.

When the finite element method is used to calculate flexibility coefficients of arbitrary quadrilateral panels, a mesh of quadrilateral isoparametric elements, as is shown in Fig. 6.4(a), is suggested. The coordinates of corner nodes of the elements (x, y) can be obtained from their local natural coordinates [60,62] (ξ,η), by using the following formulae:

$$x = \sum_{j=1}^{4} N_j x_j, \quad y = \sum_{j=1}^{4} N_j y_j \tag{6.8}$$

where

$$N_j = N_j(\xi,\eta) = \frac{1}{4}(1 + \xi\xi_j)(1 + \eta\eta_j) \tag{6.9}$$

and (x_j, y_j) and (ξ_j, η_j) (j = 1, 2, 3, 4) are the global coordinates and local natural coordinates of node j of the panel, respectively. The 'parent' mesh in local natural coordinates is shown in Fig. 6.4(b).

The following Examples 6.1 and 6.2 in the next section, illustrate the calculations of flexibility matrices of a flat and a shallow-warped arbitrary quadrilateral panel, respectively. The nodal displacements of the panels are calculated using PAFEC package, in global coordinates, and then transformed into the flexibility coefficients, i.e. the generalised displacements using a purpose written program.

Example 6.1

Fig. 6.5 shows a flat arbitrary quadrilateral panel with the material properties as follows: Young's modulus $E = 0.62 \times 10^8\ k\ N/m^2$, Poisson ratio $\nu = 0.33$, and the thickness $t = 0.9 \times 10^{-3} m$.

The 'parent' mesh, from which the mesh shown in Fig. 6.5 is produced, is the same as in Fig. 5.4(a), but in local natural coordinates. The mesh in Fig. 6.5 is composed of the second-order quadrilateral isoparametric plate elements, each having eight nodes. The panel is supported to prevent rigid body movement.

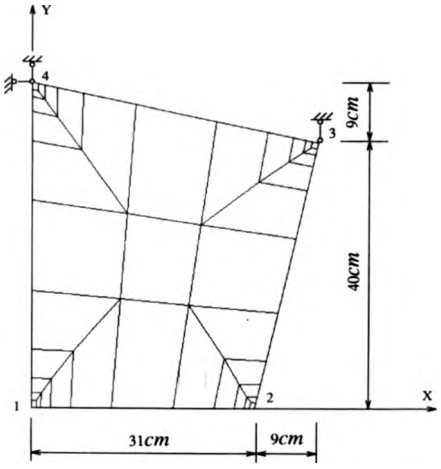

Fig. 6.5 The flat panel in Example 6.1 and
the finite element mesh

To calculate the coefficients in the k-th column (k = 1, 2, 3, 4, 5) of the flexibility matrix, a unit force $\bar{F}_k = 1$ is applied. In this example $\lambda = 0.9756$, calculated using the program in Appendix C. The output of nodal

displacements from PAFEC is listed in Table 6.2 where u_j and v_j (j = 1, 2, 3, 4) are the nodal displacements in x direction and y direction, respectively.

Table 6.2 Nodal displacements of the panel in Example 6.1 (Fig. 6.5) (Unit : mm)

Forces	u_1	v_1	u_2	v_2	u_3	v_3	u_4	v_4
$\bar{F}_1 = 1$	-0.187	0.112	0.153	0.070	-0.001	0	0	0
$\bar{F}_2 = 1$	-0.278	0.013	-0.381	-0.316	-0.117	0	0	0
$\bar{F}_3 = 1$	0.300	0.125	0.299	0.147	0.432	0	0	0
$\bar{F}_4 = 1$	0.236	-0.441	0.124	-0.043	-0.129	0	0	0
$\bar{F}_5 = 1$	-0.337	0.046	-0.306	0.018	-0.031	0	0	0

For arbitrary quadrilateral panels, it is convenient to use a purpose written program to calculate flexibility coefficients from the nodal displacements caused by unit forces. Such a program is listed in Appendix D. The calculated flexibility matrix of the panel in this example is:

$$[\bar{f}] = \begin{bmatrix} 0.340 & -0.103 & -0.001 & -0.112 & 0.030 \\ -0.103 & 0.366 & -0.114 & -0.013 & 0.043 \\ -0.001 & -0.114 & 0.421 & -0.126 & -0.030 \\ -0.112 & -0.013 & -0.126 & 0.441 & -0.046 \\ 0.030 & 0.043 & -0.030 & -0.046 & 0.358 \end{bmatrix} \qquad (6.10)$$

6.3 Five-force model for shallow-warped arbitrary quadrilateral panels

For a shallow-warped arbitrary quadrilateral panel in equilibrium, a plane close to it can be chosen so that the out-of-plane forces applied to the panel can be considered as perpendicular to this plane. The panel with the applied forces acting along its sides is projected on the plane (Fig. 6.6). As explained in Section 6.2, the projected forces can be expressed in terms of five groups of self-balancing forces, each represented by one parameter. The factor λ' is determined by the geometry of the projected panel and can be calculated using suitable formulae from Table 6.1.

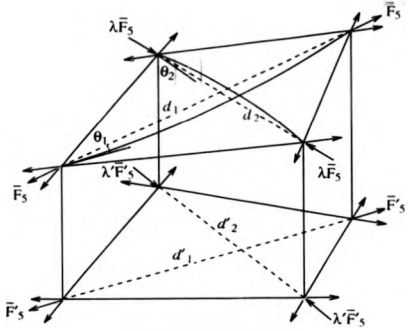

Fig. 6.6 Warped panel projected to a plane

Projected back to the original panel, the five-force model for the warped panel is thus established, its nodal force vector being

$$\{ \bar{F} \} = [\bar{F}_1 \; \bar{F}_2 \; \bar{F}_3 \; \bar{F}_4 \; \bar{F}_5]^T$$

and the formula for λ can be derived as shown below.

It can be seen from Fig. 6.6 that

$$\bar{F}'_5 = \bar{F}_5 \cos\theta_1 \tag{6.11}$$

and

$$\lambda'\bar{F}'_5 = (\lambda\bar{F}_5) \cos\theta_2 \tag{6.12}$$

where θ_1 and θ_2 are the inclinations of the diagonals 1-3 and 2-4 to the projection plane, respectively. Dividing both sides of eq. (6.12) by those of eq. (6.11), respectively, gives

$$\lambda' = \lambda \frac{\cos\theta_2}{\cos\theta_1}$$

or

$$\lambda = \lambda' \frac{\cos\theta_1}{\cos\theta_2} \tag{6.13}$$

Applying eq. (6.7) gives

$$\lambda' = \frac{d'_2 \sin(\alpha_2+\beta_2)\sin(\alpha_4+\beta_4)}{d'_1 \sin(\alpha_1+\beta_1)\sin(\alpha_3+\beta_3)} \tag{6.14}$$

where d'_1 and d'_2 are the lengths of two projected diagonals and all the angles are measured from the projection of the panel. Substitution of eq. (6.14) into eq.

(6.13) gives

$$\lambda' = \frac{d'_2 cos\theta_1 sin(\alpha_2+\beta_2) sin(\alpha_4+\beta_4)}{d'_1 cos\theta_2 sin(\alpha_1+\beta_1) sin(\alpha_3+\beta_3)}$$

but

$$\frac{d'_1}{cos\theta_1} = d_1, \quad \frac{d'_2}{cos\theta_2} = d_2,$$

therefore

$$\lambda = \frac{d_2 sin(\alpha_2+\beta_2) sin(\alpha_4+\beta_4)}{d_1 sin(\alpha_1+\beta_1) sin(\alpha_3+\beta_3)} \tag{6.15}$$

where d_1 and d_2 are the lengths of diagonals which do not meet in space, because the panel is warped.

A finite element mesh used to calculate flexibility coefficients of a warped panel is three dimensional. It can be, however, defined by a two dimensional mesh in local natural coordinate system by using the following formulae:

$$x = \sum_{j=1}^{4} N_j x_j, \quad y = \sum_{j=1}^{4} N_j y_j, \quad z = \sum_{j=1}^{4} N_j z_j, \tag{6.16}$$

where

$$N_j = N_j(\xi,\eta) = \frac{1}{4} (1 + \xi\xi_j) (1 + \eta\eta_j) \tag{6.17}$$

and (x_j, y_j, z_j) and (ξ_j, η_j) (j = 1, 2, 3, 4) are global Cartesian coordinates and local natural coordinates of node j of the panel, respectively. Fig. 6.7 shows the 'parent' mesh in local natural coordinates and the produced mesh in global Cartesian coordinates. In the case of warped rectangular panels, eq. (6.16) defines a hyperbolic paraboloid.

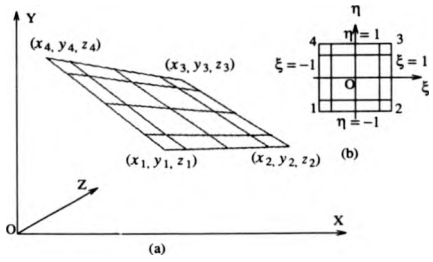

Fig. 6.7 Mesh of elements of a warped panel in

(a) global Cartesian coordinates;

(b) local natural coordinates.

Example 6.2

Fig. 6.8 shows a warped panel with the material properties as follows: Young's modulus E = 0.62 $\times 10^8\ kN/m^2$, Poisson ratio v = 0.33, and the thickness t = $0.9 \times 10^{-3} m$.

The 'parent' mesh from which the mesh shown in Fig. 6.8 is produced is the same as in Fig. 5.4, but in local natural coordinates. The mesh in Fig. 6.8 is

composed of the second-order quadrilateral isoparametric shell elements, each having eight nodes. The panel is supported to prevent rigid body movements, so that

$$w_1 = v_3 = w_3 = u_4 = v_4 = w_4 = 0. \tag{6.18}$$

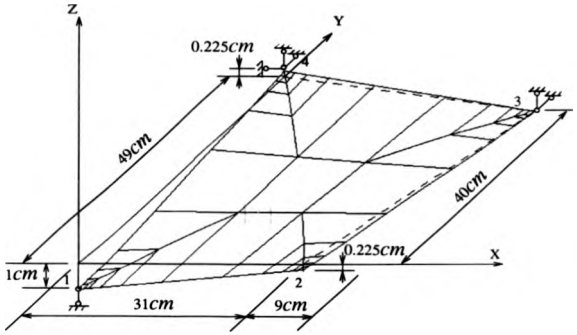

Fig. 6.8 The warped panel in Example 6.2 and the finite element mesh

To calculate the coefficients in the k-th column (k = 1, 2, 3, 4, 5) of the flexibility matrix a unit force $\bar{F}_k = 1$ is applied. In this example $\lambda = 0.9755$, calculated using the program in Appendix C. The output of nodal displacements from PAFEC is listed in Table 6.3 where u_i, v_i and w_i (i = 1, 2, 3, 4) are the nodal displacements in x direction, y direction and z direction, respectively. The nodal displacements which are zero in eq. (6.18) are not shown in the Table.

Table 6.3 Nodal displacements of the panel in Example 6.2 (Fig. 6.8) (Unit : *mm*)

Forces	u_1	v_1	u_2	v_2	w_2	u_3
$\bar{F}_1 = 1$	-0.035	0.092	0.066	0.009	10.765	0.002
$\bar{F}_2 = 1$	-0.059	-0.010	-0.532	-0.416	15.647	-0.097
$\bar{F}_3 = 1$	0.463	0.105	0.196	0.096	10.774	0.460
$\bar{F}_4 = 1$	0.472	-0.488	-0.014	-0.120	15.755	-0.107
$\bar{F}_5 = 1$	-2.554	0.037	-2.445	0.533	-3.686	-0.018

The purpose written program (Appendix D) converts the nodal displacements into the flexibility matrix as in:

$$[\bar{f}] = \begin{bmatrix} 0.370 & -0.082 & 0.002 & -0.092 & 0.016 \\ -0.082 & 0.416 & -0.094 & 0.010 & 0.033 \\ 0.002 & -0.094 & 0.449 & -0.105 & -0.018 \\ -0.092 & 0.010 & -0.105 & 0.488 & -0.037 \\ 0.017 & 0.033 & -0.018 & -0.037 & 3.505 \end{bmatrix} \quad (6.19)$$

Comparing the two flexibility matrices in eq. (6.19) and eq. (6.10), it can be seen that the conclusions concerning the influence of curvature on flexibility of rectangular panels, drawn in Section 5.4, are principally true for all quadrilateral panels.

6.4 Four-force model

As discussed in Section 5.3, the four-force model is produced from the five-force model by simply ignoring the presence of fifth force. Hence the flexibility matrix is 4 × 4, which, if adopted for the panel in Example 6.2, would be as follows:

$$[\bar{f}] = \begin{bmatrix} 0.370 & -0.082 & 0.002 & -0.092 \\ -0.082 & 0.416 & -0.094 & 0.010 \\ 0.002 & -0.094 & 0.449 & -0.105 \\ -0.092 & 0.010 & -0.105 & 0.488 \end{bmatrix} \quad (6.20)$$

It has been pointed out in Section 5.3 that employing the four-force model would reduce the stiffness of the panel and the whole structure. On the other hand, it has been argued that the four-force model can give satisfactory results if the angular distortion of the panels is not significant, and that the fifth force becomes less important when the panel is warped, because the stiffness associated with the fifth force is reduced due to curvature. These arguments remain true for arbitrary quadrilateral panels as is demonstrated futher in Chapter 9, where numerical examples are given.

CHAPTER 7

Solution of Governing Equations

7.1 Introduction

In Chapter 4 the governing equations of clad cable structures under static loadings have been established as:

$$\sum_{m=1}^{M} \frac{\partial U_m}{\partial \Delta_{ji}} - P_{ji} + \sum_{e=1}^{M_c} \frac{\partial \{\bar{\Delta}\}^{(e)T}}{\partial \Delta_{ji}} \{\bar{F}\}^{(e)} = 0$$

$$(j = 1, 2, ..., N;\ i = 1, 2, 3) \qquad (7.1)$$

and

$$\{\bar{F}\}^{(e)} = [\bar{K}]^{(e)} \{\bar{\Delta}\}^{(e)} \qquad (e = 1, 2, ..., M_c) \qquad (7.2)$$

which are the same as eqs. (4.5) and (4.8) in Chapter 4, respectively.

In this Chapter the solution of the governing equations is discussed using the dynamic relaxation method, which in itself introduces an additional equation of dynamic equilibrium and hence allowing the unknown displacements of sub-region 1 and unknown forces of sub-region 2 to be found.

7.2 Discussion of equilibrium equations

Eqs. (7.1) and (7.2) are the equilibrium equations and the compatibility equations, respectively, governing the static response of the structure. The physical meaning of eq. (7.2) is very clear while that of eq. (7.1) is not, because there are two terms of partial derivative involved in which the relationship between the original functions and the primary variables is not explicit. This section is aimed to give physical interpretation of eq. (7.1).

7.2.1 Contribution of cable links to equilibrium

The first term on the right-hand side of eq. (7.1), $\sum_{m=1}^{M} \frac{\partial U_e}{\partial \Delta_{ji}}$, represents the contribution of the cable links to equilibrium. It has been proved [5,30] that

$$\sum_{m=1}^{M} \frac{\partial U_m}{\partial \Delta_{ji}} = -\sum_{1}^{N_k} t_{jk} \left[\left(x_{ki} - x_{ji} \right) + \left(\Delta_{ki} - \Delta_{ji} \right) \right] \tag{7.3}$$

where

$$t_{jk} = \frac{F_{jk}}{L_{jk} + \delta L_{jk}}, \tag{7.4}$$

known as the tension coefficient of cable link $j-k$, in which

$$F_{jk} = F_{jk}^{0} + \frac{(EA)_{jk}}{L_{jk}^{0}} \delta L_{jk}. \tag{7.5}$$

The notation in eqs. (7.3), (7.4) and (7.5) is explained with help of Fig. 7.1 as follows:

N_{jc} = the total number of cable links which meet at node j ;

x_{ki} , x_{ji} = Cartesian coordinates of nodes k , j, in the i −th direction (i = 1, 2, 3);

Δ_{ki} , Δ_{ji} = the displacements of nodes k , j, in the i −th direction ;

F_{jk} = the internal force in cable link j−k ;

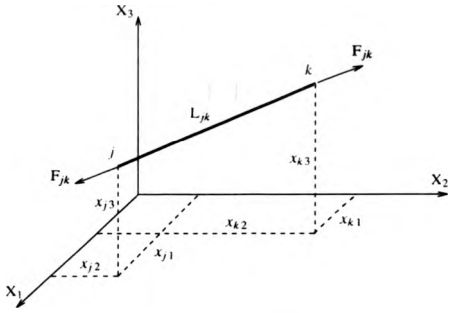

Fig. 7.1 Current state of cable member j−k

F_{jk}^{0} = the initial (prestress) force in cable link $j-k$;

L_{jk}^{0} = the initial (prestressed) length of cable link $j-k$;

δL_{jk} = the increase in current length L_{jk} ;

E, A = Young's modulus and cross–section area .

Eq. (7.3) can be rewritten as follows:

$$\sum_{m=1}^{M} \frac{\partial U_e}{\partial \Delta_{ji}} = -\sum_{1}^{N_k} F_{jk} \cos(jk, X_i) \tag{7.6}$$

where $\cos(jk, X_i)$ is the cosine of the angle between cable link $j-k$ and X_i axis and therefore $F_{jk} \cos(jk, X_i)$ represents the force component of member $j-k$ in X_i direction.

The second term of eq. (7.1), P_{ji}, represents the component of the external force vector at node j in the i-th direction. The final term, $\sum_{e=1}^{M_e} \frac{\partial [\bar{\Delta}]^{(e)T}}{\partial \Delta_{ji}} \{\bar{F}\}^{(e)}$, represents the contribution of cladding panel to equilibrium, as discussed below.

7.2.2 Contribution of panels to equilibrium

A quadrilateral panel e is shown in Fig. 7.2. The equilibrium at node j is now considered. In the case of the five-force model, the displacement vector of the

panel, $\{\bar{\Delta}\}^{(e)}$, has five components as defined in Chapter 6:

$$\bar{\Delta}_1^{(e)} = \delta L_{jk}, \quad \bar{\Delta}_2^{(e)} = \delta L_{kl}, \quad \bar{\Delta}_3^{(e)} = \delta L_{mi}, \quad \bar{\Delta}_4^{(e)} = \delta L_{jm},$$

$$\bar{\Delta}_5^{(e)} = \delta L_{jl} - \lambda^{(e)} \delta L_{km}, \tag{7.7}$$

where λ is a multiplication factor, determined by the geometry of the panel, as discussed in Chapter 6.

In order to reveal the physical meaning of $\sum_{e=1}^{M_j} \frac{\partial \{\bar{\Delta}\}^{(e)T}}{\partial \Delta_{ji}} \{\bar{F}\}^{(e)}$, an explanation for $\frac{\partial \{\bar{\Delta}\}^{(e)T}}{\partial \Delta_{ji}}$ is required. In eq. (7.7) only the displacements $\bar{\Delta}_1^{(e)}$, $\bar{\Delta}_4^{(e)}$ and $\bar{\Delta}_5^{(e)}$ are related to the nodal displacement Δ_{ji}. The expressions of these generalised displacements in terms of components of $\{\bar{\Delta}\}^{(e)}$ are:

$$\bar{\Delta}_1^{(e)} = \sqrt{\sum_{i=1}^{3} [(x_{ki} - x_{ji}) + (\Delta_{ki} - \Delta_{ji})]^2} - \sqrt{\sum_{i=1}^{3} (x_{ki} - x_{ji})^2} \tag{7.8a}$$

$$\bar{\Delta}_4^{(e)} = \sqrt{\sum_{i=1}^{3} [(x_{mj} - x_{ji}) + (\Delta_{mi} - \Delta_{ji})]^2} - \sqrt{\sum_{i=1}^{3} (x_{mi} - x_{ji})^2} \tag{7.8b}$$

$$\bar{\Delta}_5^{(e)} = \left(\sqrt{\sum_{i=1}^{3} [(x_{li} - x_{ji}) + (\Delta_{li} - \Delta_{ji})]^2} - \sqrt{\sum_{i=1}^{3} (x_{li} - x_{ji})^2} \right)$$

$$- \lambda^{(e)} \left(\sqrt{\sum_{i=1}^{3} [(x_{mi} - x_{ki}) + (\Delta_{mi} - \Delta_{ki})]^2} - \sqrt{\sum_{i=1}^{3} (x_{mi} - x_{ki})^2} \right)$$

(7.8c)

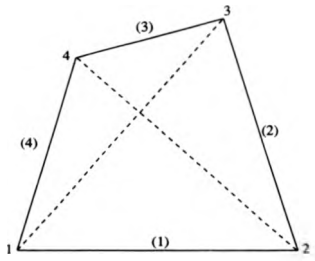

Fig. 7.2 Quadrilateral panel e

The partial derivative of $\bar{\Delta}l^{(e)}$ with respect to Δ_{ji} then is

$$\frac{\partial \bar{\Delta}l^{(e)}}{\partial \Delta_{ji}} = \frac{-[(x_{ki} - x_{ji}) + (\Delta_{ki} - \Delta_{ji})]}{\sqrt{\sum_{i=1}^{3}[(x_{ki} - x_{ji}) + (\Delta_{ki} - \Delta_{ji})]^2}}$$

which can be further developed into the direction cosine of side $j-k$ in the deformed state of the panel:

$$\frac{\partial \bar{\Delta}l^{(e)}}{\partial \Delta_{ji}} = -\cos(jk, X_i) \tag{7.9a}$$

because

$$\sqrt{\sum_{i=1}^{3}[(x_{ki} - x_{ji}) + (\Delta_{ki} - \Delta_{ji})]^2} = L_{jk} + \delta L_{jk} .$$

Similarly, the partial derivatives of $\bar{\Delta}l^{(e)}$ and $\bar{\Delta}s^{(e)}$ with respect to Δ_{ji} are

$$\frac{\partial \bar{\Delta}_j^{(e)}}{\partial \Delta_{ji}} = -\cos(jm, X_i) \tag{7.9b}$$

and

$$\frac{\partial \bar{\Delta}_j^{(e)}}{\partial \Delta_{ji}} = -\cos(jl, X_i) \tag{7.9c}$$

If the node under consideration is at an end of the other diagonal of panel e, say, node k, the corresponding partial derivative of $\bar{\Delta}_j^{(e)}$ is

$$\frac{\partial \bar{\Delta}_j^{(e)}}{\partial \Delta_{ki}} = \lambda^{(e)} \cos(km, X_i) \tag{7.9d}$$

Multiplied by the corresponding force components (Fig. 7.2) of panel e, eqs. (7.9) become

$$\bar{F}_1^{(e)} \frac{\partial \bar{\Delta}_1^{(e)}}{\partial \Delta_{ji}} = -\bar{F}_1^{(e)} \cos(jk, X_i) = -F_{jk}^{(e)} \cos(jk, X_i), \tag{7.10a}$$

$$\bar{F}_4^{(e)} \frac{\partial \bar{\Delta}_4^{(e)}}{\partial \Delta_{ji}} = -\bar{F}_4^{(e)} \cos(jm, X_i) = -F_{jm}^{(e)} \cos(jm, X_i), \tag{7.10b}$$

$$\bar{F}_5^{(e)} \frac{\partial \bar{\Delta}_5^{(e)}}{\partial \Delta_{ji}} = -\bar{F}_5^{(e)} \cos(jl, X_i) = -F_{jl}^{(e)} \cos(jl, X_i) \tag{7.10c}$$

and

$$\bar{F}_5^{(e)} \frac{\partial \bar{\Delta}_5^{(e)}}{\partial \Delta_{ki}} = \lambda^{(e)} \bar{F}_5^{(e)} \cos(km, X_i) = -F_{kn}^{(g)} \cos(km, X_i). \tag{7.10d}$$

Summation for all the panels meeting at joint j yields that

$$\sum_{e=1}^{M_j} \frac{\partial(\bar{\Delta})^{(e)T}}{\partial \Delta_{ji}} (\bar{F})^{(e)} = -\sum_{e=1}^{M_j} \sum_{k=1}^{3} F_{jk}^{(e)} \cos(jk, X_i) \qquad (7.11)$$

where M_j = the number of panels meeting at joint j;

k = number of nodes connected at node j by panel e .

Hence the final term in the right-hand side in eq. (7.1), given now by eq. (7.11), represents the summation of the projections of all panel forces, of which the lines of action pass through node j, in the i-th direction.

7.2.3 Unification of cable links and panels in equilibrium equations

Comparison of eq. (7.11) and eq. (7.6) shows that a quadrilateral panel is equivalent to a group of six straight bar links (Fig. 7.3(b)), fictitiously added to the cable system, as their contribution to equilibrium of the structure. For this to be true, the following conditions must be satisfied:

(i) The four nodes of the bar links must have the same location as those of the panel;

(ii) The internal forces of the bar links are always equal to the corresponding forces in the five-force model, as shown in Fig. 7.3(a). Therefore, there are only five independent forces although there are six bars.

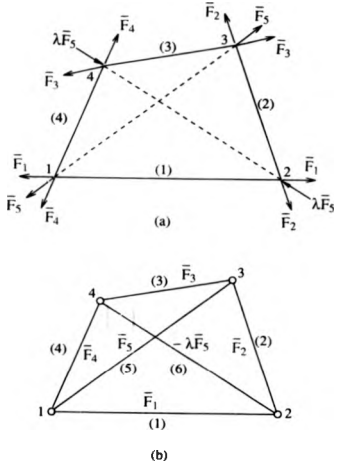

Fig. 7.3 (a) Five-force model of panel

(b) Six bar group

Hence, the relationship between the forces and the corresponding displacements of the six bar group can be described by eq. (7.2).

The six bar group can now replace the panel under consideration without introducing any changes in the mechanical properties of the structure. The structure becomes a combination of cable members and grouped bars, as illustrated in Fig.7.4, and the contribution of cable members and panels can be expressed in a unified form in the equilibrium equations, which replace eq. (7.1) as follows

$$\sum_{1}^{N_j} F_{jk} \cos(jk, X_i) + P_{ji} = 0 \qquad (7.12)$$

where the summation is extended to both the cable links and bar links. It should be noted that in order to obtain the forces in the bar links a panel has to be solved according to eq. (7.2).

A panel is now defined by the six bars. For example, panel 2 in Fig.7.4(a) is defined in Fig.7.4(b) as "0 0 3 1 7 8", where the first four numbers give its four sides, "0" indicating the boundary line of the structure, and the last two numbers define the two diagonal bars.

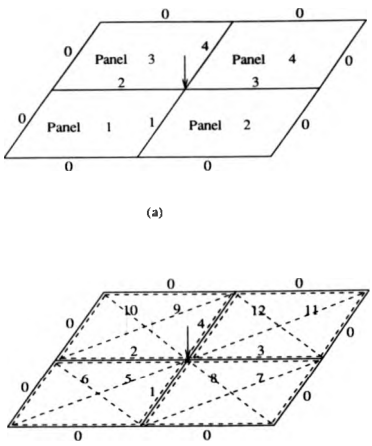

Fig. 7.4 Concept of clad cable structure with panels being replaced by six bar groups (a) original structure (b) replacement

7.3 Solution of governing equations

Through the work in the previous section, the governing equilibrium equations of a clad cable structure have been changed into the form of eq. (7.12) which in essence does not differ from those of an unclad cable structure. Any numerical approach suitable for the analysis of unclad structures can be easily adopted to solve these equations. In the present section the solution of the governing equations by the dynamic relaxation method is introduced.

7.3.1 Dynamic relaxation with viscous damping

The dynamic relaxation method deals with a problem of static equilibrium using an approach of dynamic analysis. The structure under consideration becomes a system of vibration. Due to the damping action, the structure reaches its static equilibrium as the consequence of a dynamic process, in which the behaviour of individual nodes, denoted by j, is considered.

If the structure is not in equilibrium, the left hand side of eq. (7.12) is not zero but equal to a residual force R_{ji}, representing the difference between the external force and internal force vectors:

$$R_{ji} = \sum_{1}^{N_j} F_{jk} \cos(jk, X_i) + P_{ji}$$

$$(j = 1, 2, ..., N;\ i = 1, 2, 3) \qquad (7.13)$$

where N = the total number of nodes in the structure;

i = 1, 2, 3, corresponds to X, Y, Z coordinates;

N_j = the total number of links (including cable links and bar links) connected to node j.

Under the action of the residual forces, the structure vibrates about its position of equilibrium. According to the theory of vibration [51], the equations of motions are:

$$R_{ji} = m_{ji} \ddot{\Delta}_{ji} + c_{ji} \dot{\Delta}_{ji} \tag{7.14}$$

where m_{ji} = the mass, assumed be concentrated at the nodes;

c_{ji} = the viscous damping coefficient;

$\dot{\Delta}_{ji}$, $\ddot{\Delta}_{ji}$ = the velocity and acceleration, respectively .

At this stage the structure is being discretised using centred finite difference grid in both space and time. The first and second derivatives in eq. (7.14) are replaced by their centred finite difference approximations, giving the recurrence formulae [63] described below.

The residual forces at time t are given by

$$R_{ji}{}^{t} = \sum_{1}^{N_j} F_{jk}{}^{t} \cos (jk, X_i)^{t} + P_{ji} \tag{7.15}$$

where the internal forces F_{jk}^{t} are calculated from the present geometry of the structure. If link $j-k$ is a cable member then

$$F_{jk}^{t} = F_{jk}^{0} + \frac{(EA)_{jk}}{L_{jk}^{0}} \delta L_{jk}^{t} , \tag{7.16}$$

or, if the link belongs to the six bar group representing panel e then

$$\{\bar{F}\}^{(e)t} = [\bar{K}]^{(e)} \{\bar{\Delta}\}^{(e)t} , \tag{7.17}$$

and the current direction cosines of link $j-k$ is

$$cos\ (jk, X_i)^{t} = \frac{(X_{ki} - X_{ji}) + (\Delta_{ki} - \Delta_{ji})^{t}}{L_{jk}^{t}} \tag{7.18}$$

The velocity component of node j in X_i direction at time ($t+\delta t/2$) is calculated from the current residual force and its previous value, δt being a time increment:

$$\dot{\Delta}_{ji}^{t+\delta t/2} = \dot{\Delta}_{ji}^{t-\delta t/2} \frac{\frac{m_{ji}}{\delta t} - \frac{c_{ji}}{2}}{\frac{m_{ji}}{\delta t} + \frac{c_{ji}}{2}} + R_{ji}^{t} \frac{1}{\frac{m_{ji}}{\delta t} + \frac{c_{ji}}{2}} \tag{7.19}$$

The new geometry of the structure at time ($t+\delta t$) is then:

$$\Delta_{ji}^{t+\delta t} = \Delta_{ji}^{t} + \dot{\Delta}_{ji}^{t+\delta t/2} \delta t \tag{7.20}$$

The iterative process starts from $t = 0$ and the initial displacements and velocities are assumed to be zero. The first iteration requires a value of $\dot{\Delta}_{ji}^{-\delta t/2}$. Using the concept of linear difference and substituting $\dot{\Delta}_{ji}^{-\delta t/2} = -\dot{\Delta}_{ji}^{\delta t/2}$ into eq. (7.19) gives

$$\dot{\Delta}_{ji}^{\delta t/2} = R_{ji}^{0} \frac{\delta t}{2m_{ji}} \tag{7.19a}$$

Repetitive use of eqs. (7.15) - (7.20) allows the unknown displacements Δ_{ji} to be calculated from eq. (7.20) and the forces from eqs. (7.16) and (7.17). In the above equations the time increment δt can be chosen arbitrarily, but the mass m_{ji} must be based on the stability criterion to ensure the convergence of the calculation [49]. Viscous damping coefficients can be calculated from undamped vibration, to give faster convergence. The consideration of choice of these parameters is discussed in Chapters 8 and 9.

7.3.2 Dynamic relaxation with kinetic damping

Kinetic damping, suggested by Cundall in 1967 [48], is considered to be more effective than viscous damping for dynamic relaxation [50]. In the procedure of dynamic relaxation with kinetic damping, the structure is actually in a state of free vibration without damping, except for those moments when a peak value of the kinetic energy of the system is found. At each such moment, the vibration is forced to stop, namely, all velocity components are set to zero, and then the vibration is restarted from the current geometry of the structure. After each stop the total mechanical energy of the system, i.e. the sum of kinetic energy and potential energy, is being reduced, and step by step, the system reaches its equilibrium state. Because there is no viscous damping, eq. (7.19) takes the following simplified form:

$$\dot{\Delta}_{ji}^{t+\delta t/2} = \dot{\Delta}_{ji}^{t-\delta t/2} + R_{ji}^{t} \frac{\delta t}{m_{ji}} \tag{7.21}$$

At $t = t^*$ when a peak in kinetic energy is detected the vibration is stopped, and then restarted from a zero velocity state, letting $\dot{\Delta}_{ji}^{t+\delta t/2} = -\dot{\Delta}_{ji}^{t-\delta t/2}$ in eq. (7.21) gives

$$\dot{\Delta}_{ji}^{t^*+\delta t/2} = R_{ji}^{t^*} \frac{\delta t}{2m_{ji}} \tag{7.21a}$$

Hence, the recurrent formulae of the procedure with kinetic damping include eqs. (7.15) - (7.18), (7.21), (7.21a) and (7.20). In addition, for every iteration the kinetic energy of the system, denoted by K, is calculated and compared with that of the previous iteration:

$$K^{t+\delta t/2} = \frac{1}{2} \sum_{j=1}^{N} \sum_{i=1}^{3} m_{ji} (\dot{\Delta}_{ji}^{t+\delta t/2})^2 \tag{7.22a}$$

$$K^{t-\delta t/2} = \frac{1}{2} \sum_{j=1}^{N} \sum_{i=1}^{3} m_{ji} (\dot{\Delta}_{ji}^{t-\delta t/2})^2 \tag{7.22b}$$

If $K^{t+\delta t/2}$ is found less than $K^{t-\delta t/2}$, a peak value of K must have been reached between $t-\delta t/2$ and $t+\delta t/2$. This peak value can be assumed to take place approximately at the mid-point of the time interval, i.e. $t^* = t$ (Fig.7.5); More precise position of this point can be found by regarding the K–t curve, shown in Fig. 7.5, as a parabola, and consequently using the following formula:

$$t^* = t - \alpha\, \delta t \tag{7.23}$$

where

$$\alpha = \frac{K^{t+\delta t/2} - K^{t-\delta t/2}}{K^{t-3\delta t/2} - 2K^{t-\delta t/2} + K^{t+\delta t/2}} \tag{7.24}$$

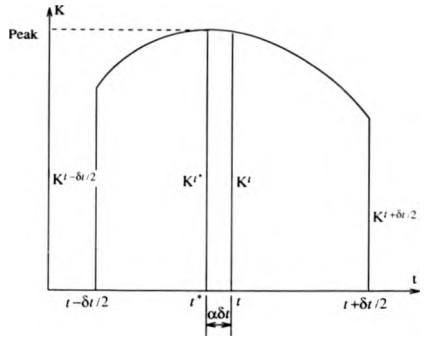

Fig. 7.5 K–t curve

The displacements at t^*, from which the vibration restarts, are then given by

$$\Delta_{ji}^{t^*} = \Delta_{ji}^{t} - \dot{\Delta}_{ji}^{t-\delta t/2}\,\alpha\delta t \tag{7.25}$$

Substituting for Δ_{ji}^{t} and $\dot{\Delta}_{ji}^{t-\delta t/2}$ from eqs. (7.20) and (7.21) gives

$$\Delta_{ji}^{t^*} = (\Delta_{ji}^{t+\delta t} - \dot{\Delta}_{ji}^{t+\delta t/2}\,\delta t) - (\dot{\Delta}_{ji}^{t+\delta t/2} - R_{ji}^{t}\,\frac{\delta t}{m_{ji}})\,\alpha\delta t$$

$$= \Delta_{ji}^{t+\delta t} - \dot{\Delta}_{ji}^{t+\delta t/2}\,(1-\alpha)\,\delta t + R_{ji}^{t}\,\frac{\alpha\,(\delta t)^2}{m_{ji}} \tag{7.26}$$

CHAPTER 8

Dynamic Relaxation Parameters and Computer Programming

8.1 Introduction

In this chapter, four programs for the static analysis of cable structures are introduced. They are:

SACSV1 – Dynamic relaxation procedure with viscous damping;

SACSK1, SACSK2 and SACSK3 – Dynamic relaxation procedures with kinetic damping.

These programs are based on the recurrent formulae discussed in the previous chapter. In addition, some optimisation of the dynamic relaxation parameters has been carried out to improve the rate of convergence of the method, as discussed in Section 8.2. The complete programs are listed in Appendix E. The effects of using these programs on speed of convergence are shown in Chapter 9, where numerical examples are given.

8.2 Optimisation of dynamic relaxation parameters

There are three kinds of parameters in the dynamic relaxation procedure with viscous damping which influence the stability of the solution and the speed of convergence: the masses m_{ji}, which can have fictitious values (the method only simulates a dynamic process); the time increment δt, and the damping coefficients c_{ji}. If viscous damping is used, the values of damping coefficients have to be found from undamped oscillation of the structure [63] which is somewhat tedious; and the method which uses kinetic damping, described briefly in Section 7.3.2, offers a better solution. In this section optimisation of certain dynamic relaxation parameters, which control the size of the iterative step and hence the speed of convergence, is performed for both kinetic and viscous damping procedures.

8.2.1 Kinetic damping

A stability condition to ensure the convergence of dynamic relaxation has been suggested as follows [64]:

$$m_{ji} > \frac{1}{2} \delta t^2 s_{ji} \tag{8.1a}$$

or

$$\delta t < \sqrt{2 \frac{m_{ji}}{s_{ji}}} \tag{8.1b}$$

where s_{ji} is the stiffness component of the structure at node j in X_i direction.

Hence, to ensure numerical stability, one may proceed in two ways:

(i) Arbitrarily choosing δt first, and then calculating m_{ji} from condition (8.1a); or

(ii) Arbitrarily choosing m_{ji} and then determining δt which satisfies condition (8.1b) for all nodes of the structure.

In the second case, if the masses m_{ji} are not proportional to the stiffness components s_{ji}, the value of $\sqrt{2\frac{m_{ji}}{s_{ji}}}$ on the right hand side of (8.1b) would differ about j and i and its minimum would be the critical time increment. A small δt is safe to ensure convergence, but it also results in slow convergence. Hence constant ratio of mass to stiffness throughout the structure is recommended.

In eq. (8.1b), 2 is a somewhat arbitrary constant [50] which, for some problems, gives a very conservative value for δt and hence, to speed up the convergence, another constant, say, BI, can be introduced.

Let

$$\delta t = \sqrt{\mathrm{BI}\,\frac{m_{ji}}{s_{ji}}} \tag{8.2}$$

In the case of kinetic damping, starting with $\dot{\Delta}_{ji}^{0} = 0$ and $\Delta_{ji}^{0} = 0$ and using eqs.

(7.21a), (7.21) and (7.20) successively, gives

$$\dot{\Delta}_{ji}^{(2k+1)\delta t/2} = R_{ji}^{0} \frac{\delta t}{2m_{ji}} + R_{ji}^{\delta t} \frac{\delta t}{m_{ji}} + R_{ji}^{2\delta t} \frac{\delta t}{m_{ji}} + \cdots + R_{ji}^{k\delta t} \frac{\delta t}{m_{ji}}$$

$$= \frac{\frac{1}{2} R_{ji}^{0} + \sum_{i=1}^{k} R_{ji}^{i\delta t}}{m_{ji}} \delta t$$

$$(k = 0, 1, ..., n ; n = t / \delta t) \qquad (8.3)$$

and

$$\Delta_{ji}^{t+\delta t} = \dot{\Delta}_{ji}^{\delta t/2} \delta t + \dot{\Delta}_{ji}^{3\delta t/2} \delta t + \dot{\Delta}_{ji}^{5\delta t/2} \delta t + \cdots + \dot{\Delta}_{ji}^{(2n+1)\delta t/2} \delta t$$

$$= \frac{\sum_{k=0}^{n} (\frac{1}{2} R_{ji}^{0} + \sum_{i=1}^{k} R_{ji}^{i\delta t})}{m_{ji}} \delta t^2 \qquad (8.4)$$

Substitution of eq. (8.2) into eq. (8.4) gives

$$\Delta_{ji}^{t+\delta t} = \frac{\sum_{k=0}^{n} (\frac{1}{2} R_{ji}^{0} + \sum_{i=1}^{k} R_{ji}^{i\delta t})}{m_{ji}} BI \frac{m_{ji}}{s_{ji}}$$

$$= BI \frac{\sum_{k=0}^{n} (\frac{1}{2} R_{ji}^{0} + \sum_{i=1}^{k} R_{ji}^{i\delta t})}{s_{ji}} \qquad (8.5)$$

It can be seen from eq. (8.5) that the calculated displacements are independent of δt, provided eq. (8.2) is true. Given δt, the ratio of m_{ji} to s_{ji} can be determined:

$$\frac{m_{ji}}{s_{ji}} = \frac{\delta t^2}{BI} \qquad (8.6)$$

For convenience $\delta t = 1$ can be taken and eq. (8.6) thus becomes

$$\frac{m_{ji}}{s_{ji}} = \frac{1}{BI} \qquad (8.7)$$

BI is now the only parameter that needs to be considered to optimise the procedure of dynamic relaxation with kinetic damping. It affects the stability of iterations and the convergence rate, because the ratio between masses and stiffness of a system determines the basic period of vibration, and, given a certain time increment, it determines how many time intervals a basic period is divided into. It is easy to get a conceptual understanding of this, through examination of a system with one degree of freedom. Fig. 8.1 shows the displacement-time curve of free vibration of such system. The period is

$$T = 2\pi \sqrt{\frac{m}{s}} \tag{8.8}$$

where the subscripts of m and s disappear, because there is only one degree of freedom. Comparing eqs. (8.2) and (8.8) gives

$$\frac{T}{\delta t} = \frac{2\pi}{\sqrt{BI}} \tag{8.9}$$

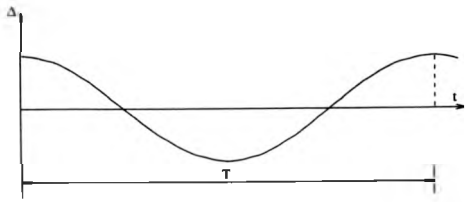

Fig. 8.1 Displacement-time curve of free vibration of a system with one degree of freedom

Substituting $\delta t = 1$ and (from eq. (8.7)) $m_{ji} = \frac{s_{ji}}{BI}$ into the recurrent formulae for dynamic relaxation with kinetic damping, as derived in Chapter 7 (eqs. (7.15) to (7.21)) results in the equations (8.10) to (8.18) given below, in which superscript n replaces t, since the time increment $\delta t = 1$.

Residual force components at $t = n\ \delta t$:

$$R_{ji}^{n} = \sum_{k=1}^{N_i} F_{jk}^{n}\ cos\ (jk, X_i)^n + P_{ji} \tag{8.10}$$

where

$$F_{jk}^{n} = F_{jk}^{0} + \frac{(EA)_{jk}}{L_{jk}^{0}} \delta L_{jk}^{n}\ , \tag{8.11}$$

for a cable member $j-k$; or F_{jk}^{n} is a element of $\{\overline{F}\}^{(e)n}$, and

$$\{\overline{F}\}^{(e)n} = [\overline{K}]^{(e)} \{\overline{\Delta}\}^{(e)n}\ , \tag{8.12}$$

if the member $j-k$ belongs to the six bar group representing panel e;

and

$$cos\ (jk, X_i)^n = \frac{(x_{ki} - x_{ji}) + (\Delta_{ki} - \Delta_{ji})^n}{L_{jk}^{n}}. \tag{8.13}$$

Velocity components at $t = (n+\frac{1}{2})\ \delta t$:

$$\dot{\Delta}_{ji}^{n+1/2} = \dot{\Delta}_{ji}^{n-1/2} + R_{ji}^{n}\ \frac{BI}{s_{ji}} \tag{8.14}$$

or

$$\dot{\Delta}^{*}_{ji} = R^{*}_{ji} \frac{BI}{2 s_{ji}} \tag{8.14a}$$

if the vibration of the structure is restarted after reaching a peak value of kinetic energy.

Displacements at $t = (n+1)\,\delta t$:

$$\Delta^{n+1}_{ji} = \Delta^{n}_{ji} + \dot{\Delta}^{n+1/2}_{ji} \tag{8.15}$$

Kinetic energy at $t = (n+\frac{1}{2})\,\delta t$ and $t = (n-\frac{1}{2})\,\delta t$:

$$K^{n+1/2} = \frac{BI}{2} \sum_{j=1}^{N} \sum_{i=1}^{3} \frac{(\dot{\Delta}^{n+1/2}_{ji})^2}{s_{ji}} \tag{8.16a}$$

$$K^{n-\frac{1}{2}} = \frac{BI}{2} \sum_{j=1}^{N} \sum_{i=1}^{3} \frac{(\dot{\Delta}^{n-1/2}_{ji})^2}{s_{ji}} \tag{8.16b}$$

Displacements at $t = t^{*}$:

$$\begin{aligned} \Delta^{*}_{ji} &= \Delta^{n}_{ji} - \dot{\Delta}^{n-1/2}_{ji}\,\alpha \\ &= (\Delta^{n+1}_{ji} - \dot{\Delta}^{n+1/2}_{ji}) - (\dot{\Delta}^{n+1/2}_{ji} - \frac{BI\,R^{n}_{ji}}{s_{ji}})\,\alpha \\ &= \Delta^{n+1}_{ji} - (1-\alpha)\,\dot{\Delta}^{n+1/2}_{ji} + \frac{\alpha\,BI\,R^{n}_{ji}}{s_{ji}} \end{aligned} \tag{8.17}$$

where

$$\alpha = \frac{K^{n+1/2} - K^{n-1/2}}{K^{n-3/2} - 2K^{n-1/2} + K^{n+1/2}} \tag{8.18}$$

which is obtained from quadratic interpolation as shown previously in Section 7.3.2, Fig. 7.5.

8.2.2 Viscous damping

In the case of viscous damping, the factor BI can still be used as with kinetic damping, but another constant, CI, concerning the damping coefficient, is introduced, as shown below. Substitution of eq. (8.2) into eq. (7.19) yields

$$\dot{\Delta}_{ji}^{t+\delta t/2} = \dot{\Delta}_{ji}^{t-\delta t/2} \frac{\sqrt{\frac{m_{ji} s_{ji}}{BI}} - \frac{c_{ji}}{2}}{\sqrt{\frac{m_{ji} s_{ji}}{BI}} + \frac{c_{ji}}{2}} + R_{ji}^{t} \frac{1}{\sqrt{\frac{m_{ji} s_{ji}}{BI}} + \frac{c_{ji}}{2}} \tag{8.19}$$

Letting

$$c_{ji} = CI\, c_{cji} = CI \times 2\sqrt{m_{ji}\, s_{ji}} \tag{8.20}$$

where $c_{cji} = 2\sqrt{m_{ji}\, s_{ji}}$ is the critical damping of a system with one degree of freedom; and substituting this into eq. (8.19) gives

$$\dot{\Delta}_{ji}^{t+\delta t/2} = \dot{\Delta}_{ji}^{t-\delta t/2} \frac{\sqrt{\frac{1}{BI}} - CI}{\sqrt{\frac{1}{BI}} + CI} + R_{ji}^{t} \frac{1}{\left(\sqrt{\frac{1}{BI}} + CI\right)\sqrt{m_{ji}\, s_{ji}}}$$

Further development leads to

$$\dot{\Delta}_{ji}^{t+\delta t/2} = \dot{\Delta}_{ji}^{t-\delta t/2} \frac{1 - CI\sqrt{BI}}{1 + CI\sqrt{BI}} + \frac{R_{ji}^{t}\, BI}{(1 + CI\sqrt{BI})\, s_{ji}}\, \delta t \tag{8.21}$$

At $t = 0$ the corresponding formula is

$$\dot{\Delta}_{ji}^{\delta t/2} = \frac{R_{ji}^{0}\ BI}{2 s_{ji}\ \delta t} \qquad (8.21a)$$

Starting with $\Delta_{ji}^{0} = 0$ and $\dot{\Delta}_{ji}^{0} = 0$, eqs. (8.21a), (8.21) and (7.20) successively give $\dot{\Delta}_{ji}^{\delta t/2}$, $\dot{\Delta}_{ji}^{3\delta t/2}$, ..., $\dot{\Delta}_{ji}^{(2k+1)\delta t/2}$, each containing a factor $\frac{1}{\delta t}$; and $\Delta_{ji}^{\delta t}$, $\Delta_{ji}^{2\delta t}$, ..., $\Delta_{ji}^{(2k+1)\delta t/2}$, independent of δt. The expressions are similar to eqs. (8.4) and (8.5) but much more tedious; and hence are left out. Again, the time increment can be chosen arbitrarily, and for convenience $\delta t = 1$ is taken, giving the recurrent formulae for viscous damping procedure, summarised below.

Residual force components at $t = n\ \delta t$: given by eqs. (8.10) - (8.13) as before.

Velocity components at $t = (n + \frac{1}{2})\ \delta t$:

$$\dot{\Delta}_{ji}^{n+1/2} = \dot{\Delta}_{ji}^{n-1/2} \times \frac{1 - CI\sqrt{BI}}{1 + CI\sqrt{BI}} + \frac{R_{ji}^{n}\ BI}{(1 + CI\sqrt{BI})\ s_{ji}} \quad (n \neq 0); \qquad (8.22)$$

or, if $n = 0$:

$$\dot{\Delta}_{ji}^{1/2} = R_{ji}^{0}\ \frac{BI}{2 s_{ji}} \qquad (8.22a)$$

Displacements at $t = (n+1)\ \delta t$: given by eq. (8.15) as before.

8.3 Computer programs

Appendix E lists and describes four computer programs for static analysis of cable structures using dynamic relaxation. They can be used for static analysis of plane or space trusses as well. The programs are:

(i) SACSV1

In this program viscous damping is used. The mass components are proportional to the initial stiffness components, given by eq. (8.7), and stay constant during iterations. The viscous damping coefficients are given by eq. (8.20).

(ii) SACSK1, SACSK2 and SACSK3

In all the three programs kinetic damping is used. The difference between them lies only in the adoption of fictitious masses:

In SACSK1, the mass components at a given node are identical in all directions. Masses at different nodes are proportional to the sum of the elastic and geometric stiffnesses of all the links (except diagonal bars) meeting at a node.

In SACSK2, the mass components are proportional to nodal stiffness components, they vary not only from node to node, but also with directions, as in SACSV1.

In SACSK3, the mass components are proportional to nodal stiffness components, as in SACSK2 and SACSV1; in addition, they are recalculated each time a peak value of kinetic energy of the system is detected.

CHAPTER 9

Numerical Examples and Study of Convergence Rate

9.1 Introduction

In this chapter, numerical examples of clad cable networks as well as some unclad cable structures are calculated, using the programs introduced in the previous chapter and listed in Appendix E. The results obtained from the four-force model and the five-force model are given and they are further compared with those obtained for a bare network, to assess the stiffening effect of cladding. In one case, numerical results are compared with those from experimental measurements. The use of different programs, which can have significant effect on the rate of convergence, is discussed.

9.2 Numerical examples

Example 9.1

A flat cable net, attached to a rigid boundary and fully clad with square panels, is shown in Fig. 9.1. The data used are as follows:

Young's modulus of cables	$128.3 \times 10^6\ k\,\mathrm{N}/m^2$
Cross–section area of cables	$0.785 \times 10^{-6}\ m^2$
Pretension in cables	$0.2\ k\,\mathrm{N}$
Young's modulus of panels	$62 \times 10^6\ k\,\mathrm{N}/m^2$
Poisson ratio of panels	0.33
Thickness of panels	$0.9 \times 10^{-3}\ m$

The accuracy of computation, given by the final maximum residual force, ER, is assumed to be 0.00003 k N, or 0.15% of the external load P.

This structure is calculated using the four-force model and the five-force model, respectively. The flexibility matrices of the panels have been calculated in Example 5.1 in Section 5.2.2 and they can be easily inverted to give the stiffness matrices. The results of the vertical displacement of node 5 (there is no horizontal movement at the node because of symmetry), the force and extension of the cable members, and the forces in panel 1 (representing all the other panels as well, because of symmetry), are listed in Tables 9.1, 9.2 and 9.3, respectively. The results of the corresponding unclad net are also listed for comparison.

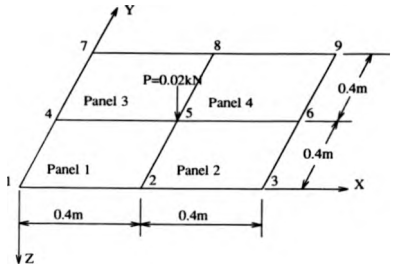

Fig. 9.1 Fully clad flat net in Example 9.1

Table 9.1 Vertical displacement of node 5 in Example 9.1 (Fig. 9.1)

Panel model	Δ_{53} (*cm*)
Five-force model	0.438
Four-force model	0.455
Unclad	0.889

Table 9.2 Force and extension of cable members in Example 9.1 (Fig. 9.1)

Panel model	Force (kN)	Extension ($\times 10^{-4}$ m)
Five-force model	0.2060	0.239
Four-force model	0.2065	0.258
Unclad	0.2249	0.988

Table 9.3 Forces of panel 1 in Example 9.1 (Fig. 9.1)

Panel model	$\bar{F}_1$, $\bar{F}_4$ (kN)	$\bar{F}_2$, $\bar{F}_3$ (kN)	$\bar{F}_5$ (kN)
Five-force model	0.048	0.108	0.049
Four-force model	0.051	0.117	-
Unclad	-	-	-

The nodal force components calculated from different numerical models for panel 1, in X-Y plane, are shown in Fig. 9.2.

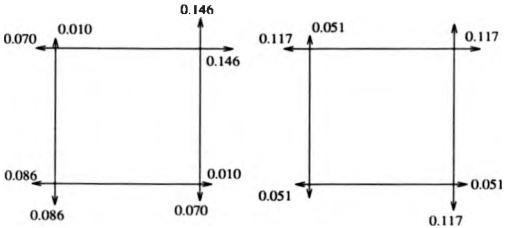

Fig. 9.2 Nodal force components in X-Y plane of panel 1

(a) five-force model (b) four-force model

From Tables 9.1, 9.2, 9.3 and Fig. 9.2 it is seen that

i) The panels can make a great deal of contribution to the stiffness of the structure;

ii) The four-force model is more flexible than the five-force model, because it ignores the stiffness of the panel corresponding to the anti-symmetrical deformation.

iii) In this example, it is obvious that the panels undergo angular distortion, hence the state of equilibrium of panel 1 shown in Fig. 9.2(a) is more realistic than that in Fig. 9.2(b).

Example 9.2

A flat cable net, fully clad with quadrilateral panels, is shown in Fig. 9.3. The area, square in plan, and surrounded by the rigid boundary, is divided by the cable members into four equal quadrilaterals and the cross-section area of cables is 1.018×10^{-6} m^2. The remaining data and the accuracy requirement are the same as in Example 9.1.

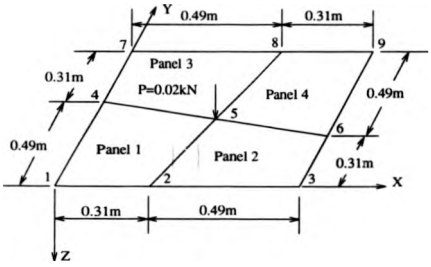

Fig. 9.3 Fully clad flat net in Example 9.2

The flexibility matrices of the panels have been calculated in Example 6.1 in Section 6.2.2. The results produced with four-force and five-force models of the clad structure, and those of the corresponding unclad net are listed in Tables 9.4, 9.5 and 9.6. The nodal force components calculated from

different numerical models for panel 1, in X-Y plane, are shown in Fig. 9.4.

Table 9.4 Vertical displacement of node 5
in Example 9.2 (Fig. 9.3)

Panel model	Δ_{53} (cm)
Five-force model	0.448
Four-force model	0.464
Unclad	0.889

Table 9.5 Force and extension of cable members
in Example 9.2 (Fig. 9.3)

Panel model	Force (kN)	Extension ($\times 10^{-4}$ m)
Five-force model	0.2078	0.245
Four-force model	0.2084	0.263
Unclad	0.2307	0.964

Table 9.6 Forces of panel 1 in Example 9.2 (Fig. 9.3)

(Unit : kN)

Panel model	$\bar{F}_1$	$\bar{F}_2$	$\bar{F}_3$	$\bar{F}_4$	$\bar{F}_5$
Five-force model	0.045	0.109	0.106	0.050	0.048
Four-force model	0.054	0.124	0.110	0.048	-
Unclad	-	-	-	-	-

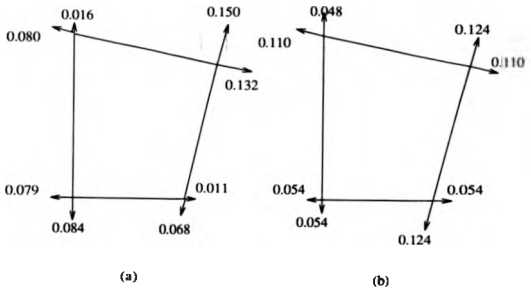

Fig. 9.4 Nodal force components in X-Y plane of panel 1

(a) five-force model (b) four-force model

From the results in Tables 9.4, 9.5, 9.6 and Fig. 9.4 the same conclusion can be drawn as in Example 9.1. In addition, when comparing the results from Table 9.4 with those in Table 9.1, it can be seen that the two nets have the same displacement at node 5 under P = 0.02 kN when they are unclad; but the clad net in Example 9.1 has a smaller displacement than that in Example 9.2. This implies that a square panel is generally stiffer than an arbitrary quadrilateral one, provided their material properties and plan area are identical.

Example 9.3

A saddle-shaped net, fully clad with quadrilateral panels, is shown in Fig. 9.5. The net is obtained by lowering nodes 1 and 9 and raising nodes 3 and 7 at the boundary by 0.01 m; the overall plan dimension are the same as in Example 9.2. Cables 2-5-8 and 4-5-6 are no longer straight lines but polylines, meeting at node 5. The panels are warped quadrilaterals. The cross-section area of cables is $0.907 \times 10^{-4}\ m^2$. The remaining data used and the accuracy requirement are the same as in Example 9.1.

The flexibility matrices of the panels have been calculated in Example 6.2 in Section 6.3. The results for the clad structure and for the corresponding unclad net are listed in Tables 9.7, 9.8 and 9.9, respectively. The forces in cable members 1 and 4 are not equal to the forces in members 2 and 3, and similarly the forces in panels 1 and 3 are not equal to those in 2 and 4, after deformation. The nodal force components calculated from different numerical models of panels 1 and 2, in X-Y plane, are shown in Fig. 9.6.

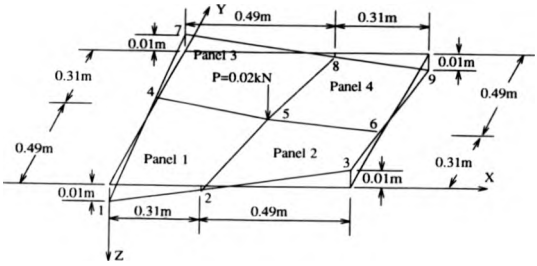

Fig. 9.5 Fully clad saddle-shaped net in Example 9.3

Table 9.7 Vertical displacement of node 5 in Example 9.3 (Fig. 9.5)

Panel model	Δ_{53} (cm)
Five-force model	0.452
Four-force model	0.473
Unclad	0.889

Table 9.8a Force and extension of cable members 1 and 4 in Example 9.3 (Fig. 9.5)

Panel model	Force (kN)	Extension ($\times 10^{-4}$ m)
Five-force model	0.2141	0.497
Four-force model	0.2151	0.533
Unclad	0.2412	1.451

Table 9.8b Force and extension of cable members 2 and 3 in Example 9.3 (Fig. 9.5)

Panel model	Force (kN)	Extension ($\times 10^{-4}$ m)
Five-force model	0.2000	0.001
Four-force model	0.2004	0.014
Unclad	0.2135	0.476

Table 9.9a Forces of panel 1 in Example 9.3 (Fig. 9.5)

(Unit : kN)

Panel model	$\bar{F}_1$	$\bar{F}_2$	$\bar{F}_3$	$\bar{F}_4$	$\bar{F}_5$
Five-force model	0.030	0.130	0.031	0.012	0.027
Four-force model	0.034	0.143	0.035	0.011	-
Unclad	-	-	-	-	-

Table 9.9b Forces of panel 2 in Example 9.3 (Fig. 9.5)

(Unit : kN)

Panel model	$\bar{F}_1$	$\bar{F}_2$	$\bar{F}_3$	$\bar{F}_4$	$\bar{F}_5$
Five-force model	0.014	0.032	0.123	0.027	-0.017
Four-force model	0.015	0.036	0.133	0.031	-
Unclad	-	-	-	-	-

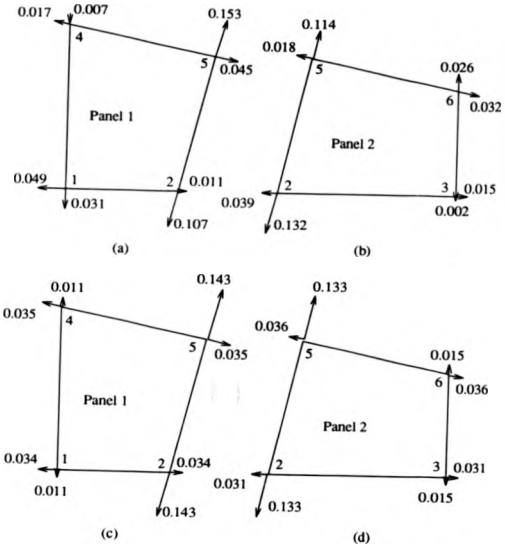

Fig. 9.6 Nodal force components in X-Y plane of panels 1 and 2

(a) five-force model, panel 1 (b) five-force model, panel 2

(c) four-force model, panel 1 (d) four-force model, panel 2

Comparison of results from Table 9.7 and Table 9.4 shows a reduction in stiffness of the clad net in Example 9.3, due to the influence of curvature on stiffness of the panels, as has been discussed in Chapter 5, Section 5.4.

Example 9.4

Hyperbolic paraboloid (HYPAR) net, partly clad with square panels. The net is subjected to two groups of loads:

i) The weight of the panels,

ii) The external loads,

as shown in Figs. 9.7(a) and (b), respectively. The clad area is shaded. The following data is used:

Young's modulus of cables	$128.3 \times 10^6\ k\,\mathrm{N}/m^2$
Cross–section area of cables	$0.785 \times 10^{-6}\ m^2$
Pretension in cables	$0.2\ k\,\mathrm{N}$
Young's modulus of panels	$62 \times 10^6\ k\,\mathrm{N}/m^2$
Poisson ratio of panels	0.33
Thickness of panels	$0.9 \times 10^{-3}\ m$
Weight of quarter panel W	$0.0009\ k\,\mathrm{N}$
External load P	$0.0157\ k\,\mathrm{N}$

The task of this example is to calculate the deformation of the partly clad net due to the external loads only, and compare it with the deformation of the corresponding unclad net under the same loads. The accuracy is required by ER = 0.00003,

i.e. the final maximum residual force must not exceed 0.00003 kN.

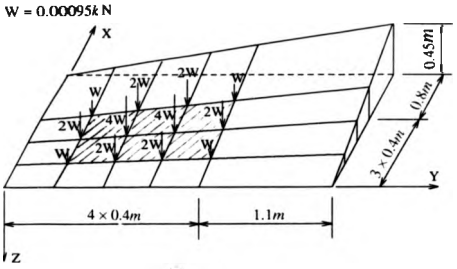

(a)

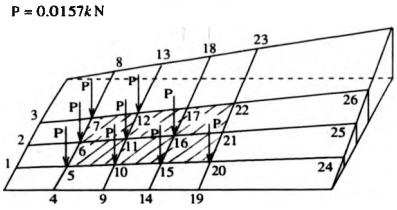

(b)

Fig. 9.7 Partly clad "hypar" net

(a) Weight of panels (b) External loads

To calculate the deformation of the net due to the external loads only, the following two group of displacements are to be calculated:

(i) The displacements caused by the weight of the panels (abbreviated as " W " in Tables 9.10 and 9.11);

(ii) The displacements caused by the weight of the panels plus the external loads (abbreviated as " W + P " in Tables 9.10 and 9.11).

The difference between cases (ii) and (i) gives the deformation due to the external loads only.

The above two groups of displacements are calculated employing the four-force model and the five-force model for the cladding, and the results are shown in Tables 9.10 and 9.11, respectively. The differences between the two groups of displacements are in Table 9.12, where the displacements of the corresponding unclad net under the external loads are also given.

The increase in stiffness of the net due to cladding can be seen when comparing the relevant columns of vertical displacements (Δ_z) in Table 9.12. The five-force model is once again shown to be stiffer than the four-force model. The difference in vertical and horizontal displacements, between the unclad and clad cases, is illustrated in Figs. 9.8 and 9.9, respectively.

Table 9.10 Inner nodal displacements calculated using four-force model for the panels (Unit : *mm*)

Node	Load: W			Load: W + P		
	Δ_x	Δ_y	Δ_z	Δ_x	Δ_y	Δ_z
5	0.09	0.09	2.79	0.45	0.38	19.29
6	0.14	0.29	4.48	0.63	1.22	25.67
7	0.11	0.35	0.36	0.56	1.87	23.15
10	0.32	0.16	4.89	1.38	0.55	25.89
11	0.50	0.50	7.82	1.90	1.74	34.98
12	0.39	0.60	6.20	1.57	2.52	30.14
15	0.51	0.17	5.21	2.19	0.57	26.06
16	0.81	0.53	8.31	2.83	1.61	32.95
17	0.64	0.65	6.64	1.77	1.80	23.34
20	0.52	0.12	3.92	2.55	0.41	21.81
21	0.82	0.39	6.24	2.60	0.74	22.00
22	0.66	0.49	5.09	1.81	1.04	16.25

Table 9.11 Inner nodal displacements calculated using five-force model for the panels (Unit : *mm*)

Node	Load: W			Load: W + P		
	Δ_x	Δ_y	Δ_z	Δ_x	Δ_y	Δ_z
5	0.14	0.21	1.89	0.88	1.04	14.99
6	0.18	0.21	3.15	1.10	1.16	22.73
7	0.16	0.09	2.58	1.24	1.30	26.51
10	0.26	0.27	3.29	1.33	1.25	21.18
11	0.39	0.35	5.33	1.77	1.52	28.90
12	0.32	0.25	4.34	1.68	2.34	27.32
15	0.32	0.28	3.56	1.79	1.34	23.12
16	0.52	0.37	5.64	2.15	1.38	26.87
17	0.41	0.26	4.51	1.25	0.39	18.66
20	0.27	0.25	2.76	2.21	1.32	22.27
21	0.47	0.29	4.32	1.62	0.70	18.01
22	0.36	0.16	3.47	0.94	-0.18	13.00

Table 9.12 Displacements due to external loads only

(Unit : *mm*)

Node	Unclad net			Clad net					
				Four-force model			Five-force model		
	Δ_x	Δ_y	Δ_z	Δ_x	Δ_y	Δ_z	Δ_x	Δ_y	Δ_z
5	0.35	0.29	19.51	0.36	0.29	16.50	0.74	0.83	13.10
6	0.68	1.07	25.63	0.49	0.93	21.19	0.92	0.95	19.58
7	0.77	1.78	23.30	0.45	1.52	22.79	1.08	1.21	23.93
10	1.18	0.56	25.85	1.06	0.39	21.00	1.07	0.98	17.89
11	1.94	1.72	34.06	1.40	1.24	27.16	1.38	1.17	23.57
12	1.91	2.49	29.50	1.18	1.92	23.94	1.36	2.09	22.98
15	1.99	0.67	25.78	1.68	0.40	20.85	1.47	1.06	19.56
16	2.76	1.72	31.31	2.02	1.08	24.64	1.63	1.01	21.23
17	1.91	1.74	21.42	1.13	1.15	16.70	0.84	0.13	14.15
20	2.42	0.62	21.48	2.03	0.29	17.89	1.94	1.07	19.51
21	2.37	0.99	20.00	1.58	0.35	15.76	1.15	0.41	13.69
22	1.74	1.13	14.41	1.15	0.55	11.16	0.58	-0.34	9.53

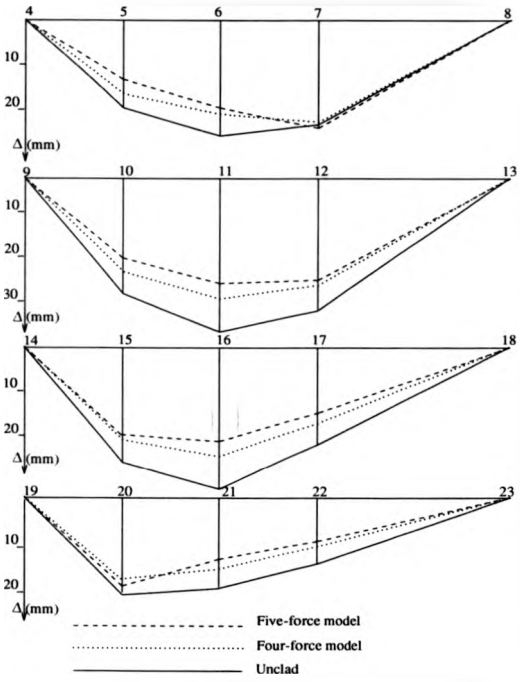

Fig. 9.8 Vertical displacements of nodes under external loads

(vertical scale exaggerated)

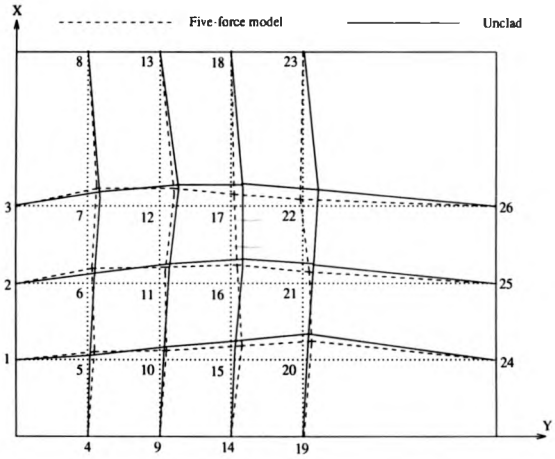

Fig. 9.9 Deformation of net in X-Y plane (exaggerated)
under external loads

The numerical results are compared against the experimental measurements, given in Ref. [9] and reproduced in Tables 9.13, 9.14 and Fig. 9.11. The size of elements used to calculate the flexibility matrix of panels is adjusted to the size of the area of the nodal connector [9], as shown in Fig. 9.10.

From Tables 9.13, 9.14 and Fig. 9.11 it can be seen that the results produced with the five-force model give better agreement with the experimental measurements than those from the four-force model. It can also be observed that the use of the four-force model in comparison with the five-force model increases the flexibility of the structure. The largest discrepancy between numerical and experimental results occurs at the boundary of the clad area, where the connectors suffer large unsymmetrical forces from the panels and the cables, which may cause the rotations of the connectors and hence reduce the accuracy of the measurements.

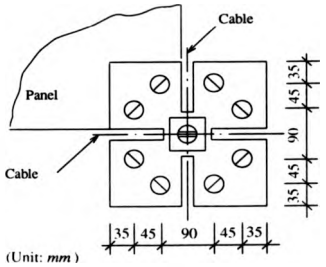

Fig. 9.10 Nodal connector design

Table 9.13 Comparison of numerical results with experimental measurement: horizontal displacements (Unit : *mm*)

Node	Experimental		Numerical			
			Four-force model		Five-force model	
	Δ_x	Δ_y	Δ_x	Δ_y	Δ_x	Δ_y
5	0.5	1.1	0.36	0.29	0.74	0.83
6	0.7	0.8	0.49	0.93	0.92	0.95
7	0.7	1.1	0.45	1.52	1.08	1.21
10	1.0	1.2	1.06	0.39	1.07	0.98
11	1.4	1.1	1.40	1.24	1.38	1.17
12	1.3	1.0	1.18	1.92	1.36	2.09
15	1.4	1.1	1.68	0.40	1.47	1.06
16	2.4	0.2	2.02	1.08	1.63	1.01
17	0.8	-0.2	1.13	1.15	0.84	0.13
20	2.1	1.4	2.03	0.29	1.94	1.07
21	1.3	0.6	1.58	0.35	1.15	0.41
22	0.8	-0.5	1.15	0.55	0.58	-0.34

Table 9.14 Comparison of numerical results with experimental measurement: vertical displacements

Node	Experimental	Numerical			
		Four-force model		Five-force model	
	Δ_z (*mm*)	Δ_z (*mm*)	Error (%)	Δ_z (*mm*)	Error (%)
5	14.4	16.50	14.58	13.10	-9.03
6	20.4	21.19	3.87	19.58	-4.02
7	22.4	22.79	1.74	23.93	6.83
10	19.4	21.00	8.25	17.89	-7.78
11	24.2	27.16	12.23	23.57	-2.60
12	25.1	23.94	-4.62	22.98	-8.45
15	22.0	20.85	-5.23	19.56	-11.09
16	22.8	24.64	8.07	21.23	-6.89
17	15.5	16.70	7.74	14.15	-8.71
20	21.6	17.89	-17.18	19.51	-9.68
21	16.1	15.76	-2.11	13.69	-14.97
22	10.7	11.16	4.30	9.53	-10.93

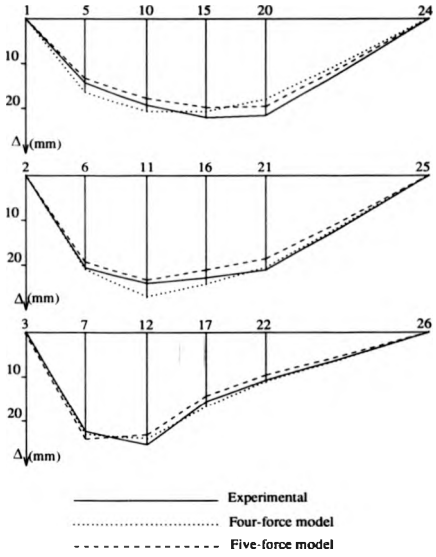

Fig. 9.11 Comparison of numerical results with experimental measurements: vertical displacements

9.3 Study of the rate of convergence

The four programs introduced in Chapter 8 are developed to study the effects of different forms of damping (viscous or kinetic) and mass arrangements on stability and convergence of the calculation. In program SACSV1, the mass components and the viscous damping coefficients are proportional to the stiffness components, and the values of two parameters BI and CI have to be chosen. These can be determined by trial and error and this can be done with a much relaxed accuracy of the solution. In programs SACSK1, SACSK2 and SACSK3, the only parameter to be chosen is BI, i.e. the ratio between stiffness and masses. Hence, for these programs, the stability and the convergence rate of the solution depend only on the one or two parameters.

The process of finding the optimum value of BI is illustrated in Table 9.15 in which the number of iterations used, for example by program SACSK2, at a lower level and a higher level of accuracy, is given. Several cases of Example 9.4 are considered, as listed below:

Case 1 – Unclad net under the external loads;

Case 2 – Clad net under the weight of the panels, analysed with the four-force model;

Case 3 – Clad net under the weight of the panels, analysed with the five-force model;

Case 4 – Clad net under the weight of the panels plus the external loads, analysed with the four-force model;

Case 5 – Clad net under the weight of the panels plus the external loads, analysed with the five-force model.

In all cases, except case 4, the approach of relaxed accuracy, aimed at finding the optimum BI, is successful.

Table 9.16 lists the least number of iterations, found by trail and error, using different programs for the solution of cases 1-5 at the same higher level of accuracy of 0.00003 kN. Three more cases of unclad cable net structures, shown in Figs. 9.12, 9.13 and 9.14, are studied in similar manner and the results are also included in Table 9.16.

Table 9.15 Iterations required by different levels of accuracy

(Program SACSK2)

Case	Max. load	ER (kN)		BI	Iterations	
		Level 1	Level 2		Level 1	Level 2
1	0.0157	0.0155	0.00003	0.8	26	86
				0.9	28	94
				1.0	27	86
				1.1	191	>1000
2	0.0038	0.0037	0.00003	0.8	67	209
				0.9	63	198
				1.0	72	200
3	0.0038	0.0037	0.00003	0.7	75	189
				0.8	72	179
				0.9	67	177
				1.0	64	164
				1.1	*	*
4	0.0195	0.0194	0.00003	0.6	95	264
				0.7	88	273
				0.8	100	230
				0.9	202	361
5	0.0195	0.0194	0.00003	0.7	99	264
				0.8	85	254
				0.9	85	242
				1.0	*	*

* Divergence.

Table 9.16 The least number of iterations to achieve equilibrium using different programs

Case	SACSK1	SACSK2	SACSK3	SACSV1
1	202	86	82	53
2	529	198	187	165
3	361	164	172	173
4	671	264	229	207
5	614	242	209	199
6	79	53	52	38
7	122	123	126	103
8	262	99	98	72

In most cases in Table 9.16, the programs which use mass components proportional to stiffness components in X, Y, Z directions (SACSK2, SACSK3 and SACSV1) show a much quicker convergence than the program with identical mass components in all directions (SACSK1). Program SACSV1 (with viscous damping) shows the quickest convergence, but the difference in convergence rate between SACSV1 and SACSK2 or SACSK3 is not significant; and this slight advantage can not offset the disadvantage that the program uses two parameters

(BI and CI) to regulate the convergence, which increase the difficulty of optimisation. The improvement made in program SACSK3 i.e. the adjustment in mass components according to the change in stiffness, due to deformations, does not make a significant difference as expected, because the deformations of the static analysis of the structures, although large, are not large enough. It is expected that in cases when geometry changes drastically, as in form finding problems, program SACSK3 will display its advantage over SACSK2 in achieving a faster convergence.

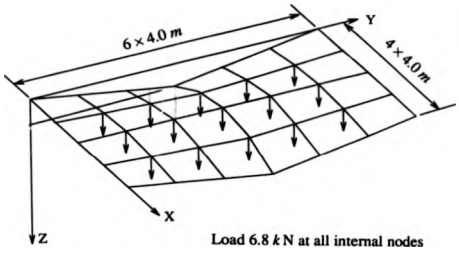

Fig. 9.12 Case 6 in Table 9.16

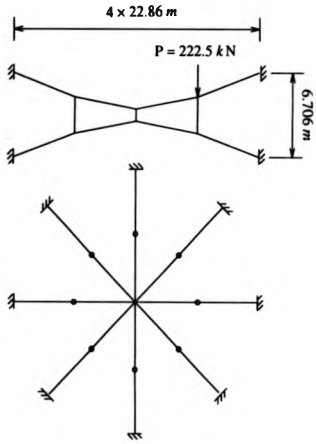

Fig. 9.13 Case 7 in Table 9.16

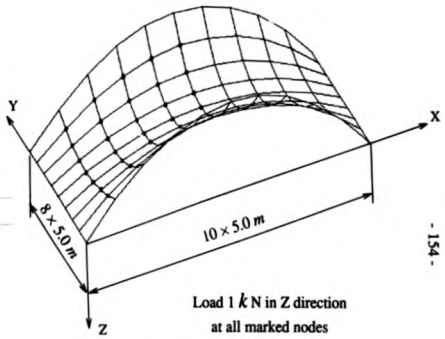

Fig. 9.14 Case 8 in Table 9.16

CHAPTER 10

Conclusions and Suggestions for Further Work

10.1 Conclusions

From the work presented in this thesis the following conclusions can be drawn:

(i) The formulation of the sub-region mixed energy principle that includes geometrically non-linear problems, and its subsequent application to the analysis of clad cable net structures has been completed successfully. The use of local coordinate system for the analysis of cladding allows the linear aspect of the behaviour of the panels, given by the in-plane force-displacement relationship, to be treated separately from the non-linear aspect caused by the large out-of-plane displacements. Hence, the proposed approach helps to overcome the difficulty of expressing the complex strain-displacement relationship of cladding panels.

(ii) Two numerical models, referred to as the four-force model and the five-force model, are developed for the analysis of panels with four straight edges. The

models apply to panels of rectangular or arbitrary quadrilateral shapes, which can be flat or doubly curved. The five-force model is shown to be more complete in expressing the state of equilibrium of a panel than the four-force model, in which the deformation associated with the fifth force is ignored.

(iii) It is shown that a quadrilateral panel can be replaced by a group of six bars, in the case of the five-force model, or four bars, if the four-force model is used. The bars obey the same force-displacement relationship as derived for the panel. The advantage of this replacement is that the contribution of the bars to achieving static equilibrium can be calculated in the same way as that of cable members, resulting in a more unified approach. This treatment simplifies the computational procedure, and allows the analysis of cable networks, clad with arbitrary quadrilateral panels, to be performed more easily.

(iv) A study of the efficiency of the dynamic relaxation technique is carried out with respect to kinetic and viscous damping as well as the use of fictitious masses. Viscous damping is shown to have the potential for achieving a faster convergence than kinetic damping, but it involves the optimisation of not one, but two parameters controlling the iterations, and this counteracts its possible advantage. The use of the fictitious masses that are proportional to stiffness components at each node of the structure, and in X, Y, Z directions, is found to be beneficial in term of convergence. In most examples that have been analysed, the convergence rate is increased by more than 100%, compared with that when identical mass components in X, Y, Z directions at each node are employed. The scheme of

adjusting mass components to the ever changing stiffness of the structure during iterations, does not seem to produce significant advantage for the static analysis of clad cable nets.

In view of this, program SACSK2, in which kinetic damping and constant (time-independent) mass components, proportional to nodal stiffness components are employed, is recommended for the static analysis of clad or unclad cable net structures.

(v) The success of the present application of the sub-region mixed energy principle demonstrates once again the potential of the principle for developing a simplified approach to complex problems, linear or geometrically non-linear, hence encourages further applications of the principle.

10.2 Suggestions for Further Work

Further work should be carried out to include:

(i) Experimental studies of several more models of clad cable networks to verify the proposed numerical method. These experiments should be designed to allow for a variety of shapes and curvatures of cladding panels to be considered

as well as for different ratios between stiffnesses of panels and cable members.

(ii) Experimental study of the force-displacement relationship of panels with various shapes and curvatures, to verify the numerical results obtained from the finite element method. Establishment of tables or charts relating flexibility/stiffness components to geometry (thickness, curvature, *etc.*) of mass-produced panels for design purpose.

(iii) Numerical modelling and experimental studies of continuous cladding surfaces under static load.

(iv) Extended application of the proposed numerical method to include the form finding of clad cable networks with both discrete and continuous cladding surfaces. Examination of the effects of the choice of mass components, within the dynamic relaxation method, on convergence of the solution and verification of the prediction that the scheme of adjusting the mass components during iterations (program SACSK3) is beneficial to the convergence rate.

References

[1] Birdsall, B. "Footnotes to suspension bridge history prior to 1950 with some rambling recollections of a cable construction engineer." *1st Oleg Kerensky Memorial Conference*, London, Session 1, pp.1-14, 1988.

[2] Lan, T. "Development of cable-roof structures in China." *1st Oleg Kerensky Memorial Conference*, London, Session 1, pp.24-27, 1988.

[3] Tang, H. *Ancient Chinese Bridges*. Cultural Relic Press, Beijing, 1987.

[4] Happold, E. "Tensile building development", *1st Oleg Kerensky Memorial Conference*, London, Session 3, pp.1-5, 1988.

[5] Buchholdt, H. A. *Introduction to Cable Roof Structures*. Cambridge University Press, 1985.

[6] Happold, T. "Chariots of fire." *Patterns*, 5, pp.2-7, Buro Happold Consulting Engineers, 1989.

[7] Shan, J. & Lewis, W. J. "Application of the sub-region mixed energy principle to the analysis of stressed membrane roofing forms." *Proc. of Int. Conf. FEMCAD*, Vol.1, pp.453-461, Paris, 1988.

[8] Lewis, W. J. & Shan, J. "Numerical modeling of the non-linear static response of clad cable net structures." *Computers & Structures*, Vol.35, No.1, pp.15-22, 1990.

[9] Lewis, W. J. *Investigation into the Structural Characteristics of Stressed Membrane Roof Structures*. Ph.D. Thesis, CNAA, Wolverhampton Polytechnic, 1982.

[10] Otto, F. *Tensile Structures*. MIT Press, Cambridge, Mass., 1962.

[11] Irvine, H. H. *Cable Structures*. MIT Press, Cambridge, Mass., 1981.

[12] Tauchert, T. R. *Energy Principle in Structural Mechanics*. McGraw-Hill, 1974.

[13] Reissner, E. "On a variational theorem in elasticity." *Journal of Mathematics and Physics*, 29, 2, pp.90-95, 1950.

[14] Reissner, E. "On variational principles in elasticity." *Proceedings of Symposia in Applied Mathematics*, McGraw-Hill, 8, pp.1-6, 1958.

[15] Hu, H. "On some variational principles in the theory of elasticity and plasticity." *Acta Phsica Sinica*, Vol.10, No.3, pp.259-290, 1954.

[16] Washizu, K. "On the variational principles of elasticity and plasticity." *Aeroelastic and Structures Research Laboratory*, Massachusetts Institute of Technology, Technical Report 25-18, March 1955.

[17] Courant, R. & Hilbert, J. N. *Methods of Mathematical Physics*, Vol.1, Interscience, New York, 1953.

[18] Chien, W. *Variational Methods and Finite Element*. Vol. 1, Science Press, Beijing, 1980.

[19] Long, Y. "Sub-region generalized variational principle in elasticity." *Shanghai Mechanics*, 2, pp.1-9, 1981.

[20] Long, Y., Zhi, B. & Yuan, S. "Sub-region, Sub-item and sub-layer generalized variational principle in elasticity." *Proc. Conf. FEM*, pp.607-609, 1982.

[21] Jones, R. E. "A generalization of direct-stiffness method of structural analysis." *AIIA Journal*, 2, 5, pp.821-826, 1966.

[22] Green, B. E., Jones, R. E., Mckey, R. W. & Strome, D. R. "General variational principles in the finite element methods." *AIIA Journal*, 7, pp.1254-1260, 1969.

[23] Pian, T. H., Tong, P. & Luk, C. H. "Elastic crack analysis by a finite element hybrid method." *Proc. of Conference on Matrix Methods in Structural Mechanics 3rd*, 1971.

[24] Bryan, E. *The Stressed Skin Design of Steel Buildings*. Constrado Monographs, 1973.

[25] Bryan, E. "Stressed skin design and construction: a state of art report." *The Structural Engineer*, Vol.54, No.9, pp.347-351, 1976.

[26] Davies, J. & Bryan, E. *Manual of Stressed Skin Diaphragm Design*. Granada, 1982.

[27] E.C.C.S. *European Recommendations for the Stressed Skin Design of Steel Structures*. Pub. no. XVII-77-1E, European Convention for Constructional Steelwork. English version published by Constrado, 1977.

[28] Timoshenko, S. & Wojnowski-Krieger, S. *Theory of Plates and Shells*, McGraw-Hill, 1959.

[29] Lewis, W. J., Jones, M. S., Lewis, G. & Rushton, K. R. "Cladding-network interaction in pretensioned cable roofs, studied by dynamic relaxation." *Computers & Structures*, Vol. 19, No. 5/6, pp.885-897, 1984.

[30] Buchholdt, H. A., Davies, M. & Hussey, M. "The analysis of cable nets." *J. Inst. Maths Applics*, Vol.4, pp.339-358, 1968.

[31] Buchholdt, H. A. "Tension structures." *The Structural Engineer*, Vol.48, No.2, pp.45-54, 1970.

[32] Shore, S. & Bathish, G. "Membrane analysis of cable roofs." *Int. Conf. on Space Structures*, 1966.

[33] Bhupinter, P. & Bhushan, L. "Membrane Analogy for anisotropic cable networks." *J. Struct. Div. ASCE* (ST5), pp1053-1066, 1974.

[34] Krishna, P. & Agrawal, T. "Approximate analysis of cable structures." *Int. Conf. on Tension Roof Structures*, 1974.

[35] Siev, A. "A general analysis of prestressed nets." *Publs. Int. Ass. Bridge Struct. Engng*, 23, pp.283-292, 1963.

[36] Siev, A. & Eidelman, J. "Stress analysis of prestressed suspended roofs." *J. Struct. Div.,ASCE* 90(ST4), pp.103-121, 1964.

[37] Hood, G. "A general stiffness method for the solution of non-linear cable networks with arbitrary loading." *Computers & structures*, 6, pp.391-396, 1976.

[38] Krishna, P. *Cable Suspended Roofs*. McGraw-Hill, 1978.

[39] Argyris, J. & Scharpe, W. "Large deflection analysis of prestressed networks." *J. Struct. Div.,ASCE* (ST3), pp.633-654, 1972.

[40] Hussey, M. "Skeletal assemblies subject to geometrically significant displacements." *IInd Pan-American Conference on Structures*, Lima, 1964.

[41] Buchholdt, H. A. "Deformation of prestressed cable nets."*Acta Polytech. Scand.* Series(b), No.38, 3, 1966.

[42] Braga, F. & Care, A. "Study of cable network subject to loads however distributed." *Int. Conf. on Tension Roof Structures*, London, 1974.

[43] Buchholdt, H. A. & McMillan, B. "Iterative methods for the solution of pretensioned cable structures and pinjointed assemlies having significant geometrical displacements." *IASS Int. Symposium on Tension Structures and Space Frames*, Tokyo, 1971.

[44] Businger, O. A. "Matrices which can be optimally scaled." *Num. Maths.* **12**, 346-8, 1968.

[45] Charlton, T. M. *Energy Principles in Theory of Structures*. Oxford University Press, 1973.

[46] Barnes, M. R. "Non-linear numerical solution methods for static and dynamic relaxation." *Institute of Lightweight Structures*, 15, pp.150-159, University of Stuttgart, 1982.

[47] Day, A. S. & Bunce, J. H. "Analysis of cable networks by dynamic relaxation." *Civil Eng. & Public Works Review*, April, pp.383-386, 1970.

[48] Cundall, P. A. "Explicit finite-difference methods in geometrics." *Proc. EF conf. numerical methods in geomechanics*, Blacksburg, Va., 1976.

[49] Barnes, M. R. "Form-finding and analysis of prestressed nets and membranes." *Proc. Int. Conf. on Non-conventional Structures*, London, Vol.1, pp.327-338, 1987.

[50] Barnes, M. R. & Wakefield, D. S. "Form-finding, analysis and patterning of surface-stressed structures." *1st Oleg Kerensky Memorial Conference*, London, Session 4, pp.8-15, 1988.

[51] Fried, I. "A gradient computational procedure for the solution of large problems arising from the finite element discretisation method." *Int. J. for Numerical Methods in Engineering*, 2(2), 1970.

[52] Greenburg, D. P. "An 'equivalent stiffness' method for suspension roof analysis." *Ninth Congress, Int. Association for Bridge and Structural Engineering*, 1972.

[53] Otter, J. R. H. "Computations for prestressed concrete reactor pressure vessels using dynamic relaxation." *Nuclear Struct. Eng.* 1, pp.61-75, 1964.

[54] Timoshenko, S. P., Young, D. H. & Weaver, W. *Vibration Problems in Engineering*. Wiley, 1974.

[55] Lewis, W. J. "A comparative study of numerical methods for the solution of pretensioned cable networks." *Proc. Int. Conf. on Non-conventional Structures*, London, Vol.2, pp.27-33, 1987.

[56] Long, Y. & Bao, S. *Structural Mechanics*. National Educational Press, Bejing, Vol.2, 1981.

[57] Ghali, A. & Neville, A. M. *Structural Analysis*. Intext Educational Publishers, 1972.

[58] Long, Y., Zhi, B., Kuang, W. & Shan, J. "Sub-region mixed finite element method for the calculation of stress intensity factor." *Acta Mechaniica Sinica*, No.4, pp.341-353, 1982.

[59] Long, Y. & Zhao, Y. "Technical Note: Calculation of stress intensity factors in plane problems by the sub-region mixed finite element method." *Adv. Eng. Software*, Vol.7, No.1, pp.32-35, 1985.

[60] Dawe, D. J. *Matrix and Finite Element Displacement Analysis of Structures*. Oxford University Press, 1984.

[61] *Data Preparation User Manual*.Level 6.1, Pafec Ltd, 1989.

[62] Zienkiewicz, O. C. & Taylor, R. L. *The Finite Element Method - 4th Edition*. McGraw-Hill, Vol.1, 1989.

[63] Lewis, W. J., Jones, M. S. & Rushton, K. R. "Dynamic relaxation analysis of the non-linear static response of pretensioned cable roofs." *Computers & Structures*, Vol. 18, No. 6, pp.989-997, 1984.

[64] Barnes, M. R. " Non-linear numerical solution methods for static and dynamic analysis of tension structures." *Symp. on air supported structures*, IStructE, London, 1980.

APPENDIX A

Tensor Notation

Tensor notation provides a convenient means for describing many quantities in the study of deformable media, such as stress and strain, which can not be described by vectors. Like vectors, tensors are independent of any particular frame of reference. But also like vectors, tensors are most conveniently described by specifying their components in an appropriate system of coordinates. The following discussion is restricted to Cartesian coordinate systems and hence Cartesian tensors.

The conventions adopted to shorten the writing of equations involving tensors in this thesis are listed as the following:

(i) *Range convention*. Whenever a subscript appears only once in a term, the subscript takes all the values 1, 2, and 3.

According to this convention, a set of three independent quantities, representing for example the coordinates of a point or the components of a vector, can be denoted simply by a_i, where it is understood that the *index* or subscript i take the

values 1, 2, and 3. Hence, a_i stands for a_1, a_2, and a_3. Similarly, both the indices i and j in b_{ij} can take on the values 1, 2, and 3, hence b_{ij} represents 9 quantities, namely, b_{11}, b_{12}, b_{13}, b_{21}, b_{22}, b_{23}, b_{31}, b_{32}, b_{33}.

(ii) *Summation convention*. Whenever a subscript appears twice in the same term, the repeated index is summed from 1 to 3. No index can be repeated more than once.

For example,

$$a_i b_i = \sum_{i=1}^{3} a_1 b_i = a_1 b_1 + a_2 b_2 + a_3 b_3 ;$$

$$a_{ij} b_j = \sum_{j=1}^{3} a_{ij} b_j = a_{i1} b_1 + a_{i2} b_2 + a_{i3} b_3 .$$

(iii) *Comma convention*. A subscript comma followed by an index i indicates partial differentiation with respect to each coordinate x_i.

For example,

$$a_{i,j} = \frac{\partial a_i}{\partial x_j} ;$$

$$b_{ij,k} = \frac{\partial b_{ij}}{\partial x_k} .$$

According to the range convention, $a_{i,j}$ stands for 9 quantities ($\frac{\partial a_1}{\partial x_1}$, $\frac{\partial a_1}{\partial x_2}$, ...

$\frac{\partial a_3}{\partial x_3}$); and $b_{ij,k}$ stands for 27 quantities ($\frac{\partial b_{11}}{\partial x_1}$, $\frac{\partial b_{11}}{\partial x_2}$, ..., $\frac{\partial b_{33}}{\partial x_3}$. The summation convention applies to indices following the comma as well. Hence

$$a_{i,i} = \frac{\partial a_i}{\partial x_i} = \frac{\partial a_1}{\partial x_1} + \frac{\partial a_2}{\partial x_2} + \frac{\partial a_3}{\partial x_3} ;$$

$$b_{ij,j} = \frac{\partial b_{ij}}{\partial x_j} = \frac{\partial b_{i1}}{\partial x_1} + \frac{\partial b_{i2}}{\partial x_2} + \frac{\partial b_{i3}}{\partial x_3} .$$

APPENDIX B

Factor λ in Quadrilaterals

The factor λ is introduced in Chapter 7 for establishing the five force model for arbitrary quadrilateral panels. It has been indicated that λ is a factor determined by the geometry of the panel (see Fig. B.1) only, which can be calculated by the following equation:

$$\lambda = \frac{sin\alpha_1 sin(\alpha_2+\beta_2)}{sin\alpha_2 sin(\alpha_1+\beta_1)} \tag{B.1}$$

which includes the angles connected with side (1) only. In this appendix a rather symmetrical (in terms of the angles involved) formula is derived, and some special cases discussed in which the calculation of λ can be simplified.

(i) For an arbitrary quadrilateral as shown in Fig. B.1,

$$\lambda = \frac{d_2 sin(\alpha_2+\beta_2) sin(\alpha_4+\beta_4)}{d_1 sin(\alpha_1+\beta_1) sin(\alpha_3+\beta_3)} \tag{B.2}$$

where d_1 and d_2 are the lengths of the diagonals.

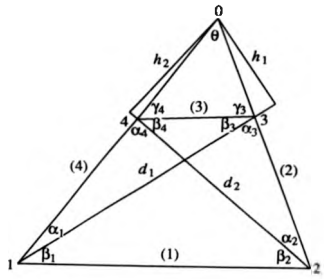

Fig. B.1

PROOF. Applying the sine rule to Δ1-3-4 and Δ2-3-4, respectively, gives

$$\frac{s_3}{\sin\alpha_1} = \frac{d_1}{\sin(\alpha_4+\beta_4)}$$

and

$$\frac{s_3}{\sin\alpha_2} = \frac{d_2}{\sin(\alpha_3+\beta_3)},$$

and hence

$$\frac{\sin\alpha_1}{\sin\alpha_2} = \frac{d_2\sin(\alpha_4+\beta_4)}{d_1\sin(\alpha_3+\beta_3)}. \qquad \text{(a)}$$

Substituting eq. (a) into (B.1) gives eq. (B.2).

(ii) For a trapezium (Fig. B.2),

$$\lambda = \frac{d_2}{d_1} \tag{B.3}$$

where d_1 and d_2 are the lengths of the diagonals.

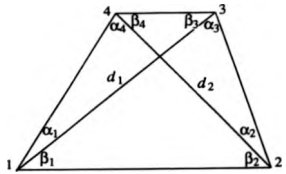

Fig. B.2

PROOF. Assume for example that side (1) is parallel to side (3). Because

$$(\alpha_1+\beta_1) + (\alpha_4+\beta_4) = 180^o$$

and

$$(\alpha_2+\beta_2) + (\alpha_3+\beta_3) = 180^o,$$

the following equations are true:

$$sin(\alpha_1+\beta_1) = sin(\alpha_4+\beta_4), \qquad sin(\alpha_2+\beta_2) = sin(\alpha_3+\beta_3). \tag{b}$$

Substituting eq. (b) into (B.2) produces eq. (B.3).

Assuming that side (2) is parallel to side (4) leads to the same conclusion and here the discussion is left out.

For isosceles trapezia of which rectangles are a special case, $\lambda = 1$ because the diagonals are equal in length.

(iii) If a quadrilateral has two opposite sides (say, side (2) and (4) in Fig. B.1) which are not parallel, then

$$\lambda = \frac{h_1}{h_2} \tag{B.4}$$

where h_1 and h_2 are the distances from the intersection of the linear extensions of the two sides (point 0 in Fig. B.1) to the diagonals (or their extensions), respectively.

PROOF. In Fig. B.1

$$sin\gamma_3 = sin(\alpha_3+\beta_3), \quad sin\gamma_4 = sin(\alpha_4+\beta_4) \tag{c}$$

because $\gamma_3 + \alpha_3 + \beta_3 = 180^o$, $\gamma_4 + \alpha_4 + \beta_4 = 180^o$. Substituting eq. (c) into (B.2) gives

$$\lambda = \frac{d_2 sin(\alpha_2+\beta_2) sin\gamma_4}{d_1 sin(\alpha_1+\beta_1) sin\gamma_3}. \tag{d}$$

Applying the sine rule in Δ 0-4-3 and Δ 0-1-2 respectively gives

$$\frac{\overline{04}}{\sin\gamma_3} = \frac{\overline{03}}{\sin\gamma_4}, \quad \frac{\overline{01}}{\sin(\alpha_2+\beta_2)} = \frac{\overline{02}}{\sin(\alpha_1+\beta_1)}$$

or

$$\frac{\sin\gamma_4}{\sin\gamma_3} = \frac{\overline{03}}{\overline{04}}, \quad \frac{\sin(\alpha_2+\beta_2)}{\sin(\alpha_1+\beta_1)} = \frac{\overline{01}}{\overline{02}}. \tag{e}$$

where the two numbers with a bar over them represent the length of the corresponding line segment.

Substituting eq. (e) into (d) yields

$$\lambda = \frac{d_2\,\overline{01}\,\overline{03}}{d_1\,\overline{02}\,\overline{04}}. \tag{f}$$

Using the formula for the area of Δ 0-1-3:

$$A_{\Delta 013} = \frac{1}{2}\,\overline{01}\,\overline{03}\sin\theta$$

and

$$A_{\Delta 013} = \frac{1}{2}d_1h_1$$

it is found that

$$\overline{01}\,\overline{03} = \frac{d_1h_1}{\sin\theta}; \tag{g}$$

Similarly,

$$\overline{02}\,\overline{04} = \frac{d_2h_2}{\sin\theta}. \tag{h}$$

Substituting eqs. (g) and (h) into (f) and eliminating the common factors gives eq. (B.4).

APPENDIX C

Computer Program for Calculation of λ

This appendix lists the program for the calculation of factor λ in arbitrary quadrilateral panels. The program is based on the formula derived in Appendix B:

$$\lambda = \frac{d_2 sin(\alpha_2+\beta_2) sin(\alpha_4+\beta_4)}{d_1 sin(\alpha_1+\beta_1) sin(\alpha_3+\beta_3)}$$

with reference to Fig.B.1. In the case of a warped panel, the angels in this formula are referred to the projection of the panel on a close plane, but d_1 and d_2 are the real lengths of the diagonals, as discussed in Chapter 6.

The information required by the program is the coordinates of the four nodes. The output information includes the value of λ, the lengths of the sides and the diagonals, and the components in Cartesian coordinates of the five unit forces, acting along the sides or diagonals.

```
      PROGRAM LAMBDA
      DIMENSION X(6,3),DX(6,3),S(6),A(5),AREA(4),F(6,3)
      REAL LAMBDA
       CHARACTER*32 FILEIN,FILEO
       PRINT *, 'INPUT FILENAME:'
       READ(*,'(A)') FILEIN
       OPEN(7,FILE=FILEIN)
       PRINT *, 'OUTPUT FILENAME:'
       READ(*,'(A)') FILEO
       OPEN(8,FILE=FILEO,STATUS='MODIFY')
      DO 1 I=1,4
    1 READ(7,*) (X(I,J),J=1,3)
      DO 2 J=1,3
      X(0,J)=X(4,J)
    2 X(5,J)=X(1,J)
      DO 5 I=1,4
      DO 3 J=1,3
    3 DX(I,J)=X(I+1,J)-X(I,J)
    5 A(I)=SQRT(DX(I,1)**2+DX(I,2)**2)
      A(0)=A(4)
      DO 6 J=1,3
      DX(5,J)=X(3,J)-X(1,J)
    6 DX(6,J)=X(4,J)-X(2,J)
      S(5)=SQRT(DX(5,1)**2+DX(5,2)**2+DX(5,3)**2)
      S(6)=SQRT(DX(6,1)**2+DX(6,2)**2+DX(6,3)**2)
      DO 10 I=1,4
   10 AREA(I)=0.5*(X(I-1,1)*X(I,2)-X(I-1,2)*X(I,1)+
     *            X(I,1)*X(I+1,2)-X(I,2)*X(I+1,1)+
     *            X(I+1,1)*X(I-1,2)-X(I+1,2)*X(I-1,1))
      LAMBDA=S(6)*AREA(2)*AREA(4)/(S(5)*AREA(1)*AREA(3))
      DO 15 I=1,4
   15 S(I)=SQRT(A(I)**2+DX(I,3)**2)
      DO 17 I=1,6
      DO 17 J=1,3
   17 F(I,J)=DX(I,J)/S(I)
      DO 18 J=1,3
   18 F(6,J)=LAMBDA*F(6,J)
      WRITE(8,20) ((X(I,J),J=1,3),I=1,4),(S(I),I=1,6),
     *            LAMBDA,((F(I,J),J=1,3),I=1,6)
   20 FORMAT(//10X,21HCOORDINATES OF NODES:/15X,1H1,3(5X,F14.6)
     *       /15X,1H2,3(5X,F14.6)/15X,1H3,3(5X,F14.6)
     *       /15X,1H4,3(5X,F14.6)//10X,17HLENGTHS OF SIDES:
     *       /15X,8HSIDE 1-2,5X,F14.6/15X,8HSIDE 2-3,5X,F14.6
     *       /15X,8HSIDE 3-4,5X,F14.6/15X,8HSIDE 4-1,5X,F14.6/
     *       /10X,21HLENGTHS OF DIAGOLALS:
     *       /15X,8HDIAL 1-3,5X,F14.6/15X,8HDIAL 2-4,5X,F14.6/
     *       /10X,7HLAMBDA-,5X,F14.6/
     *       /10X,26HCOMPONENTS OF UNIT FORCES:
     *       /15X,1HF,3X,4HNODE,10X,1HX,13X,1HY,13X,1HZ
     *       /15X,1H1,5X,1H2,1X,3F14.6/15X,1H2,5X,1H3,1X,3F14.6
     *       /15X,1H3,5X,1H4,1X,3F14.6/15X,1H4,5X,1H1,1X,3F14.6
     *       /15X,1H5,5X,1H3,1X,3F14.6/15X,1H5,5X,1H2,1X,3F14.6)
      CLOSE(7)
      CLOSE(8)
      END
```

APPENDIX D

Computer Program for Calculation of Flexibility Matrices of Quadrilateral Panels

The program listed below transfers the nodal diaplacements, obtained from finite element calculation, into the five generalised displacements, corresponding to the five-force model. If the nodal displacements are caused by a unit force in the five-force model, the program yields a column of elements of the flexibility matrix. The panel is supported to prevent rigid body movements, as shown in Fig. 6.8, where

$$w_1 = v_3 = w_3 = u_4 = v_4 = w_4 = 0.$$

Hence only six components of the nodal displacement array needs to be input. The other information required includes the coordinates of the nodes, the value of λ, and a integer NC, which indicates how many columns of the flexibility matrix are to be calculated.

```
      PROGRAM FLEX
      IMPLICIT REAL*8 (A-H,O-Z)
      REAL*8 LAMBDA
       character*32 filein,fileo
      DIMENSION A(6),B(5,5),X(5,3),DE(5,3),S0(4),S(4),
     *          D0(2),D(2)
       print *,'Input filename:'
       read(*,'(A)') filein
       open(7,file=filein)
       print *,'Output filename:'
       read(*,'(A)') fileo
       open(8,file=fileo,status='modify')
      DO 5 I=1,4
      DO 5 J=1,3
    5 DE(I,J)=0.
      READ(7,*) NC,LAMBDA
      DO 10 I=1,4
   10 READ(7,*) (X(I,J),J=1,3)
      DO 15 J=1,3
   15 X(5,J)=X(1,J)
      DO 50 IC=1,NC
      READ(7,*) (A(J),J=1,6)
      DE(1,1)=A(1)/10000.
      DE(1,2)=A(2)/10000.
      DE(2,1)=A(3)/10000.
      DE(2,2)=A(4)/10000.
      DE(2,3)=A(5)/10000.
      DE(3,1)=A(6)/10000.
      DO 20 J=1,3
   20 DE(5,J)=DE(1,J)
      DO 30 I=1,4
      S0(I)=0.
      S(I)=0.
      DO 25 J=1,3
      S0(I)=S0(I)+(X(I,J)-X(I+1,J))**2
   25 S(I)=S(I)+(X(I,J)+DE(I,J)-X(I+1,J)-DE(I+1,J))**2
      S0(I)=SQRT(S0(I))
   30 S(I)=SQRT(S(I))
      DO 40 I=1,2
      D0(I)=0.
      D(I)=0.
      DO 35 J=1,3
      D0(I)=D0(I)+(X(I,J)-X(I+2,J))**2
   35 D(I)=D(I)+(X(I,J)+DE(I,J)-X(I+2,J)-DE(I+2,J))**2
      D0(I)=SQRT(D0(I))
   40 D(I)=SQRT(D(I))
      DO 45 I=1,4
   45 B(I,IC)=10000.*(S(I)-S0(I))
      B(5,IC)=10000.*((D(1)-D0(1))-LAMBDA*(D(2)-D0(2)))
   50 CONTINUE
      DO 55 I=1,5
   55 WRITE(8,60) (B(I,J),J=1,NC)
   60 FORMAT(1X,5E12.4)
      CLOSE(5)
      CLOSE(6)
      END
```

APPENDIX E

Computer Programs for Static Analysis of Cable Structures

E.1 Introduction

This Appendix lists four programs for static analysis of cable structures, using dynamic relaxation. They can be used for static analysis of plane or space trusses as well. The cable structures can be clad or unclad; the cladding panels are flat or warped quadrilaterals with straight edges, and can be represented by either four-force or five-force models.

E.2 The main routine

The structure of all the four programs consists of a main routine and four subroutines, as illustrated by the flow chart in Fig. E.1.

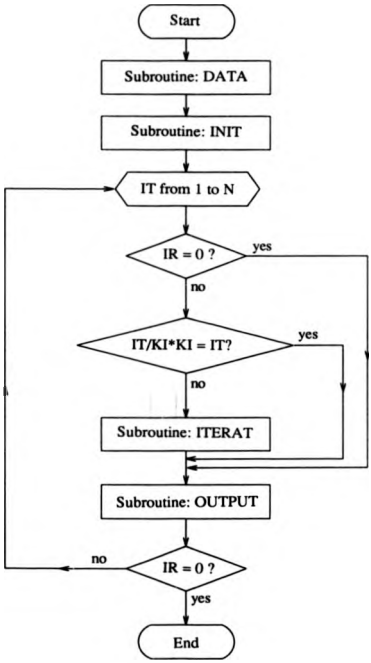

Fig. E.1 Flow chart of the main routine

Following the subroutines DATA and INIT, the main body of the program recurrently operates subroutine ITERAT. This recursive routine is controlled by three variables read into the subroutine DATA, which are:

N – the upper limit of the iteration number IT;

ER – a real variable representing the error or the residual force components; it does not appear in the body of the main routine but controls the iterative procedure through the value of another variable, IR. IR is initialised as 1 in subroutine INIT, and reset to 0 in subroutine ITERAT once all the residuals are found less than ER. The procedure continues if IR = 1 and stops to give the final output when IR = 0;

KI – a control integer for intermediate outputs during iterations: whenever the iteration number, IT, divides by KI (IT/KI*KI=IT in FORTRAN language) the subroutine OUTPUT is called.

A detailed discussion of one of the programs is presented, with the remaining programs discussed only in terms of the relative differences.

E.3 Program SACSV1

In this program viscous damping is used. The program is based on the recurrent formulae listed in Section 8.2.2. The subroutines DATA, INIT and ITERAT are

discussed below.

E.3.1 Subroutine DATA

All the data concerning the structure is input, through an input file, in free format. The subroutine requires the following information:

NJTS – Number of joints (including boundary joints);

NBJ – Number of boundary joints;

NCABL – Number of cable members (or bars in the case of a truss or pin-jointed frame);

NPANL – Number of panels;

ND – Dimension of the problem (ND = 2 or 3);

EMODE1, EMODE2 – Young's moduli of cable members (or bars);

MGF – Number of generalised forces in the panel model (MGF = 4 or 5);

ER – Error or residual;

KI – Control integer, stating after how many iterations an intermediate output should be printed.

N – Allowed maximum number of iterations;

BI, CI – Optimised dynamic relaxation parameters;

PNODE – Nodal load components;

XNODE – Nodal coordinates;

NBJT – Number of boundary joints;

MCABL – Cable member (including substitutive bars for panels) end numbers;

PREST – Prestresses of cable members;

AR – Cross section areas of cable members;

LAMBDA – λ of a panel (discussed in Section 6.2.1);

MPANL – Reference numbers of panels (identified by cable member numbers);

STIFF – Stiffness matrices of panels.

The two Young's moduli are considered only in the case of a truss, in which members in tension can be different in material from those in compression.

As has been discussed in Section 7.2.3, a quadrilateral panel can be replaced by a group of six bars, provided the five-force model is used (In the case of four force model, obviously, a group of four bars is a suitable substitute). In this program, and in the other three, a panel is defined by these bars, with a bar and a cable member that coincide, identified by the same number, as shown in Fig. 7.4.

In the subroutine, three further constants are introduced, concerning the panel-bar interchange:

NM – A constant depending on MGF: NM = 0 when MGF = 4; NM = 1 when MGF = 5 (NM=MGF/5 in FORTRAN language);

NI – Total number of cable members and additional diagonal bars (this is transmitted to other subroutines through the common block, C3);

NMS – Number of bars replacing a panel.

E.3.2 Subroutine INIT

In this subroutine, the following arrays are initialized as zero:

VNODE – Nodal velocity components;

DNODE – Nodal displacement components;

DCABL – Cable member extensions;

FPANL – Panel forces

LCABL, the array of original cable member lengths, is calculated from the coordinates of cable ends:

$$L_{jk}^{0} = \sqrt{\sum_{i=1}^{3} (X_{ki} - X_{ji})^2}$$

FCABL, the array of cable member forces, is initially given the values of PREST.

SNODE, the array of nodal stiffness components, is calculated using the following formula:

$$s_{ji} = \sum_{n=1}^{N_j} (s_{ni}^{e} + s_{ni}^{g})$$

where (See Ref. [39])

N_j is the number of cable members and bars (for simplification the diagonal bars are excluded) meeting at node j;

s_{ni}^{e} represents the elastic stiffness components in direction i, contributed by link n; if n is a panel link (a bar), s_{ni}^{e} is equal to the corresponding stiffness multiplied by c_{ni}^2, c_{ni} being the direction cosine of link n; if n represents a cable member, s_{ni}^{e} equals $\left(\frac{EA}{L_0} \right)_n \times c_{ni}^2$;

s_{ni}^{g} is the geometrical stiffness components in direction i, contributed by link n; for panel links this term is zero; for cable link n it is calculated by

$$s_{ni}^{g} = \frac{F_n^0}{L_n^0} (1 - c_{ni}^2) .$$

E.3.3 Subroutine ITERAT

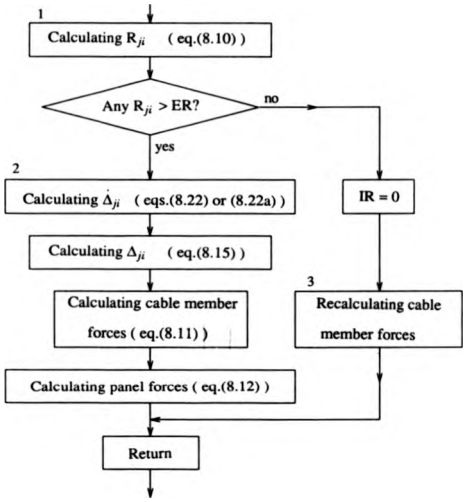

Fig. E.2 Flow chart of subroutine ITERAT

This subroutine performs calculation according to the recurrent formulae in Section 8.2.2. A flow chart of the subroutine is shown in Fig. E.2 in which the

superscripts denoting time are left out for simplicity. Further explanations of steps 1, 2 and 3 as marked on the flow chart are given below.

Step "1". The residual force components are calculated in the following order. Firstly, all the panel forces are added to relevant links; Secondly, the link forces (in cable members and bars) are transferred (projected) into nodal force components and these, when added to the external nodal loads, yield the residual forces.

Step "2". To simplify the expression for Δ_{ji} in eq.(8.22), two parameters are introduced:

$$A = 1 - CI\sqrt{BI},$$

and

$$C = 1 + CI\sqrt{BI} = 2 - A.$$

Step "3". The array of cable member forces, FCABL, which includes both the values of cable links and panel links (bars) after step "1", is restored to give the real cable forces before the final output.

```
C
C
C PROGRAM FOR STATIC ANALYSIS OF CABLE STRUCTURES
C  USING DYNAMIC RELAXATION WITH VISCOUS DAMPING
C    AND MASSES DIFFERING ABOUT DIRECTIONS
C
C
      PROGRAM SACSV1
      IMPLICIT REAL*8 (A-H,O-Z), INTEGER*4 (I-N)
       character*32 filein,fileo
      REAL*8 LCABL,LAMBDA
      COMMON XNODE(96,3),PNODE(96,3),FNODE(96,3),RNODE(96,3),
     1       VNODE(96,3),DNODE(96,3),SNODE(96,3),NBJT(40),
     2       MCABL(150,2),LCABL(150),FCABL(150),DCABL(150),
     3       PREST(150),AR(150),SE(150),MPANL(81,6),
     4       FPANL(81,5),STIFF(81,5,5),LAMBDA(81),GDM(5)
      COMMON /C1/NJTS,NBJ,NCABL,NI,NPANL,ND
      COMMON /C2/EMOD1,EMOD2
      COMMON /C3/KI,N,ER,IR,AI,BI,CI,MGF
       print *,'Input filename:'
       read(*,'(A)') filein
       open(7,file=filein)
       print *,'Output filename:'
       read(*,'(A)') fileo
       open(8,file=fileo,status='modify')
      CALL DATA
      CALL INIT
      DO 10 IT=1,N
      CALL ITERAT
      IF(IR.NE.0.AND.IT/KI*KI.NE.IT) GOTO 10
      CALL OUTPUT(IT)
      IF(IR.EQ.0) GOTO 20
   10 CONTINUE
   20 close(7)
      close(8)
      END
C
C
C INPUT DATA
C
C
      SUBROUTINE DATA
      IMPLICIT REAL*8 (A-H,O-Z), INTEGER*4 (I-N)
      REAL*8 LCABL,LAMBDA
      COMMON XNODE(96,3),PNODE(96,3),FNODE(96,3),RNODE(96,3),
     1       VNODE(96,3),DNODE(96,3),SNODE(96,3),NBJT(40),
     2       MCABL(150,2),LCABL(150),FCABL(150),DCABL(150),
     3       PREST(150),AR(150),SE(150),MPANL(81,6),
     4       FPANL(81,5),STIFF(81,5,5),LAMBDA(81),GDM(5)
      COMMON /C1/NJTS,NBJ,NCABL,NI,NPANL,ND
      COMMON /C2/EMOD1,EMOD2
      COMMON /C3/KI,N,ER,IR,AI,BI,CI,MGF
```

```
      READ(7,*) NJTS,NBJ,NCABL,NPANL,ND
      READ(7,*) EMOD1,EMOD2,MGF
      READ(7,*) ER,KI,N,BI,CI
      DO 5 I=1,NJTS
    5 READ(7,*) (PNODE(I,J),J=1,3),(XNODE(I,J),J=1,3)
      READ(7,*) (NBJT(I),I=1,NBJ)
      DO 10 I=1,NCABL
   10 READ(7,*) (MCABL(I,J),J=1,2),PREST(I),AR(I)
      NM=MGF/5
      NI=NCABL+2*NPANL*NM
      NMS=4+NM*2
      DO 15 I=NCABL+1,NI
   15 READ(7,*) (MCABL(I,J),J=1,2)
      DO 20 I=1,NPANL
   20 READ(7,*) LAMBDA(I),(MPANL(I,J),J=1,NMS)
      DO 25 I=1,NPANL
      DO 25 II=1,5
      READ(7,*) (STIFF(I,II,JJ),JJ=1,5)
   25 CONTINUE
      RETURN
      END
C
C
C INITIALISATION OF NODAL DISPLACEMENTS, NODAL VELOSITIES
C      AND OTHER VARIABLES
C
C
      SUBROUTINE INIT
      IMPLICIT REAL*8 (A-H,O-Z), INTEGER*4 (I-N)
      REAL*8 LCABL,LAMBDA
      COMMON XNODE(96,3),PNODE(96,3),FNODE(96,3),RNODE(96,3),
     1       VNODE(96,3),DNODE(96,3),SNODE(96,3),NBJT(40),
     2       MCABL(150,2),LCABL(150),FCABL(150),DCABL(150),
     3       PREST(150),AR(150),SE(150),MPANL(81,6),
     4       FPANL(81,5),STIFF(81,5,5),LAMBDA(81),GDM(5)
      COMMON /C1/NJTS,NBJ,NCABL,NI,NPANL,ND
      COMMON /C2/EMOD1,EMOD2
      COMMON /C3/KI,N,ER,IR,AI,BI,CI,MGF
      DO 5 I=1,NJTS
      DO 5 J=1,3
      VNODE(I,J)=0.
      DNODE(I,J)=0.
      SNODE(I,J)=0.
    5 CONTINUE
```

```
C
C  CALCULATING INITIAL LENGTH OF CABLE MEMBERS
C
      DO 15 I=1,NI
      DCABL(I)=0.
      SE(I)=0.
      M1=MCABL(I,1)
      M2=MCABL(I,2)
      S=0.
      DO 10 J=1,ND
   10 S=S+(XNODE(M2,J)-XNODE(M1,J))**2
   15 LCABL(I)=SQRT(S)
C
C  CALCULATING NODAL STIFFNESS
C
      DO 20 I=1,NPANL
      DO 20 J=1,4
      MJ=MPANL(I,J)
   20 IF(MJ.NE.0) SE(MJ)=SE(MJ)+STIFF(I,J,J)
      DO 25 I=1,NCABL
      M1=MCABL(I,1)
      M2=MCABL(I,2)
      FCABL(I)=PREST(I)
      TF=FCABL(I)/LCABL(I)
      IF(PREST(I).GE.0.)  SE(I)=SE(I)+EMOD1*AR(I)/LCABL(I)-TF
      IF(PREST(I).LT.0.)  SE(I)=SE(I)+EMOD2*AR(I)/LCABL(I)-TF
      DO 25 J=1,ND
      SNODE(M1,J)=SNODE(M1,J)+SE(I)*((XNODE(M1,J)-XNODE(M2,J))
     1            /LCABL(I))**2+TF
      SNODE(M2,J)=SNODE(M2,J)+SE(I)*((XNODE(M1,J)-XNODE(M2,J))
     1            /LCABL(I))**2+TF
   25 CONTINUE

      DO 30 I=1,NPANL
      DO 30 K=1,5
   30 FPANL(I,K)=0.
      IR=1
      AI=0.5
      WRITE(8,40)
   40 FORMAT(/45X,32(1H*)/45X,1H*,30X,1H*/45X,14H* ANALYSIS OF ,
     1       18HCLADDING-NETWORK */45X,1H*,11(1H ),8H(SACSV1),
     2       11(1H ),1H*/45X,1H*,30X,1H*/45X,32(1H*)
     3       //40X,9H***UNITS:,5X,12HFORCES IN KN,5X,
     4       11HLENGTH IN M//55X,9HNODE DATA/55X,9(1H-)
     5       /15X,9HJOINT NO.,5X,6HLOAD X,8X,6HLOAD Y,8X,
     6       6HLOAD Z,8X,7HCOORD X,7X,7HCOORD Y,7X,7HCOORD Z//)
      DO 45 I=1, NJTS
   45 WRITE(8,50) I, (PNODE(I,J),J=1,3),(XNODE(I,J),J=1,3)
   50 FORMAT(16X,I4,2X,6(3X,F11.6))
```

```
      WRITE(8,55)
   55 FORMAT(//52X,17HCABLE MEMBER DATA/52X,17(1H-)
     1 /27X,12HMEMBER NODES,9X,4HAREA,
     2 11X,13HINITIAL FORCE,5X,14HINITIAL LENGTH/)
      DO 60 I=1,NCABL
   60 WRITE(8,65) MCABL(I,1),MCABL(I,2),AR(I),PREST(I),LCABL(I)
   65 FORMAT(28X,I3,2X,I3,3(5X,F14.8))
      WRITE(8,70)
   70 FORMAT(//51X,5HEMOD1,9X,5HEMOD2)
      WRITE(8,75) EMOD1,EMOD2
   75 FORMAT(44X,2(3X,E11.4))
      IF(NPANL.GT.0) WRITE(8,80)
   80 FORMAT(//50X,11HPANEL SIDES,4X,6HLAMBDA
     1        /50X,11(1H-),4X,6(1H-))
      DO 85 I=1,NPANL
   85 WRITE(8,90) (MPANL(I,J),J=1,4),LAMBDA(I)
   90 FORMAT(47X,4(I3,1X),1X,F8.5)
      WRITE(8,95)
   95 FORMAT(//45X,2HBI,12X,2HCI,12X,2HER)
      WRITE(8,100) BI,CI,ER
  100 FORMAT(36X,3(4X,F10.6))
      RETURN
      END
C
C
C DYNAMIC RELAXATION PROCEDURE
C
C
      SUBROUTINE ITERAT
      IMPLICIT REAL*8 (A-H,O-Z), INTEGER*4 (I-N)
      REAL*8 LCABL,LAMBDA
      DIMENSION XTF(3)
      COMMON XNODE(96,3),PNODE(96,3),FNODE(96,3),RNODE(96,3),
     1       VNODE(96,3),DNODE(96,3),SNODE(96,3),NBJT(40),
     2       MCABL(150,2),LCABL(150),FCABL(150),DCABL(150),
     3       PREST(150),AR(150),SE(150),MPANL(81,6),
     4       FPANL(81,5),STIFF(81,5,5),LAMBDA(81),GDM(5)
      COMMON /C1/NJTS,NBJ,NCABL,NI,NPANL,ND,/C2/EMOD1,EMOD2
      COMMON /C3/KI,N,ER,IR,AI,BI,CI,MGF
      A=1.-CI*SQRT(BI)
      C=2.-A
      DO 5 I=1,NJTS
      DO 5 J=1,3
    5 FNODE(I,J)=0.
```

```
C
C  ADDING PANEL FORCES TO RELEVANT LINKS
C
      DO 10 I=1,NPANL
      I1=MPANL(I,1)
      I2=MPANL(I,2)
      I3=MPANL(I,3)
      I4=MPANL(I,4)
      IF(I1.NE.0) FCABL(I1)=FCABL(I1)+FPANL(I,1)
      IF(I2.NE.0) FCABL(I2)=FCABL(I2)+FPANL(I,2)
      IF(I3.NE.0) FCABL(I3)=FCABL(I3)+FPANL(I,3)
      IF(I4.NE.0) FCABL(I4)=FCABL(I4)+FPANL(I,4)
      IF(MGF.EQ.4) GOTO 10
      I5=MPANL(I,5)
      I6=MPANL(I,6)
      FCABL(I5)=FPANL(I,5)
      FCABL(I6)=-FPANL(I,5)*LAMBDA(I)
   10 CONTINUE
C
C  TRANSFERING LINK FORCES INTO NODAL FORCE COMPONENTS
C
      DO 20 I=1,NI
      M1=MCABL(I,1)
      M2=MCABL(I,2)
      CL=LCABL(I)+DCABL(I)
      TF=FCABL(I)/CL
      DO 15 J=1,ND
      DJ=XNODE(M2,J)+DNODE(M2,J)-XNODE(M1,J)-DNODE(M1,J)
      XTF(J)=TF*DJ
   15 CONTINUE
      DO 20 J=1,ND
      FNODE(M1,J)=FNODE(M1,J)-XTF(J)
      FNODE(M2,J)=FNODE(M2,J)+XTF(J)
   20 CONTINUE
C
C  CURRENT RESIDUALS AT INNER JOINTS
C
      DO 30 I=1, NJTS
      DO 30 J=1,3
      RNODE(I,J)=-FNODE(I,J)+PNODE(I,J)
   30 CONTINUE
C
C  CHECKING WHETHER RESIDUALS ARE CLOSE TO ER-ACCURACY
C
      DO 50 I=1,NJTS
      DO 40 K=1,NBJ
   40 IF(I.EQ.NBJT(K)) GOTO 50
      DO 45 J=1,ND
   45 IF(ABS(RNODE(I,J)).GT.ER) GOTO 60
   50 CONTINUE
      IR=0
```

```
C
C  CALCULATING REAL CABLE MEMBER FORCES FOR OUTPUT
C
      DO 55 I=1,NPANL
      I1=MPANL(I,1)
      I2=MPANL(I,2)
      I3=MPANL(I,3)
      I4=MPANL(I,4)
      IF(I1.NE.0) FCABL(I1)=FCABL(I1)-FPANL(I,1)
      IF(I2.NE.0) FCABL(I2)=FCABL(I2)-FPANL(I,2)
      IF(I3.NE.0) FCABL(I3)=FCABL(I3)-FPANL(I,3)
      IF(I4.NE.0) FCABL(I4)=FCABL(I4)-FPANL(I,4)
   55 CONTINUE
      GOTO 150
C
C  CALCULATING VELOCITIES AND DISPLACEMENTS AT INNER JOINTS
C
   60 DO 75 I=1,NJTS
      DO 65 K=1,NBJ
   65 IF(I.EQ.NBJT(K)) GOTO 75
      DO 70 J=1,ND
      VNODE(I,J)=(A*VNODE(I,J)+BI*RNODE(I,J)/SNODE(I,J))/C
      IF(AI.LT.0.8) VNODE(I,J)=BI*RNODE(I,J)/SNODE(I,J)/2.
   70 DNODE(I,J)=DNODE(I,J)+VNODE(I,J)
   75 CONTINUE
      AI=1.
C
C  CHANGE IN LENGTH OF CABLE MEMBERS
C
      DO 125 I=1,NI
      M1=MCABL(I,1)
      M2=MCABL(I,2)
      S=0.
      DO 120 J=1,ND
  120 S=S+(XNODE(M1,J)+DNODE(M1,J)-XNODE(M2,J)-DNODE(M2,J))**2
      DCABL(I)=SQRT(S)-LCABL(I)
C
C  CURRENT FORCE IN CABLE MEMBERS
C
      IF(PREST(I).GE.0.)
     1 FCABL(I)=PREST(I)+DCABL(I)*EMOD1*AR(I)/LCABL(I)
      IF(PREST(I).LT.0.)
     1 FCABL(I)=PREST(I)+DCABL(I)*EMOD2*AR(I)/LCABL(I)
      IF(FCABL(I).LT.0.0.AND.PREST(I).GT.0.0) FCABL(I)=0.0
  125 CONTINUE
```

```
C
C  CURRENT FORCE IN PANELS
C
      DO 145 I=1,NPANL
      DO 130 J=1,5
  130 GDM(J)=0.
      I1=MPANL(I,1)
      I2=MPANL(I,2)
      I3=MPANL(I,3)
      I4=MPANL(I,4)
      IF(I1.NE.0) GDM(1)=DCABL(I1)
      IF(I2.NE.0) GDM(2)=DCABL(I2)
      IF(I3.NE.0) GDM(3)=DCABL(I3)
      IF(I4.NE.0) GDM(4)=DCABL(I4)
      IF(MGF.EQ.4) GOTO 135
      I5=MPANL(I,5)
      I6=MPANL(I,6)
      GDM(5)=DCABL(I5)-DCABL(I6)*LAMBDA(I)
  135 DO 140 II=1,MGF
      FPANL(I,II)=0.
      DO 140 JJ=1,MGF
      FPANL(I,II)=FPANL(I,II)+STIFF(I,II,JJ)*GDM(JJ)
  140 CONTINUE
  145 CONTINUE
  150 CONTINUE
      RETURN
      END
```

```
C
C
C FINAL OUTPUT
C
C
      SUBROUTINE OUTPUT(IT)
      IMPLICIT REAL*8 (A-H,O-Z), INTEGER*4 (I-N)
      REAL*8 LCABL,LAMBDA
      COMMON XNODE(96,3),PNODE(96,3),FNODE(96,3),RNODE(96,3),
     1       VNODE(96,3),DNODE(96,3),SNODE(96,3),NBJT(40),
     2       MCABL(150,2),LCABL(150),FCABL(150),DCABL(150),
     3       PREST(150),AR(150),SE(150),MPANL(81,6),
     4       FPANL(81,5),STIFF(81,5,5),LAMBDA(81),GDM(5)
      COMMON /C1/NJTS,NBJ,NCABL,NI,NPANL,ND
      WRITE(8,5) IT
    5 FORMAT(//8X,15H**ITERATION NO.,1X,I5/10X,19(1H-))
      WRITE(8,10)
   10 FORMAT(/15X,9HJOINT NO.,5X,6HDISP X,7X,6HDISP Y,7X,
     1       6HDISP Z,10X,5HRES X,8X,5HRES Y,8X,5HRES Z/)
      DO 25 I=1, NJTS
      DO 15 K=1,NBJ
   15 IF(I.EQ.NBJT(K)) GOTO 20
      WRITE(8,30) I,(DNODE(I,J),J=1,3),(RNODE(I,J),J=1,3)
      GOTO 25
   20 WRITE(8,35) I,(DNODE(I,J),J=1,3),(RNODE(I,J),J=1,3)
   25 CONTINUE
   30 FORMAT(17X,I4,5X,3(E11.4,2X),3(2X,E11.4))
   35 FORMAT(15X,2H**,I4,5X,3(E11.4,2X),3(2X,E11.4))
      WRITE(8,40)
   40 FORMAT(//32X,10HJOINT REFS,12X,11HCABLE FORCE,14X,
     1       9HEXTENSION/)
      DO 45 I=1,NCABL
   45 WRITE(8,50) MCABL(I,1),MCABL(I,2),FCABL(I),DCABL(I)
   50 FORMAT(33X,I3,2X,I3,2(10X,F14.8))
      IF(NPANL.GT.0) WRITE(8,55)
   55 FORMAT(//17X,9HSIDE REFS,40X,11HPANEL FORCE/)
      DO 60 I=1,NPANL
   60 WRITE(8,65) (MPANL(I,J),J=1,4),(FPANL(I,J),J=1,5)
   65 FORMAT(13X,4(I3,1X),2X,5(1X,F14.8))
      RETURN
      END
```

E.4 Programs SACSK1, SACSK2 and SACSK3

In all the three programs kinetic damping is used. The difference between them lies only in the adoption of fictitious masses:

In SACSK1 (pp.198-205), the mass components at a given node are identical in all directions. Masses at different nodes are proportional to the sums of the stiffnesses of all the links (except diagonal bars) meeting at the relevent node.

In SACSK2 (pp.206-213), as in SACSV1, the mass components are proportional to nodal stiffness components, namely, they vary not only from node to node, but also with directions.

In SACSK3 (pp.214-221), the mass components are proportional to nodal stiffness components, as in SACSK2 and SACSV1; in addition, the nodal stiffness components are recalculated each time when a peak value of kinetic energy of the system is detected. Unlike the other three programs, the nodal stiffness components in SACSK3 are calculated in subroutine ITERATE, instead of INIT.

```
C
C
C PROGRAM FOR STATIC ANALYSIS OF CABLE STRUCTURES
C  USING DYNAMIC RELAXATION WITH KINETIC DAMPING
C   AND MASSES IDENTICAL IN ALL DIRECTIONS
C
C
      PROGRAM SACSK1
      IMPLICIT REAL*8 (A-H,O-Z), INTEGER*4 (I-N)
       character*32 filein,fileo
      REAL*8 LCABL,LAMBDA
      COMMON XNODE(96,3),PNODE(96,3),FNODE(96,3),RNODE(96,3),
     1       VNODE(96,3),DNODE(96,3),SI(96),NBJT(40),
     2       MCABL(150,2),LCABL(150),FCABL(150),DCABL(150),
     3       PREST(150),AR(150),SE(150),MPANL(81,6),
     4       FPANL(81,5),STIFF(81,5,5),LAMBDA(81),GDM(5)
      COMMON /C1/NJTS,NBJ,NCABL,NI,NPANL,N
      COMMON /C2/EMOD1,EMOD2
      COMMON /C3/KI,ER,IR,ENERGY(3),MGF,AI,BI
       print *,'Input filename:'
       read(*,'(A)') filein
       open(7,file=filein)
       print *,'Output filename:'
       read(*,'(A)') fileo
       open(8,file=fileo,status='modify')
      CALL DATA
      CALL INIT
      DO 10 IT=1,N
      CALL ITERAT
      IF(IR.NE.0.AND.IT/KI*KI.NE.IT) GOTO 10
      CALL OUTPUT(IT)
      IF(IR.EQ.0) GOTO 20
   10 CONTINUE
   20 close(7)
      close(8)
      END
C
C
C INPUT DATA
C
C
      SUBROUTINE DATA
      IMPLICIT REAL*8 (A-H,O-Z), INTEGER*4 (I-N)
      REAL*8 LCABL,LAMBDA
      COMMON XNODE(96,3),PNODE(96,3),FNODE(96,3),RNODE(96,3),
     1       VNODE(96,3),DNODE(96,3),SI(96),NBJT(40),
     2       MCABL(150,2),LCABL(150),FCABL(150),DCABL(150),
     3       PREST(150),AR(150),SE(150),MPANL(81,6),
     4       FPANL(81,5),STIFF(81,5,5),LAMBDA(81),GDM(5)
      COMMON /C1/NJTS,NBJ,NCABL,NI,NPANL,N
      COMMON /C2/EMOD1,EMOD2
      COMMON /C3/KI,ER,IR,ENERGY(3),MGF,AI,BI
```

```
      READ(7,*) NJTS,NBJ,NCABL,NPANL
      READ(7,*) EMOD1,EMOD2,MGF
      READ(7,*) ER,KI,N,BI
      DO 5 I=1,NJTS
    5 READ(7,*) (PNODE(I,J),J=1,3),(XNODE(I,J),J=1,3)
      READ(7,*) (NBJT(I),I=1,NBJ)
      DO 10 I=1,NCABL
   10 READ(7,*) (MCABL(I,J),J=1,2),PREST(I),AR(I)
      NM=MGF/5
      NI=NCABL+2*NPANL*NM
      NMS=4+NM*2
      DO 15 I=NCABL+1,NI
   15 READ(7,*) (MCABL(I,J),J=1,2)
      DO 20 I=1,NPANL
   20 READ(7,*) LAMBDA(I),(MPANL(I,J),J=1,NMS)
      DO 25 I=1,NPANL
      DO 25 II=1,5
      READ(7,*) (STIFF(I,II,JJ),JJ=1,5)
   25 CONTINUE
      RETURN
      END
C
C
C INITIALISATION OF NODAL DISPLACEMENTS, NODAL VELOSITIES
C      AND OTHER VARIABLES
C
C
      SUBROUTINE INIT
      IMPLICIT REAL*8 (A-H,O-Z), INTEGER*4 (I-N)
      REAL*8 LCABL,LAMBDA
      COMMON XNODE(96,3),PNODE(96,3),FNODE(96,3),RNODE(96,3),
     1       VNODE(96,3),DNODE(96,3),SI(96),NBJT(40),
     2       MCABL(150,2),LCABL(150),FCABL(150),DCABL(150),
     3       PREST(150),AR(150),SE(150),MPANL(81,6),
     4       FPANL(81,5),STIFF(81,5,5),LAMBDA(81),GDM(5)
      COMMON /C1/NJTS,NBJ,NCABL,NI,NPANL,N
      COMMON /C2/EMOD1,EMOD2
      COMMON /C3/KI,ER,IR,ENERGY(3),MGF,AI,BI
      DO 5 I=1,NJTS
      SI(I)=0.
      DO 5 J=1,3
      VNODE(I,J)=0.
      DNODE(I,J)=0.
    5 CONTINUE
```

```
C
C  CALCULATING INITIAL LENGTH OF CABLE MEMBERS
C
      DO 15 I=1,NI
      DCABL(I)=0.
      IF(I.LE.NCABL) SE(I)=0.
      M1=MCABL(I,1)
      M2=MCABL(I,2)
      S=0.
      DO 10 J=1,3
   10 S=S+(XNODE(M2,J)-XNODE(M1,J))**2
   15 LCABL(I)=SQRT(S)
C
C CALCULATING MAXIMUM POSSIBLE STIFFNESS AT INNER JOINTS
C
      DO 20 I=1,NPANL
      DO 20 J=1,4
      MJ=MPANL(I,J)
   20 IF(MJ.NE.0) SE(MJ)=SE(MJ)+STIFF(I,J,J)
      DO 25 I=1,NCABL
      FCABL(I)=PREST(I)
      M1=MCABL(I,1)
      M2=MCABL(I,2)
      IF(PREST(I).GE.0.)
     1  SE(I)=SE(I)+(EMOD1*AR(I)+PREST(I))/LCABL(I)
      IF(PREST(I).LT.0.)
     1  SE(I)=SE(I)+(EMOD2*AR(I)+PREST(I))/LCABL(I)
      SI(M1)=SI(M1)+SE(I)
      SI(M2)=SI(M2)+SE(I)
   25 CONTINUE
      AI=0.5
      DO 30 I=1,NPANL
      DO 30 K=1,5
   30 FPANL(I,K)=0.
      IR=1
      DO 35 I=1,3
   35 ENERGY(I)=0.
      WRITE(8,40)
   40 FORMAT(/45X,32(1H*)/45X,1H*,30X,1H*/45X,14H* ANALYSIS OF ,
     1       18HCLADDING-NETWORK */45X,1H*,11(1H ),8H(SACSK1),
     2       11(1H ),1H*/45X,1H*,30X,1H*/45X,32(1H*)
     3       //40X,9H***UNITS:,5X,12HFORCES IN KN,5X,
     4       11HLENGTH IN M//55X,9HNODE DATA/55X,9(1H-)
     5       /15X,9HJOINT NO.,5X,6HLOAD X,8X,6HLOAD Y,8X,
     6       6HLOAD Z,8X,7HCOORD X,7X,7HCOORD Y,7X,7HCOORD Z//)
      DO 45 I=1, NJTS
   45 WRITE(8,50) I, (PNODE(I,J),J=1,3),(XNODE(I,J),J=1,3)
   50 FORMAT(16X,I4,2X,6(3X,F11.6))
```

```
      WRITE(8,55)
   55 FORMAT(//52X,17HCABLE MEMBER DATA/52X,17(1H-)
     1 /27X,12HMEMBER NODES,9X,4HAREA,
     2 11X,13HINITIAL FORCE,5X,14HINITIAL LENGTH/)
      DO 60 I=1,NCABL
   60 WRITE(8,65) MCABL(I,1),MCABL(I,2),AR(I),PREST(I),LCABL(I)
   65 FORMAT(28X,I3,2X,I3,3(5X,F14.8))
      WRITE(8,70)
   70 FORMAT(//51X,5HEMOD1,9X,5HEMOD2)
      WRITE(8,75) EMOD1,EMOD2
   75 FORMAT(44X,2(3X,E11.4))
      IF(NPANL.GT.0) WRITE(8,80)
   80 FORMAT(//50X,11HPANEL SIDES,4X,6HLAMBDA
     1        /50X,11(1H-),4X,6(1H-))
      DO 85 I=1,NPANL
   85 WRITE(8,90) (MPANL(I,J),J=1,4),LAMBDA(I)
   90 FORMAT(47X,4(I3,1X),1X,F8.5)
      WRITE(8,95)
   95 FORMAT(//53X,2HBI,12X,2HER)
      WRITE(8,100) BI,ER
  100 FORMAT(44X,2(4X,F10.6))
      RETURN
      END
C
C
C DYNAMIC RELAXATION PROCEDURE
C
C
      SUBROUTINE ITERAT
      IMPLICIT REAL*8 (A-H,O-Z), INTEGER*4 (I-N)
      REAL*8 LCABL,LAMBDA
      DIMENSION XTF(3)
      COMMON XNODE(96,3),PNODE(96,3),FNODE(96,3),RNODE(96,3),
     1       VNODE(96,3),DNODE(96,3),SI(96),NBJT(40),
     2       MCABL(150,2),LCABL(150),FCABL(150),DCABL(150),
     3       PREST(150),AR(150),SE(150),MPANL(81,6),
     4       FPANL(81,5),STIFF(81,5,5),LAMBDA(81),GDM(5)
      COMMON /C1/NJTS,NBJ,NCABL,NI,NPANL,N
      COMMON /C2/EMOD1,EMOD2
      COMMON /C3/KI,ER,IR,ENERGY(3),MGF,AI,BI
      DO 5 I=1,NJTS
      DO 5 J=1,3
    5 FNODE(I,J)=0.
```

```
C
C  ADDING PANEL FORCES TO RELEVANT LINKS
C
      DO 10 I=1,NPANL
      I1=MPANL(I,1)
      I2=MPANL(I,2)
      I3=MPANL(I,3)
      I4=MPANL(I,4)
      IF(I1.NE.0) FCABL(I1)=FCABL(I1)+FPANL(I,1)
      IF(I2.NE.0) FCABL(I2)=FCABL(I2)+FPANL(I,2)
      IF(I3.NE.0) FCABL(I3)=FCABL(I3)+FPANL(I,3)
      IF(I4.NE.0) FCABL(I4)=FCABL(I4)+FPANL(I,4)
      IF(MGF.EQ.4) GOTO 10
      I5=MPANL(I,5)
      I6=MPANL(I,6)
      FCABL(I5)=FPANL(I,5)
      FCABL(I6)=-FPANL(I,5)*LAMBDA(I)
   10 CONTINUE
C
C  TRANSFERING LINK FORCES INTO NODAL FORCE COMPONENTS
C
      DO 20 I=1,NI
      M1=MCABL(I,1)
      M2=MCABL(I,2)
      TF=FCABL(I)/(LCABL(I)+DCABL(I))
      DO 15 J=1,3
   15 XTF(J)=TF*(XNODE(M2,J)+DNODE(M2,J)-XNODE(M1,J)-DNODE(M1,J))
      DO 20 J=1,3
      FNODE(M1,J)=FNODE(M1,J)-XTF(J)
      FNODE(M2,J)=FNODE(M2,J)+XTF(J)
   20 CONTINUE
C
C  CURRENT RESIDUALS AT INNER JOINTS
C
      DO 30 I=1, NJTS
      DO 30 J=1,3
      RNODE(I,J)=-FNODE(I,J)+PNODE(I,J)
   30 CONTINUE
C
C  CHECKING WHETHER RESIDUALS ARE CLOSE TO ER-ACCURACY
C
      DO 50 I=1,NJTS
      DO 40 K=1,NBJ
   40 IF(I.EQ.NBJT(K)) GOTO 50
      DO 45 J=1,3
   45 IF(ABS(RNODE(I,J)).GT.ER) GOTO 60
   50 CONTINUE
      IR=0
```

```
C
C  CALCULATING REAL CABLE MEMBER FORCES FOR OUTPUT
C
      DO 55 I=1,NPANL
      I1=MPANL(I,1)
      I2=MPANL(I,2)
      I3=MPANL(I,3)
      I4=MPANL(I,4)
      IF(I1.NE.0) FCABL(I1)=FCABL(I1)-FPANL(I,1)
      IF(I2.NE.0) FCABL(I2)=FCABL(I2)-FPANL(I,2)
      IF(I3.NE.0) FCABL(I3)=FCABL(I3)-FPANL(I,3)
      IF(I4.NE.0) FCABL(I4)=FCABL(I4)-FPANL(I,4)
   55 CONTINUE
      GOTO 150
C
C  CALCULATING VELOCITIES AND DISPLACEMENTS AT INNER JOINTS
C
   60 DO 75 I=1,NJTS
      DO 65 K=1,NBJ
   65 IF(I.EQ.NBJT(K)) GOTO 75
      DO 70 J=1,3
      VNODE(I,J)=VNODE(I,J)+RNODE(I,J)*AI*BI/SI(I)
      DNODE(I,J)=DNODE(I,J)+VNODE(I,J)
C
C  KINETIC ENERGY
C
   70 ENERGY(3)=ENERGY(3)+VNODE(I,J)**2*SI(I)
   75 CONTINUE
      IF(ENERGY(3).GT.ENERGY(2)) GOTO 110
      ALPHA=(ENERGY(3)-ENERGY(2))/
     1      (ENERGY(1)-2.*ENERGY(2)+ENERGY(3))
      DO 100 I=1,NJTS
      DO 80 K=1,NBJ
   80 IF(I.EQ.NBJT(K)) GOTO 100
      DO 90 J=1,3
      DNODE(I,J)=DNODE(I,J)-(1.+ALPHA)*VNODE(I,J)
     1          +2.*ALPHA*RNODE(I,J)/SI(I)
   90 VNODE(I,J)=0.
  100 CONTINUE
      DO 105 I=1,3
  105 ENERGY(I)=0.
      AI=0.5
      GOTO 115
  110 ENERGY(1)=ENERGY(2)
      ENERGY(2)=ENERGY(3)
      ENERGY(3)=0.
      AI=1.
```

```
C
C  CHANGE IN LENGTH OF CABLE MEMBERS
C
  115 DO 125 I=1,NI
      M1=MCABL(I,1)
      M2=MCABL(I,2)
      S=0.
      DO 120 J=1,3
  120 S=S+(XNODE(M1,J)+DNODE(M1,J)-XNODE(M2,J)-DNODE(M2,J))**2
      DCABL(I)=SQRT(S)-LCABL(I)
C
C  CURRENT FORCE IN CABLE MEMBERS
C
      IF(PREST(I).GE.0.)
     1 FCABL(I)=PREST(I)+DCABL(I)*EMOD1*AR(I)/LCABL(I)
      IF(PREST(I).LT.0.)
     1 FCABL(I)=PREST(I)+DCABL(I)*EMOD2*AR(I)/LCABL(I)
      IF(FCABL(I).LT.0.0.AND.PREST(I).GT.0.0) FCABL(I)=0.0
  125 CONTINUE
C
C  CURRENT FORCE IN PANELS
C
      DO 145 I=1,NPANL
      DO 130 J=1,5
  130 GDM(J)=0.
      I1=MPANL(I,1)
      I2=MPANL(I,2)
      I3=MPANL(I,3)
      I4=MPANL(I,4)
      IF(I1.NE.0) GDM(1)=DCABL(I1)
      IF(I2.NE.0) GDM(2)=DCABL(I2)
      IF(I3.NE.0) GDM(3)=DCABL(I3)
      IF(I4.NE.0) GDM(4)=DCABL(I4)
      IF(MGF.EQ.4) GOTO 135
      I5=MPANL(I,5)
      I6=MPANL(I,6)
      GDM(5)=DCABL(I5)-DCABL(I6)*LAMBDA(I)
  135 DO 140 II=1,MGF
      FPANL(I,II)=0.
      DO 140 JJ=1,MGF
      FPANL(I,II)=FPANL(I,II)+STIFF(I,II,JJ)*GDM(JJ)
  140 CONTINUE
  145 CONTINUE
  150 CONTINUE
      RETURN
      END
```

```
C
C
C FINAL OUTPUT
C
C
      SUBROUTINE OUTPUT(IT)
      IMPLICIT REAL*8 (A-H,O-Z), INTEGER*4 (I-N)
      REAL*8 LCABL,LAMBDA
      COMMON XNODE(96,3),PNODE(96,3),FNODE(96,3),RNODE(96,3),
     1       VNODE(96,3),DNODE(96,3),SI(96),NBJT(40),
     2       MCABL(150,2),LCABL(150),FCABL(150),DCABL(150),
     3       PREST(150),AR(150),SE(150),MPANL(81,6),
     4       FPANL(81,5),STIFF(81,5,5),LAMBDA(81),GDM(5)
      COMMON /C1/NJTS,NBJ,NCABL,NI,NPANL,N
      WRITE(8,5) IT
    5 FORMAT(//8X,15H**ITERATION NO.,1X,I5/10X,19(1H-))
      WRITE(8,10)
   10 FORMAT(/15X,9HJOINT NO.,5X,6HDISP X,7X,6HDISP Y,7X,
     1       6HDISP Z,10X,5HRES X,8X,5HRES Y,8X,5HRES Z/)
      DO 25 I=1, NJTS
      DO 15 K=1,NBJ
   15 IF(I.EQ.NBJT(K)) GOTO 20
      WRITE(8,30) I,(DNODE(I,J),J=1,3),(RNODE(I,J),J=1,3)
      GOTO 25
   20 WRITE(8,35) I,(DNODE(I,J),J=1,3),(RNODE(I,J),J=1,3)
   25 CONTINUE
   30 FORMAT(17X,I4,5X,3(E11.4,2X),3(2X,E11.4))
   35 FORMAT(15X,2H**,I4,5X,3(E11.4,2X),3(2X,E11.4))
      WRITE(8,40)
   40 FORMAT(//32X,10HJOINT REFS,12X,11HCABLE FORCE,14X,
     1       9HEXTENSION/)
      DO 45 I=1,NCABL
   45 WRITE(8,50) MCABL(I,1),MCABL(I,2),FCABL(I),DCABL(I)
   50 FORMAT(33X,I3,2X,I3,2(10X,F14.8))
      IF(NPANL.GT.0) WRITE(8,55)
   55 FORMAT(//17X,9HSIDE REFS,40X,11HPANEL FORCE/)
      DO 60 I=1,NPANL
   60 WRITE(8,65) (MPANL(I,J),J=1,4),(FPANL(I,J),J=1,5)
   65 FORMAT(13X,4(I3,1X),2X,5(1X,F14.8))
      RETURN
      END
```

```
C
C
C PROGRAM FOR STATIC ANALYSIS OF CABLE STRUCTURES
C  USING DYNAMIC RELAXATION WITH KINETIC DAMPING
C   AND MASSES DIFFERING ABOUT DIRECTIONS
C
C
      PROGRAM SACSK2
      IMPLICIT REAL*8 (A-H,O-Z), INTEGER*4 (I-N)
       character*32 filein,fileo
      REAL*8 LCABL,LAMBDA
      COMMON XNODE(96,3),PNODE(96,3),FNODE(96,3),RNODE(96,3),
     1       VNODE(96,3),DNODE(96,3),SNODE(96,3),NBJT(40),
     2       MCABL(150,2),LCABL(150),FCABL(150),DCABL(150),
     3       PREST(150),AR(150),SE(150),MPANL(81,6),
     4       FPANL(81,5),STIFF(81,5,5),LAMBDA(81),GDM(5)
      COMMON /C1/NJTS,NBJ,NCABL,NI,NPANL,ND
      COMMON /C2/EMOD1,EMOD2
      COMMON /C3/KI,N,ER,IR,AI,BI,ENERGY(3),MGF
       print *,'Input filename:'
       read(*,'(A)') filein
       open(7,file=filein)
       print *,'Output filename:'
       read(*,'(A)') fileo
       open(8,file=fileo,status='modify')
      CALL DATA
      CALL INIT
      DO 10 IT=1,N
      CALL ITERAT
      IF(IR.NE.0.AND.IT/KI*KI.NE.IT) GOTO 10
      CALL OUTPUT(IT)
      IF(IR.EQ.0) GOTO 20
   10 CONTINUE
   20 close(7)
      close(8)
      END
C
C
C INPUT DATA
C
C
      SUBROUTINE DATA
      IMPLICIT REAL*8 (A-H,O-Z), INTEGER*4 (I-N)
      REAL*8 LCABL,LAMBDA
      COMMON XNODE(96,3),PNODE(96,3),FNODE(96,3),RNODE(96,3),
     1       VNODE(96,3),DNODE(96,3),SNODE(96,3),NBJT(40),
     2       MCABL(150,2),LCABL(150),FCABL(150),DCABL(150),
     3       PREST(150),AR(150),SE(150),MPANL(81,6),
     4       FPANL(81,5),STIFF(81,5,5),LAMBDA(81),GDM(5)
      COMMON /C1/NJTS,NBJ,NCABL,NI,NPANL,ND
      COMMON /C2/EMOD1,EMOD2
      COMMON /C3/KI,N,ER,IR,AI,BI,ENERGY(3),MGF
```

```
      READ(7,*) NJTS,NBJ,NCABL,NPANL,ND
      READ(7,*) EMOD1,EMOD2,MGF
      READ(7,*) ER,KI,N,BI
      DO 5 I=1,NJTS
    5 READ(7,*) (PNODE(I,J),J=1,3),(XNODE(I,J),J=1,3)
      READ(7,*) (NBJT(I),I=1,NBJ)
      DO 10 I=1,NCABL
   10 READ(7,*) (MCABL(I,J),J=1,2),PREST(I),AR(I)
      NM=MGF/5
      NI=NCABL+2*NPANL*NM
      NMS=4+NM*2
      DO 15 I=NCABL+1,NI
   15 READ(7,*) (MCABL(I,J),J=1,2)
      DO 20 I=1,NPANL
   20 READ(7,*) LAMBDA(I),(MPANL(I,J),J=1,NMS)
      DO 25 I=1,NPANL
      DO 25 II=1,5
      READ(7,*) (STIFF(I,II,JJ),JJ=1,5)
   25 CONTINUE
      RETURN
      END
C
C
C INITIALISATION OF NODAL DISPLACEMENTS, NODAL VELOSITIES
C   AND OTHER VARIABLES
C
C
      SUBROUTINE INIT
      IMPLICIT REAL*8 (A-H,O-Z), INTEGER*4 (I-N)
      REAL*8 LCABL,LAMBDA
      COMMON XNODE(96,3),PNODE(96,3),FNODE(96,3),RNODE(96,3),
     1       VNODE(96,3),DNODE(96,3),SNODE(96,3),NBJT(40),
     2       MCABL(150,2),LCABL(150),FCABL(150),DCABL(150),
     3       PREST(150),AR(150),SE(150),MPANL(81,6),
     4       FPANL(81,5),STIFF(81,5,5),LAMBDA(81),GDM(5)
      COMMON /C1/NJTS,NBJ,NCABL,NI,NPANL,ND
      COMMON /C2/EMOD1,EMOD2
      COMMON /C3/KI,N,ER,IR,AI,BI,ENERGY(3),MGF
      DO 5 I=1,NJTS
      DO 5 J=1,3
      VNODE(I,J)=0.
      DNODE(I,J)=0.
      SNODE(I,J)=0.
    5 CONTINUE
```

```
C
C  CALCULATING INITIAL LENGTH OF CABLE MEMBERS
C
      DO 15 I=1,NI
      DCABL(I)=0.
      SE(I)=0.
      M1=MCABL(I,1)
      M2=MCABL(I,2)
      S=0.
      DO 10 J=1,ND
   10 S=S+(XNODE(M2,J)-XNODE(M1,J))**2
   15 LCABL(I)=SQRT(S)
C
C  CALCULATING NODAL STIFFNESS
C
      DO 20 I=1,NPANL
      DO 20 J=1,4
      MJ=MPANL(I,J)
   20 IF(MJ.NE.0) SE(MJ)=SE(MJ)+STIFF(I,J,J)
      DO 25 I=1,NCABL
      M1=MCABL(I,1)
      M2=MCABL(I,2)
      FCABL(I)=PREST(I)
      TF=FCABL(I)/LCABL(I)
      IF(PREST(I).GE.0.) SE(I)=SE(I)+EMOD1*AR(I)/LCABL(I)-TF
      IF(PREST(I).LT.0.) SE(I)=SE(I)+EMOD2*AR(I)/LCABL(I)-TF
      DO 25 J=1,ND
      SNODE(M1,J)=SNODE(M1,J)+SE(I)*((XNODE(M1,J)-XNODE(M2,J))
     1            /LCABL(I))**2+TF
      SNODE(M2,J)=SNODE(M2,J)+SE(I)*((XNODE(M1,J)-XNODE(M2,J))
     1            /LCABL(I))**2+TF
   25 CONTINUE
      DO 30 I=1,NPANL
      DO 30 K=1,5
   30 FPANL(I,K)=0.
      IR=1
      AI=0.5
      DO 35 I=1,3
   35 ENERGY(I)=0.
      WRITE(8,40)
   40 FORMAT(/45X,32(1H*)/45X,1H*,30X,1H*/45X,14H* ANALYSIS OF ,
     1       18HCLADDING-NETWORK */45X,1H*,11(1H ),8H(SACSK2),
     2       11(1H ),1H*/45X,1H*,30X,1H*/45X,32(1H*)
     3       //40X,9H***UNITS:,5X,12HFORCES IN KN,5X,
     4       11HLENGTH IN M//55X,9HNODE DATA/55X,9(1H-)
     5       /15X,9HJOINT NO.,5X,6HLOAD X,8X,6HLOAD Y,8X,
     6       6HLOAD Z,8X,7HCOORD X,7X,7HCOORD Y,7X,7HCOORD Z//)
      DO 45 I=1, NJTS
   45 WRITE(8,50) I, (PNODE(I,J),J=1,3),(XNODE(I,J),J=1,3)
   50 FORMAT(16X,I4,2X,6(3X,F11.6))
```

```
      WRITE(8,55)
   55 FORMAT(//52X,17HCABLE MEMBER DATA/52X,17(1H-)
     1 /27X,12HMEMBER NODES,9X,4HAREA,
     2 11X,13HINITIAL FORCE,5X,14HINITIAL LENGTH/)
      DO 60 I=1,NCABL
   60 WRITE(8,65) MCABL(I,1),MCABL(I,2),AR(I),PREST(I),LCABL(I)
   65 FORMAT(28X,I3,2X,I3,3(5X,F14.8))
      WRITE(8,70)
   70 FORMAT(//51X,5HEMOD1,9X,5HEMOD2)
      WRITE(8,75) EMOD1,EMOD2
   75 FORMAT(44X,2(3X,E11.4))
      IF(NPANL.GT.0) WRITE(8,80)
   80 FORMAT(//50X,11HPANEL SIDES,4X,6HLAMBDA
     1         /50X,11(1H-),4X,6(1H-))
      DO 85 I=1,NPANL
   85 WRITE(8,90) (MPANL(I,J),J=1,4),LAMBDA(I)
   90 FORMAT(47X,4(I3,1X),1X,F8.5)
      WRITE(8,95)
   95 FORMAT(//53X,2HBI,12X,2HER)
      WRITE(8,100) BI,ER
  100 FORMAT(44X,2(4X,F10.6))
      RETURN
      END
C
C
C DYNAMIC RELAXATION PROCEDURE
C
C
      SUBROUTINE ITERAT
      IMPLICIT REAL*8 (A-H,O-Z), INTEGER*4 (I-N)
      REAL*8 LCABL,LAMBDA
      DIMENSION XTF(3)
      COMMON XNODE(96,3),PNODE(96,3),FNODE(96,3),RNODE(96,3),
     1       VNODE(96,3),DNODE(96,3),SNODE(96,3),NBJT(40),
     2       MCABL(150,2),LCABL(150),FCABL(150),DCABL(150),
     3       PREST(150),AR(150),SE(150),MPANL(81,6),
     4       FPANL(81,5),STIFF(81,5,5),LAMBDA(81),GDM(5)
      COMMON /C1/NJTS,NBJ,NCABL,NI,NPANL,ND,/C2/EMOD1,EMOD2
      COMMON /C3/KI,N,ER,IR,AI,BI,ENERGY(3),MGF
      DO 5 I=1,NJTS
      DO 5 J=1,3
    5 FNODE(I,J)=0.
```

```
C
C  ADDING PANEL FORCES TO RELEVANT LINKS
C
      DO 10 I=1,NPANL
      I1=MPANL(I,1)
      I2=MPANL(I,2)
      I3=MPANL(I,3)
      I4=MPANL(I,4)
      IF(I1.NE.0) FCABL(I1)=FCABL(I1)+FPANL(I,1)
      IF(I2.NE.0) FCABL(I2)=FCABL(I2)+FPANL(I,2)
      IF(I3.NE.0) FCABL(I3)=FCABL(I3)+FPANL(I,3)
      IF(I4.NE.0) FCABL(I4)=FCABL(I4)+FPANL(I,4)
      IF(MGF.EQ.4) GOTO 10
      I5=MPANL(I,5)
      I6=MPANL(I,6)
      FCABL(I5)=FPANL(I,5)
      FCABL(I6)=-FPANL(I,5)*LAMBDA(I)
   10 CONTINUE
C
C  TRANSFERING LINK FORCES INTO NODAL FORCE COMPONENTS
C
      DO 20 I=1,NI
      M1=MCABL(I,1)
      M2=MCABL(I,2)
      CL=LCABL(I)+DCABL(I)
      TF=FCABL(I)/CL
      DO 15 J=1,ND
      DJ=XNODE(M2,J)+DNODE(M2,J)-XNODE(M1,J)-DNODE(M1,J)
      XTF(J)=TF*DJ
   15 CONTINUE
      DO 20 J=1,3
      FNODE(M1,J)=FNODE(M1,J)-XTF(J)
      FNODE(M2,J)=FNODE(M2,J)+XTF(J)
   20 CONTINUE
C
C  CURRENT RESIDUALS AT INNER JOINTS
C
      DO 30 I=1, NJTS
      DO 30 J=1,3
      RNODE(I,J)=-FNODE(I,J)+PNODE(I,J)
   30 CONTINUE
C
C  CHECKING WHETHER RESIDUALS ARE CLOSE TO ER-ACCURACY
C
      DO 50 I=1,NJTS
      DO 40 K=1,NBJ
   40 IF(I.EQ.NBJT(K)) GOTO 50
      DO 45 J=1,ND
   45 IF(ABS(RNODE(I,J)).GT.ER) GOTO 60
   50 CONTINUE
      IR=0
```

```
C
C  CALCULATING REAL CABLE MEMBER FORCES FOR OUTPUT
C
      DO 55 I=1,NPANL
      I1=MPANL(I,1)
      I2=MPANL(I,2)
      I3=MPANL(I,3)
      I4=MPANL(I,4)
      IF(I1.NE.0) FCABL(I1)=FCABL(I1)-FPANL(I,1)
      IF(I2.NE.0) FCABL(I2)=FCABL(I2)-FPANL(I,2)
      IF(I3.NE.0) FCABL(I3)=FCABL(I3)-FPANL(I,3)
      IF(I4.NE.0) FCABL(I4)=FCABL(I4)-FPANL(I,4)
   55 CONTINUE
      GOTO 150
C
C  CALCULATING VELOCITIES AND DISPLACEMENTS AT INNER JOINTS
C
   60 DO 75 I=1,NJTS
      DO 65 K=1,NBJ
   65 IF(I.EQ.NBJT(K)) GOTO 75
      DO 70 J=1,ND
      VNODE(I,J)=VNODE(I,J)+AI*BI*RNODE(I,J)/SNODE(I,J)
      DNODE(I,J)=DNODE(I,J)+VNODE(I,J)
C
C  KINETIC ENERGY
C
   70 ENERGY(3)=ENERGY(3)+VNODE(I,J)**2*SNODE(I,J)
   75 CONTINUE
      IF(ENERGY(3).GT.ENERGY(2)) GOTO 110
      ALPHA=(ENERGY(3)-ENERGY(2))/
     1      (ENERGY(1)-2.*ENERGY(2)+ENERGY(3))
      DO 100 I=1,NJTS
      DO 80 K=1,NBJ
   80 IF(I.EQ.NBJT(K)) GOTO 100
      DO 90 J=1,ND
      DNODE(I,J)=DNODE(I,J)-(1.+ALPHA)*VNODE(I,J)
     1           +BI*ALPHA*RNODE(I,J)/SNODE(I,J)
   90 VNODE(I,J)=0.
  100 CONTINUE
      DO 105 I=1,3
  105 ENERGY(I)=0.
      AI=0.5
      GOTO 115
  110 ENERGY(1)=ENERGY(2)
      ENERGY(2)=ENERGY(3)
      ENERGY(3)=0.
      AI=1.
```

```
C
C  CHANGE IN LENGTH OF CABLE MEMBERS
C
  115 DO 125 I=1,NI
      M1=MCABL(I,1)
      M2=MCABL(I,2)
      S=0.
      DO 120 J=1,ND
  120 S=S+(XNODE(M1,J)+DNODE(M1,J)-XNODE(M2,J)-DNODE(M2,J))**2
      DCABL(I)=SQRT(S)-LCABL(I)
C
C  CURRENT FORCES IN CABLE MEMBERS
C
      IF(PREST(I).GE.0.)
     1 FCABL(I)=PREST(I)+DCABL(I)*EMOD1*AR(I)/LCABL(I)
      IF(PREST(I).LT.0.)
     1 FCABL(I)=PREST(I)+DCABL(I)*EMOD2*AR(I)/LCABL(I)
      IF(FCABL(I).LT.0.0.AND.PREST(I).GT.0.0) FCABL(I)=0.0
  125 CONTINUE
C
C  CURRENT FORCES IN PANELS
C
      DO 145 I=1,NPANL
      DO 130 J=1,5
  130 GDM(J)=0.
      I1=MPANL(I,1)
      I2=MPANL(I,2)
      I3=MPANL(I,3)
      I4=MPANL(I,4)
      IF(I1.NE.0) GDM(1)=DCABL(I1)
      IF(I2.NE.0) GDM(2)=DCABL(I2)
      IF(I3.NE.0) GDM(3)=DCABL(I3)
      IF(I4.NE.0) GDM(4)=DCABL(I4)
      IF(MGF.EQ.4) GOTO 135
      I5=MPANL(I,5)
      I6=MPANL(I,6)
      GDM(5)=DCABL(I5)-DCABL(I6)*LAMBDA(I)
  135 DO 140 II=1,MGF
      FPANL(I,II)=0.
      DO 140 JJ=1,MGF
      FPANL(I,II)=FPANL(I,II)+STIFF(I,II,JJ)*GDM(JJ)
  140 CONTINUE
  145 CONTINUE
  150 CONTINUE
      RETURN
      END
```

```
C
C
C FINAL OUTPUT
C
C
      SUBROUTINE OUTPUT(IT)
      IMPLICIT REAL*8 (A-H,O-Z), INTEGER*4 (I-N)
      REAL*8 LCABL,LAMBDA
      COMMON XNODE(96,3),PNODE(96,3),FNODE(96,3),RNODE(96,3),
     1       VNODE(96,3),DNODE(96,3),SNODE(96,3),NBJT(40),
     2       MCABL(150,2),LCABL(150),FCABL(150),DCABL(150),
     3       PREST(150),AR(150),SE(150),MPANL(81,6),
     4       FPANL(81,5),STIFF(81,5,5),LAMBDA(81),GDM(5)
      COMMON /C1/NJTS,NBJ,NCABL,NI,NPANL,ND
      WRITE(8,5) IT
    5 FORMAT(//8X,15H**ITERATION NO.,1X,I5/10X,19(1H-))
      WRITE(8,10)
   10 FORMAT(/15X,9HJOINT NO.,5X,6HDISP X,7X,6HDISP Y,7X,
     1       6HDISP Z,10X,5HRES X,8X,5HRES Y,8X,5HRES Z/)
      DO 25 I=1, NJTS
      DO 15 K=1,NBJ
   15 IF(I.EQ.NBJT(K)) GOTO 20
      WRITE(8,30) I,(DNODE(I,J),J=1,3),(RNODE(I,J),J=1,3)
      GOTO 25
   20 WRITE(8,35) I,(DNODE(I,J),J=1,3),(RNODE(I,J),J=1,3)
   25 CONTINUE
   30 FORMAT(17X,I4,5X,3(E11.4,2X),3(2X,E11.4))
   35 FORMAT(15X,2H**,I4,5X,3(E11.4,2X),3(2X,E11.4))
      WRITE(8,40)
   40 FORMAT(//32X,10HJOINT REFS,12X,11HCABLE FORCE,14X,
     1       9HEXTENSION/)
      DO 45 I=1,NCABL
   45 WRITE(8,50) MCABL(I,1),MCABL(I,2),FCABL(I),DCABL(I)
   50 FORMAT(33X,I3,2X,I3,2(10X,F14.8))
      IF(NPANL.GT.0) WRITE(8,55)
   55 FORMAT(//17X,9HSIDE REFS,40X,11HPANEL FORCE/)
      DO 60 I=1,NPANL
   60 WRITE(8,65) (MPANL(I,J),J=1,4),(FPANL(I,J),J=1,5)
   65 FORMAT(13X,4(I3,1X),2X,5(1X,F14.8))
      RETURN
      END
```

```
C
C
C PROGRAM FOR STATIC ANALYSIS OF CABLE STRUCTURES
C  USING DYNAMIC RELAXATION WITH KINETIC DAMPING
C   AND MASSES DIFFERING ABOUT DIRECTIONS,
C    ADJUSTED AFTER PEAK KINETIC ENERGY
C
      PROGRAM SACSK3
      IMPLICIT REAL*8 (A-H,O-Z), INTEGER*4 (I-N)
       character*32 filein,fileo
      REAL*8 LCABL,LAMBDA
      COMMON XNODE(96,3),PNODE(96,3),FNODE(96,3),RNODE(96,3),
     1       VNODE(96,3),DNODE(96,3),SNODE(96,3),NBJT(40),
     2       MCABL(150,2),LCABL(150),FCABL(150),DCABL(150),
     3       PREST(150),AR(150),SE(150),MPANL(81,6),
     4       FPANL(81,5),STIFF(81,5,5),LAMBDA(81),GDM(5)
      COMMON /C1/NJTS,NBJ,NCABL,NI,NPANL,ND
      COMMON /C2/EMOD1,EMOD2
      COMMON /C3/KI,N,ER,IR,AI,BI,ENERGY(3),MGF
       print *,'Input filename:'
       read(*,'(A)') filein
       open(7,file=filein)
       print *,'Output filename:'
       read(*,'(A)') fileo
       open(8,file=fileo,status='modify')
      CALL DATA
      CALL INIT
      DO 10 IT=1,N
      CALL ITERAT
      IF(IR.NE.0.AND.IT/KI*KI.NE.IT) GOTO 10
      CALL OUTPUT(IT)
      IF(IR.EQ.0) GOTO 20
   10 CONTINUE
   20 close(7)
      close(8)
      END
C
C
C INPUT DATA
C
C
      SUBROUTINE DATA
      IMPLICIT REAL*8 (A-H,O-Z), INTEGER*4 (I-N)
      REAL*8 LCABL,LAMBDA
      COMMON XNODE(96,3),PNODE(96,3),FNODE(96,3),RNODE(96,3),
     1       VNODE(96,3),DNODE(96,3),SNODE(96,3),NBJT(40),
     2       MCABL(150,2),LCABL(150),FCABL(150),DCABL(150),
     3       PREST(150),AR(150),SE(150),MPANL(81,6),
     4       FPANL(81,5),STIFF(81,5,5),LAMBDA(81),GDM(5)
      COMMON /C1/NJTS,NBJ,NCABL,NI,NPANL,ND
      COMMON /C2/EMOD1,EMOD2
      COMMON /C3/KI,N,ER,IR,AI,BI,ENERGY(3),MGF
```

```
      READ(7,*) NJTS,NBJ,NCABL,NPANL,ND
      READ(7,*) EMOD1,EMOD2,MGF
      READ(7,*) ER,KI,N,BI
      DO 5 I=1,NJTS
    5 READ(7,*) (PNODE(I,J),J=1,3),(XNODE(I,J),J=1,3)
      READ(7,*) (NBJT(I),I=1,NBJ)
      DO 10 I=1,NCABL
   10 READ(7,*) (MCABL(I,J),J=1,2),PREST(I),AR(I)
      NM=MGF/5
      NI=NCABL+2*NPANL*NM
      NMS=4+NM*2
      DO 15 I=NCABL+1,NI
   15 READ(7,*) (MCABL(I,J),J=1,2)
      DO 20 I=1,NPANL
   20 READ(7,*) LAMBDA(I),(MPANL(I,J),J=1,NMS)
      DO 25 I=1,NPANL
      DO 25 II=1,5
      READ(7,*) (STIFF(I,II,JJ),JJ=1,5)
   25 CONTINUE
      RETURN
      END
C
C
C INITIALISATION OF NODAL DISPLACEMENTS, NODAL VELOSITIES
C      AND OTHER VARIABLES
C
C
      SUBROUTINE INIT
      IMPLICIT REAL*8 (A-H,O-Z), INTEGER*4 (I-N)
      REAL*8 LCABL,LAMBDA
      COMMON XNODE(96,3),PNODE(96,3),FNODE(96,3),RNODE(96,3),
     1       VNODE(96,3),DNODE(96,3),SNODE(96,3),NBJT(40),
     2       MCABL(150,2),LCABL(150),FCABL(150),DCABL(150),
     3       PREST(150),AR(150),SE(150),MPANL(81,6),
     4       FPANL(81,5),STIFF(81,5,5),LAMBDA(81),GDM(5)
      COMMON /C1/NJTS,NBJ,NCABL,NI,NPANL,ND
      COMMON /C2/EMOD1,EMOD2
      COMMON /C3/KI,N,ER,IR,AI,BI,ENERGY(3),MGF
      DO 5 I=1,NJTS
      DO 5 J=1,3
      VNODE(I,J)=0.
      DNODE(I,J)=0.
      SNODE(I,J)=0.
    5 CONTINUE
```

```
C
C  CALCULATING INITIAL LENGTH OF CABLE MEMBERS
C
      DO 15 I=1,NI
      DCABL(I)=0.
      SE(I)=0.
      M1=MCABL(I,1)
      M2=MCABL(I,2)
      S=0.
      DO 10 J=1,ND
   10 S=S+(XNODE(M2,J)-XNODE(M1,J))**2
   15 LCABL(I)=SQRT(S)
C
C ADDIING PANEL STIFFNESS TO RELEVANT CABLE MEMBER STIFFNESS
C
      DO 20 I=1,NPANL
      DO 20 J=1,4
      MJ=MPANL(I,J)
   20 IF(MJ.NE.0) SE(MJ)=SE(MJ)+STIFF(I,J,J)
      DO 25 I=1,NCABL
      M1=MCABL(I,1)
      M2=MCABL(I,2)
      FCABL(I)=PREST(I)
      IF(PREST(I).GE.0.) SE(I)=SE(I)+EMOD1*AR(I)/LCABL(I)
      IF(PREST(I).LT.0.) SE(I)=SE(I)+EMOD2*AR(I)/LCABL(I)
   25 CONTINUE
      DO 30 I=1,NPANL
      DO 30 K=1,5
   30 FPANL(I,K)=0.
      IR=1
      AI=0.5
      DO 35 I=1,3
   35 ENERGY(I)=0.
      WRITE(8,40)
   40 FORMAT(/45X,32(1H*)/45X,1H*,30X,1H*/45X,14H* ANALYSIS OF ,
     1       18HCLADDING-NETWORK */45X,1H*,11(1H ),8H(SACSK3),
     2       11(1H ),1H*/45X,1H*,30X,1H*/45X,32(1H*)
     3       //40X,9H***UNITS:,5X,12HFORCES IN KN,5X,
     4       11HLENGTH IN M//55X,9HNODE DATA/55X,9(1H-)
     5       /15X,9HJOINT NO.,5X,6HLOAD X,8X,6HLOAD Y,8X,
     6       6HLOAD Z,8X,7HCOORD X,7X,7HCOORD Y,7X,7HCOORD Z//)
      DO 45 I=1, NJTS
   45 WRITE(8,50) I, (PNODE(I,J),J=1,3),(XNODE(I,J),J=1,3)
   50 FORMAT(16X,I4,2X,6(3X,F11.6))
      WRITE(8,55)
   55 FORMAT(//52X,17HCABLE MEMBER DATA/52X,17(1H-)
     1 /27X,12HMEMBER NODES,9X,4HAREA,
     2 11X,13HINITIAL FORCE,5X,14HINITIAL LENGTH/)
```

```
      DO 60 I=1,NCABL
   60 WRITE(8,65) MCABL(I,1),MCABL(I,2),AR(I),PREST(I),LCABL(I)
   65 FORMAT(28X,I3,2X,I3,3(5X,F14.8))
      WRITE(8,70)
   70 FORMAT(//51X,5HEMOD1,9X,5HEMOD2)
      WRITE(8,75) EMOD1,EMOD2
   75 FORMAT(44X,2(3X,E11.4))
      IF(NPANL.GT.0) WRITE(8,80)
   80 FORMAT(//50X,11HPANEL SIDES,4X,6HLAMBDA
     1         /50X,11(1H-),4X,6(1H-))
      DO 85 I=1,NPANL
   85 WRITE(8,90) (MPANL(I,J),J=1,4),LAMBDA(I)
   90 FORMAT(47X,4(I3,1X),1X,F8.5)
      WRITE(8,95)
   95 FORMAT(//53X,2HBI,12X,2HER)
      WRITE(8,100) BI,ER
  100 FORMAT(44X,2(4X,F10.6))
      RETURN
      END
C
C
C DYNAMIC RELAXATION PROCEDURE
C
C
      SUBROUTINE ITERAT
      IMPLICIT REAL*8 (A-H,O-Z), INTEGER*4 (I-N)
      REAL*8 LCABL,LAMBDA
      DIMENSION XTF(3),SCABL(3)
      COMMON XNODE(96,3),PNODE(96,3),FNODE(96,3),RNODE(96,3),
     1       VNODE(96,3),DNODE(96,3),SNODE(96,3),NBJT(40),
     2       MCABL(150,2),LCABL(150),FCABL(150),DCABL(150),
     3       PREST(150),AR(150),SE(150),MPANL(81,6),
     4       FPANL(81,5),STIFF(81,5,5),LAMBDA(81),GDM(5)
      COMMON /C1/NJTS,NBJ,NCABL,NI,NPANL,ND,/C2/EMOD1,EMOD2
      COMMON /C3/KI,N,ER,IR,AI,BI,ENERGY(3),MGF
      DO 5 I=1,NJTS
      DO 5 J=1,3
      IF(AI.LT.0.8) SNODE(I,J)=0.
    5 FNODE(I,J)=0.
```

```
C
C  ADDING PANEL FORCES TO RELEVANT LINKS
C
      DO 10 I=1,NPANL
      I1=MPANL(I,1)
      I2=MPANL(I,2)
      I3=MPANL(I,3)
      I4=MPANL(I,4)
      IF(I1.NE.0) FCABL(I1)=FCABL(I1)+FPANL(I,1)
      IF(I2.NE.0) FCABL(I2)=FCABL(I2)+FPANL(I,2)
      IF(I3.NE.0) FCABL(I3)=FCABL(I3)+FPANL(I,3)
      IF(I4.NE.0) FCABL(I4)=FCABL(I4)+FPANL(I,4)
      IF(MGF.EQ.4) GOTO 10
      I5=MPANL(I,5)
      I6=MPANL(I,6)
      FCABL(I5)=FPANL(I,5)
      FCABL(I6)=-FPANL(I,5)*LAMBDA(I)
   10 CONTINUE
C
C  TRANSFERING LINK FORCES INTO NODAL FORCE COMPONENTS
C    AND CALCULATING CURRENT STIFFNESS
C    ( AFTER PEAK KINETIC ENERGY )
C
      DO 20 I=1,NI
      M1=MCABL(I,1)
      M2=MCABL(I,2)
      CL=LCABL(I)+DCABL(I)
      TF=FCABL(I)/CL
      TF0=PREST(I)/LCABL(I)
      IF(AI.LT.0.8.AND.I.LE.NCABL) SE(I)=SE(I)-TF0
      DO 15 J=1,ND
      DJ=XNODE(M2,J)+DNODE(M2,J)-XNODE(M1,J)-DNODE(M1,J)
      CJ=DJ/CL
      XTF(J)=TF*DJ
      IF(AI.LT.0.8.AND.I.LE.NCABL) SCABL(J)=SE(I)*CJ*CJ+TF0
   15 CONTINUE
      DO 20 J=1,3
      FNODE(M1,J)=FNODE(M1,J)-XTF(J)
      IF(AI.LT.0.8) SNODE(M1,J)=SNODE(M1,J)+SCABL(J)
      FNODE(M2,J)=FNODE(M2,J)+XTF(J)
      IF(AI.LT.0.8) SNODE(M2,J)=SNODE(M2,J)+SCABL(J)
   20 CONTINUE
C
C  CURRENT RESIDUALS AT INNER JOINTS
C
      DO 30 I=1, NJTS
      DO 30 J=1,3
      RNODE(I,J)=-FNODE(I,J)+PNODE(I,J)
   30 CONTINUE
```

```
C
C  CHECKING WHETHER RESIDUALS ARE CLOSE TO ER-ACCURACY
C
      DO 50 I=1,NJTS
      DO 40 K=1,NBJ
   40 IF(I.EQ.NBJT(K)) GOTO 50
      DO 45 J=1,ND
   45 IF(ABS(RNODE(I,J)).GT.ER) GOTO 60
   50 CONTINUE
      IR=0
C
C  CALCULATING REAL CABLE MEMBER FORCES FOR OUTPUT
C
      DO 55 I=1,NPANL
      I1=MPANL(I,1)
      I2=MPANL(I,2)
      I3=MPANL(I,3)
      I4=MPANL(I,4)
      IF(I1.NE.0) FCABL(I1)=FCABL(I1)-FPANL(I,1)
      IF(I2.NE.0) FCABL(I2)=FCABL(I2)-FPANL(I,2)
      IF(I3.NE.0) FCABL(I3)=FCABL(I3)-FPANL(I,3)
      IF(I4.NE.0) FCABL(I4)=FCABL(I4)-FPANL(I,4)
   55 CONTINUE
      GOTO 150
C
C  CALCULATING VELOCITIES AND DISPLACEMENTS AT INNER JOINTS
C
   60 DO 75 I=1,NJTS
      DO 65 K=1,NBJ
   65 IF(I.EQ.NBJT(K)) GOTO 75
      DO 70 J=1,ND
      VNODE(I,J)=VNODE(I,J)+AI*BI*RNODE(I,J)/SNODE(I,J)
      DNODE(I,J)=DNODE(I,J)+VNODE(I,J)
C
C  KINETIC ENERGY
C
   70 ENERGY(3)=ENERGY(3)+VNODE(I,J)**2*SNODE(I,J)
   75 CONTINUE
      IF(ENERGY(3).GT.ENERGY(2)) GOTO 110
      ALPHA=(ENERGY(3)-ENERGY(2))/
     1      (ENERGY(1)-2.*ENERGY(2)+ENERGY(3))
      DO 100 I=1,NJTS
      DO 80 K=1,NBJ
   80 IF(I.EQ.NBJT(K)) GOTO 100
      DO 90 J=1,ND
      DNODE(I,J)=DNODE(I,J)-(1.+ALPHA)*VNODE(I,J)
     1           +BI*ALPHA*RNODE(I,J)/SNODE(I,J)
   90 VNODE(I,J)=0.
  100 CONTINUE
      DO 105 I=1,3
  105 ENERGY(I)=0.
      AI=0.5
      GOTO 115
```

```
  110 ENERGY(1)=ENERGY(2)
      ENERGY(2)=ENERGY(3)
      ENERGY(3)=0.
      AI=1.
C
C  CHANGE IN LENGTH OF CABLE MEMBERS
C
  115 DO 125 I=1,NI
      M1=MCABL(I,1)
      M2=MCABL(I,2)
      S=0.
      DO 120 J=1,ND
  120 S=S+(XNODE(M1,J)+DNODE(M1,J)-XNODE(M2,J)-DNODE(M2,J))**2
      DCABL(I)=SQRT(S)-LCABL(I)
C
C  CURRENT FORCE IN CABLE MEMBERS
C
      IF(PREST(I).GE.0.)
     1 FCABL(I)=PREST(I)+DCABL(I)*EMOD1*AR(I)/LCABL(I)
      IF(PREST(I).LT.0.)
     1 FCABL(I)=PREST(I)+DCABL(I)*EMOD2*AR(I)/LCABL(I)
      IF(FCABL(I).LT.0.0.AND.PREST(I).GT.0.0) FCABL(I)=0.0
  125 CONTINUE
C
C  CURRENT FORCE IN PANELS
C
      DO 145 I=1,NPANL
      DO 130 J=1,5
  130 GDM(J)=0.
      I1=MPANL(I,1)
      I2=MPANL(I,2)
      I3=MPANL(I,3)
      I4=MPANL(I,4)
      IF(I1.NE.0) GDM(1)=DCABL(I1)
      IF(I2.NE.0) GDM(2)=DCABL(I2)
      IF(I3.NE.0) GDM(3)=DCABL(I3)
      IF(I4.NE.0) GDM(4)=DCABL(I4)
      IF(MGF.EQ.4) GOTO 135
      I5=MPANL(I,5)
      I6=MPANL(I,6)
      GDM(5)=DCABL(I5)-DCABL(I6)*LAMBDA(I)
  135 DO 140 II=1,MGF
      FPANL(I,II)=0.
      DO 140 JJ=1,MGF
      FPANL(I,II)=FPANL(I,II)+STIFF(I,II,JJ)*GDM(JJ)
  140 CONTINUE
  145 CONTINUE
  150 CONTINUE
      RETURN
      END
```

```
C
C
C FINAL OUTPUT
C
C
      SUBROUTINE OUTPUT(IT)
      IMPLICIT REAL*8 (A-H,O-Z), INTEGER*4 (I-N)
      REAL*8 LCABL,LAMBDA
      COMMON XNODE(96,3),PNODE(96,3),FNODE(96,3),RNODE(96,3),
     1       VNODE(96,3),DNODE(96,3),SNODE(96,3),NBJT(40),
     2       MCABL(150,2),LCABL(150),FCABL(150),DCABL(150),
     3       PREST(150),AR(150),SE(150),MPANL(81,6),
     4       FPANL(81,5),STIFF(81,5,5),LAMBDA(81),GDM(5)
      COMMON /C1/NJTS,NBJ,NCABL,NI,NPANL,ND
      WRITE(8,5) IT
    5 FORMAT(//8X,15H**ITERATION NO.,1X,I5/10X,19(1H-))
      WRITE(8,10)
   10 FORMAT(/15X,9HJOINT NO.,5X,6HDISP X,7X,6HDISP Y,7X,
     1       6HDISP Z,10X,5HRES X,8X,5HRES Y,8X,5HRES Z/)
      DO 25 I=1, NJTS
      DO 15 K=1,NBJ
   15 IF(I.EQ.NBJT(K)) GOTO 20
      WRITE(8,30) I,(DNODE(I,J),J=1,3),(RNODE(I,J),J=1,3)
      GOTO 25
   20 WRITE(8,35) I,(DNODE(I,J),J=1,3),(RNODE(I,J),J=1,3)
   25 CONTINUE
   30 FORMAT(17X,I4,5X,3(E11.4,2X),3(2X,E11.4))
   35 FORMAT(15X,2H**,I4,5X,3(E11.4,2X),3(2X,E11.4))
      WRITE(8,40)
   40 FORMAT(//32X,10HJOINT REFS,12X,11HCABLE FORCE,14X,
     1       9HEXTENSION/)
      DO 45 I=1,NCABL
   45 WRITE(8,50) MCABL(I,1),MCABL(I,2),FCABL(I),DCABL(I)
   50 FORMAT(33X,I3,2X,I3,2(10X,F14.8))
      IF(NPANL.GT.0) WRITE(8,55)
   55 FORMAT(//17X,9HSIDE REFS,40X,11HPANEL FORCE/)
      DO 60 I=1,NPANL
   60 WRITE(8,65) (MPANL(I,J),J=1,4),(FPANL(I,J),J=1,5)
   65 FORMAT(13X,4(I3,1X),2X,5(1X,F14.8))
      RETURN
      END
```